DOCTOR OF PHILOSOPHY

Functional integration of neural signals during person perception

Greven, Inez

Award date:
2016

Awarding institution:
Bangor University

PRIFYSGOL
BANGOR
UNIVERSITY

Functional integration of neural signals during person perception

Inez Margot Greven

Thesis submitted to the School of Psychology Bangor University in partial fulfilment of the requirements for the degree of Doctor of Philosophy

Bangor, United Kingdom

March 2016

SoBA Lab
SOCIAL BRAIN IN ACTION

ACKNOWLEDGEMENTS

In the empirical chapters of this thesis, I use the pronoun ‘we’ to acknowledge the collaboration with my supervisor Richard Ramsey, and second supervisor Paul Downing. In the general chapters, I use ‘I’ to represent my thought for this thesis. This is not to say that I would have been able to produce this thesis without the fruitful discussions I’ve had with my supervisors and many other people over the past three years.

First of all, I thank Richard Ramsey. The opportunity to start my PhD under your supervision means a lot to me. You have encouraged me to think critically and independently, which is exactly the kind of supervision I wanted and needed. You enthusiastically lead by example, and showed me great directions in which I can and want to take my career.

I would like to thank Paul Downing, my second supervisor, for his valuable insights, which encouraged me to think critically about and improve my experimental design. I am also grateful to Emily Cross, my PhD committee chair. The conversations we had about science and gender equality in academia have been really encouraging and continue to motivate me in my journey to becoming an independent researcher.

Of course I thank past and present PhD and Post-Doc researchers of the Social Brain in Action laboratory, for the great atmosphere and for making it a pleasure to help each other out: Emily Butler, Louise Kirsch, Alex Jones, Tom Gardner, Dace Apšvalka, Dilini Sumanapala, Elin Harding Williams.

To the Psychology Department and Bangor Imaging Group: thanks for creating an environment where everyone could ask questions, leading to interesting discussions and new insights. The technical and administrative staff is also thanked for all the support.

Lieve Papa en Mama. Bedankt dat jullie altijd in mij geloven en achter me staan. Zonder jullie was ik hier niet geweest, en zonder jullie zou ik nooit mijn PhD op een geweldige plek hebben gedaan. Antje, André, Anna, Henri, Bert, Margriet, Martin, Anouk: bedankt voor jullie enthousiasme en interesse, waar ik ook heen ga en wat ik ook besluit te doen.

Ultimo, ma assolutamente non meno importante, grazie al mio tesoro, Antonio. Mi hai aiutato tanto, e senza di te sarei una palla ancora più grande di ansia. E dopo tre anni in una relazione a lunga distanza, io so Umberto Eco aveva ragione; l'assenza è all'amore come il vento al fuoco: spegne il piccolo, fa avvampare il grande.

SUMMARY

In every day social interactions, it is important to know who other people are and how we might expect them to behave. Neuroscientific research has identified neuroanatomically distinct networks involved in perceiving a person's physical features and reasoning about their trait characteristics. While it has been demonstrated that both these networks are engaged when linking multiple features of a person together, the neural networks integration under these circumstances has mostly been overlooked. Over four empirical chapters, this thesis aims to understand how functional integration between distinct cognitive and neural systems supports person perception during social interactions.

The first empirical chapter (Chapter 3) investigates how physical features are linked to social knowledge, similarly to how we form impressions when we initially meet someone. While in this chapter social knowledge was inferred from descriptions of the person's behaviour, Chapter 4 aimed to investigate how social signals are extracted from the visual image of the body alone. Chapter 5 investigated functional integration during the perception of bodies that cued recall of social knowledge. Finally, Chapter 6 differentiated between affective valences of trait-based judgments.

Taken together, the findings presented in this thesis highlight the importance of an integrative perspective when investigating the role of functionally segregated brain regions in a larger interconnected network. This view advocates the use of functional connectivity measures when investigating the role of person perception nodes in socially complex settings.

Rem tene, verba sequentur

- Umberto Eco, the Name of the Rose

TABLE OF CONTENTS

LIST OF FIGURES AND TABLES

Chapter 1. General Introduction

Chapter 3. Linking person perception and person knowledge in the human brain

Appendices:

Chapter 4.

Appendices:

Chapter 5.

Appendices:

Chapter 6.

Appendices:

CHAPTER 1

GENERAL INTRODUCTION

Allow me to introduce my partner, Antonio: he helps me learn his native language, does yoga every morning, and recently flew to his hometown in Italy for the weekend to attend his friend's wedding. Hearing descriptions of someone's behaviour prompts us to form impressions of them, such as 'patient', 'motivated', and 'loyal' (Uleman et al., 2008). In addition, Antonio's physical features, such as his broad shoulders and straight posture, allow me to identify him in a crowd. As these examples demonstrate, there is a rich and diverse array of information available during everyday social interactions, which helps guide social behaviour. Indeed, I would react very differently to a hug from Antonio compared to a hug from a complete stranger. The emerging field of social neuroscience has begun to uncover the neural substrates that underpin how we navigate through our social lives (Cacioppo and Berntson, 1992; Ochsner and Lieberman, 2001). In the present thesis, I take a similar approach to understanding how different dimensions of social information are bound together into a holistic representation of another person's identity.

To date, neuroscience research has largely focused on identifying how distinct neural networks contribute to the perceptual, affective, and inferential analysis of a person (Adolphs, 2009). Less research, however, has investigated how signals from these functionally segregated brain circuits are integrated (Friston et al., 2003). Although it is widely acknowledged that distributed networks are involved in social perception and cognition (Haxby et al., 2000; Fairhall and Ishai, 2007; van Overwalle, 2009), it remains largely unknown how distinct neural networks interact during social exchanges. For instance, when meeting someone and forming an impression of them, it is unclear how the visual analysis of physical features (e.g., thin, tall) is linked to trait-based inferences regarding their underlying character (e.g., friendly, hardworking).

In this thesis, I will investigate the circumstances under which distributed neural networks interact with one another during the detection and recognition of others. The rest of this introduction will provide relevant background to the thesis by outlining the key neural networks that are involved in processing social information. Section 1.1 will introduce and define the social brain. Section 1.2 will review how functionally segregated neural networks contribute to visually perceiving a person (1.2.1), reasoning about another person (1.2.2), and vicariously feeling what another person might feel (1.2.3). In section 1.3 I will outline how functional integration of neural signals from distributed networks has been shown to contribute to social perception, as well as identify outstanding questions. Lastly, in section 1.4 I will present an overview of my thesis and outline the main question that each chapter addresses.

1.1. The social brain

Over the past 25 years, researchers have intensively investigated the neurobiological bases of social abilities (Adolphs, 1999; Ochsner and Lieberman, 2001; Frith and Frith, 2010). Both in monkeys and humans, several brain circuits have been identified that show sensitivity to the processing of socially relevant stimuli, such as identifying the presence of others, tracking gaze direction and facial expressions, as well as inferring goals and intentions (Perrett et al., 1985, 1992; Brothers, 1990; Tomasello et al., 1998; Adolphs, 1999; Adolphs et al., 2003; Gallese et al., 2004). Collectively, these brain circuits have been labelled 'the social brain' because they are involved in detecting, encoding, and retrieving social information (Frith, 2007; Frith and Frith, 2010).

The ability to deal with complex social situations requires an efficient processing of the conspecifics with which we are interacting. Brain structures responsible for different aspects of social cognition (e.g., simply observing a conspecific, or actively reasoning about them) have been proposed and investigated (Frith and Frith, 1999; Adolphs, 2009; van Overwalle, 2009). While a plethora of neuroscience research has dealt with testing the functional specificity of these areas (i.e., that a particular area is engaged more for one function compared to other functions; Kanwisher, 2010), others have attempted to unify these segregated neural networks by testing how they influence each other during different circumstances (Ishai, 2008). Before describing the functional integration in section 1.3, I will first discuss the functional segregation of several systems within the social brain.

1.2. Functional segregation in the social brain

It has long been acknowledged that the brain has, in part, a functionally segregated structure (Hecaen and Angelergues, 1962; Berker et al., 1986; Rorden and Karnath, 2004). Indeed, research has demonstrated the existence of functionally segregated brain areas, i.e., cells that are grouped together to perform similar functions (Friston and Price, 2001). In the social domain, segregated groups of cells together process social stimuli, such as what someone looks like or what their beliefs and desires are (Peelen and Downing, 2007; Mitchell, 2009; Kanwisher, 2010). Of the many neural circuits that process social information, I will focus on those that span perceptual, inferential, and affective processing, as they are most relevant to the current thesis.

1.2.1. Neural networks supporting person perception

Person perception involves the detection and identification of a conspecific on the basis of their physical features (Downing and Peelen, 2011). Person perception is essential for social interaction because before we interact with someone, we must first detect their presence (Bindemann et al., 2010; Stein et al., 2012). In addition, since physical features convey many social signals, such as information about someone's identity, emotional state, and the meaning of their actions (Slaughter et al., 2004), person perception aids the navigation of complex social interactions, for instance, by helping to identify who to form alliances with and who to avoid (Cosmides and Tooby, 1994; Pascalis and Bachevalier, 1998; Parr and De Waal, 1999; Vokey et al., 2004; Stevens et al., 2005; Martin-Malivel and Okada, 2007).

Specialised brain areas localised for body and face perception have been identified for non-human primates as well as humans (Tsao et al., 2003; Peelen and Downing, 2007; Gross, 2008). Most research in humans has focused on the neural substrates of face perception. This network has been divided into a "core" and "extended" network: the core network, located along the ventral visual stream, responds selectively to faces, while the extended network further processes the faces to determine, for instance, a person's identity and associated biographical information (e.g., their name, occupation), or their emotional state (Haxby et al., 2000; Fairhall and Ishai, 2007; Ishai, 2008).

A similar cognitive and neural architecture has been proposed to underpin body perception (Minnebusch and Daum, 2009; Amoruso et al., 2011; Downing and Peelen, 2011; Ramsey et al., 2011). For example, core nodes along the ventral visual stream have been credited with processing body shape and posture (Downing and Peelen, 2011, 2015). Less research has clearly identified the functional roles performed by extended networks in body perception, although it has been proposed that they may exist in a similar manner to face perception (Minnebusch and Daum, 2009; Amoruso et al., 2011). However, while bodies, like faces, convey a multitude of relevant social signals and offer cues that faces might hide (Slaughter et al., 2004; Aviezer et al., 2012), there have been relatively few studies investigating the relationship between core and extended networks in body perception. For this reason I will focus my thesis on body perception.

In the following section I will outline non-human and human evidence for the detection of conspecifics on the basis of their body, as well as summarise functional claims for the role of two separate body-selective nodes in person perception.

Neural systems and functional claims

Body-part selectivity was demonstrated in the brain of non-human primates by analysing electrophysiological recordings from single neurons in the inferotemporal (IT) cortex (Gross et al., 1969, 1972; Desimone et al., 1984; Gross, 2008). Gross and colleagues (1969, 1972) found that neurons in IT cortex of the macaque responded more strongly to various depictions of hands compared to other stimuli such as faces. This was confirmed by comparative fMRI studies testing both macaques' and humans' category-selective responses, thereby highlighting that humans and macaques have similar brain architectures for the visual processing of faces and bodies (Tsao et al., 2003; Pinsk et al., 2005, 2009).

Two anatomically separate areas responding selectively to bodies have been identified with fMRI in the human brain. The extrastriate body area (EBA) in the occipital cortex responds stronger to whole bodies and body parts (pictures, line-drawings, and silhouettes) compared to objects and faces (Downing et al., 2001). The fusiform body area (FBA), located in the fusiform gyrus, responds more to whole bodies rather than body parts (Peelen & Downing, 2005). For instance, Brandman and Yovel (2016) presented participants with whole (intact) bodies or the sum of its parts (a whole body in a scrambled configuration). Segregated patches of cortex, selective for different categories such as objects and faces, did not show a general preference for bodies in its intact compared to scrambled configuration. Body-selective areas, on the other hand, responded more strongly to the whole bodies, suggesting their involvement in a more holistic processing of the body (see also Taylor et al., 2007).

Transcranial magnetic stimulation (TMS; Barker et al., 1985; Walsh and Cowey, 2000; Fitzgerald et al., 2006) has been used to study the neurobiological bases of body perception. By creating a 'virtual lesion' at the approximate location of EBA, participants are typically slower in deciding which of two images (body-, face-, and motor-parts) matched a previously presented sample, demonstrating that EBA is causally involved in distinguishing between bodies (e.g., Urgesi et al., 2004). Furthermore, EBA could be dissociated from two other nearby located category-selective regions (Pitcher et al., 2009): the occipital face area (OFA; Gauthier et al., 2000) and the object-selective lateral occipitotemporal complex (LO; Malach et al., 1995). The causal role of FBA has been demonstrated in a lesion study which revealed deficits in body perception (Moro et al., 2008, 2012). Altogether, these results demonstrate that the responses in EBA and FBA are specifically and causally involved in the visual analysis of bodies (Downing and Peelen, 2011).

Despite the strong evidence that EBA and FBA are selectively engaged by bodies, other lines of research have suggested that body-selective areas are responsible for a plethora of functions beyond the visual analysis of bodies. While Urgesi and colleagues (2007) demonstrated a specific role for EBA in representing body shape and posture but not bodily actions, other studies did suggest the involvement of EBA in performing and understanding the meaning of bodily actions (Astafiev et al., 2004; Kable and Chatterjee, 2006; Marsh et al., 2010). For instance, Astafiev and colleagues (2004) reported that, even without visual feedback, EBA was modulated by limb movements to a visual target stimulus. According to the authors of these studies, EBA integrates information about bodies and actions rather than solely processing visual information about the body.

Another study, where right EBA responded differentially to body parts shown from one’s own (egocentric) or someone else’s (allocentric) viewpoint, suggested that EBA may be involved in the multimodal integration of information enabling a person to maintain a sense of body ownership (Saxe et al., 2006). EBA has indeed been found to be activated when manipulating body ownership. For instance, EBA was more active when mentally imagining oneself in the position of a presented figure compared to when the figure was supposed to portray the participants’ mirror-image (Arzy et al., 2006; Blanke et al., 2010).

While people report relying primarily on the face when making identity judgments, the rest of the body also provides important cues for determining a person’s identity (O’Toole et al., 2011; Rhodes et al., 2013; Rice et al., 2013). To distinguish people based on their body, a visual analysis has to take place in body patches. However, it is not agreed upon whether EBA and FBA specifically differentiate between bodies of the self and familiar or unfamiliar others and thereby represent for person identity. While some authors found stronger responses to the participant’s own body in comparison to familiar or unfamiliar other in EBA and FBA (Sugiura et al., 2006; Hodzic et al., 2009a; Vocks et al., 2010), others found no such distinction (Chan et al., 2004; Devue et al., 2007; Hodzic et al., 2009b).

The bodies in the studies described so far did not differ in their postures. However, postures and body language can also signal a person's basic emotions such as fear, anger, and happiness (Walker and Trimboli, 1989; Atkinson et al., 2004; Sinke et al., 2012). It has been demonstrated by several laboratories that activity in EBA and FBA is modulated by emotional body postures (e.g., Hadjikhani and de Gelder, 2003; de Gelder et al., 2004; Grèzes et al., 2007, 2013; Borhani et al., 2015).

In summary, many functional claims have been made regarding the role of EBA and FBA in body perception, which extend beyond the processing of body shape and posture to include the processing emotions, identity and action goals (Downing and Peelen, 2011). However, it is not clear if the engagement of body patches in these cognitively more elaborate representations reflect a basic function of a segregated brain region or the interaction with a wider brain network. Proposals for interaction between "core" person perception nodes and "extended" networks have been put forward for many different aspects of person perception (Haxby et al., 2000; Minnebusch and Daum, 2009; Amoruso et al., 2011; Ramsey et al., 2011). The next two sub-sections will discuss two extended networks and how they might contribute to social perception.

1.2.2. Neural networks supporting person knowledge

As a social species, we are very skilled at reading social signals from others based on their non-verbal behavior and emotional body language (Walker and Trimboli, 1989; Atkinson et al., 2004; Sinke et al., 2012). In more extreme cases, we can make generalised judgments based on a person's appearance (e.g., stigma associated with obesity; Puhl and Heuer, 2009). However, the more accurate inferences about a person's trait characteristics come from learning about how people act, which I refer to as 'person knowledge' in my thesis.

Reasoning about other people's inner mental states is an ability that falls under the term Theory of Mind (ToM; Premack and Woodruff, 1978), and is proposed to develop during early childhood (Wimmer and Perner, 1983; Gopnik and Astington, 1988; Repacholi and Gopnik, 1997; Brüne and Brüne-Cohrs, 2006; Saxe, 2006a; Heyes, 2014). In a classic ToM task, the participant is asked to reason about a person who has out-dated beliefs about a situation ("false-belief" stories). To correctly complete the task, participants have to reason about a belief that is different from the state of reality, thus ensuring that the process of belief reasoning rather than reality reasoning is engaged. ToM encompasses more than just belief reasoning, however, and refers to a collection of abilities that aids understanding the content of another person's mind (Samson and Apperly, 2010; Chiavarino et al., 2012; Apperly, 2013).

Neural systems and functional roles

A network comprising bilateral temporal poles and temporoparietal junctions (TPJ), medial prefrontal cortex (mPFC), and precuneus, has been found to be engaged more in false-belief relative to control conditions (Saxe, 2006b; Carrington and Bailey, 2009; Mitchell, 2009; van Overwalle, 2009; Schurz et al., 2014). The TPJ is one of the key brain regions involved in representing others' thoughts, feelings, and desires (Saxe, 2010; Young et al., 2010). Tasks involving reasoning about out-dated beliefs or inferring someone's trait-characteristics result in greater activation of this brain area (Saxe and Kanwisher, 2003; Ma et al., 2011, 2012). While TPJ seems to be involved in holding information about another person's mental states in general, mPFC appears to distinguish between people on the basis of how similar they are to us (Mitchell, 2009), or how likeable they seem (Cloutier and Gyurovski, 2014). Furthermore, when successfully binding social information together (i.e., when the person and associated behaviour were later recognised) activity in mPFC is enhanced, suggesting its involvement in encoding person-specific social information (Mitchell et al., 2004; Gilron and Gutchess, 2012). Lastly, mPFC is shown to be sensitive to person-specific information (Hassabis et al., 2014; Welborn and Lieberman, 2014), and is involved in correctly retrieving and subsequently selecting social information (Satpute et al., 2013). Correctly encoding and storing person-specific social information is important to predict how a person might act in the future.

Less research has identified functional roles for the temporal poles and precuneus in ToM. Bilateral temporal poles have been associated with storing and recalling social information about people (Sugiura et al., 2006; Tsukiura et al., 2006; Olson et al., 2007, 2013; Simmons and Martin, 2009; Simmons et al., 2010; Drane et al., 2013). Some researchers suggest that the temporal poles play a key role in conceptual memory in general (Patterson et al., 2007). However, Olson and colleagues (2007, 2013) have argued that socialness is confounded with semantic specificity, and that the role of the temporal poles in representing and recalling social knowledge goes beyond semantic memory in general. Lastly, activity in the precuneus has been associated with reasoning about perceptually familiar people (Cavanna and Trimble, 2006; Cloutier et al., 2011), although more research is needed to better characterise the functional role of this ToM node.

Altogether, temporal poles, TPJ, mPFC, and precuneus, are involved in reasoning about another person. In the next session I will discuss the neural system enabling us to feel what another person feels.

1.2.3. Neural networks supporting affective processing

Reasoning about what a person is thinking or inferring their trait-characteristics is often based on their behaviour. However, a person's posture can also inform us about their affective states (Coulson, 2004; De Silva and Bianchi-Berthouze, 2004; Slaughter et al., 2004). As these affective states reliably influence behaviour (Pourtois et al., 2013), it is important for the observer to rapidly infer the valence of such affective signals in order to modify their own behaviour accordingly (de Gelder et al., 2004; Grèzes et al., 2013; Borhani et al., 2015). Apart from modifying our behaviour, for instance, by fleeing because we are the target of a person's anger (Grèzes et al., 2013), a person's emotional state can additionally allow us to vicariously feel what they feel in order to empathise with them (Zaki et al., 2007; Bastiaansen et al., 2009; Batson, 2009; Keysers and Gazzola, 2009).

Neural systems and functional roles

An "affective network" of brain regions comprising amygdala, insula, medial prefrontal and orbitofrontal cortex (mPFC and OFC, respectively), and striatum, has been found to be involved in affective empathy, as well as emotion and reward processing (Keysers and Gazzola, 2009; Fan et al., 2011; Bartra et al., 2013; Eres and Molenberghs, 2013). Whether we simply observe someone or actively imagining what they feel, be it positive (e.g., joy) or negative (e.g., pain, disgust), the empathetic response is associated with activity within the affective network (Singer et al., 2004; Jabbi et al., 2007; Lamm and Singer, 2010).

The amygdala processes the valence of a socially relevant stimulus (Whalen, 1998; Costafreda et al., 2008; Adolphs, 2010; Morrison and Salzman, 2010; Pessoa, 2010). By virtue of its dense connections with various other parts of the brain, the amygdala is involved in various behavioural functions, such as valence- and arousal-based modulation of memory, perception, and social responding (Phelps and LeDoux, 2005; LeDoux, 2007).

While the amygdala can be thought of as processing the "actual" valence of a stimulus, the striatum and OFC have commonly been associated with appending a subjective value (Seymour et al., 2007; Kahnt et al., 2012; Bartra et al., 2013). When evaluating several options to choose from, and when receiving a reward, responses in striatum and OFC have proven to be domain-general, as they respond to both primary (e.g., food) as well as secondary (e.g., social and monetary) rewards (Izuma et al., 2008; Levy and Glimcher, 2012; Lin et al., 2012).

The insula has been functionally subdivided in several clusters (Kurth et al., 2010; Deen et al., 2011; Jakab et al., 2012; Cauda and Vercelli, 2013), with the anterior part specifically recruited in both affective and cognitive empathy (Fan et al., 2011). Due to its functional connections to the middle and inferior temporal cortex and the anterior cingulate cortex, the anterior insula is thought to be responsible for multimodal integration of emotion and memory. By contrast, the cytoarchitectonically distinct posterior insula is involved in sensorimotor integration (Kurth et al., 2010; Cauda et al., 2011).

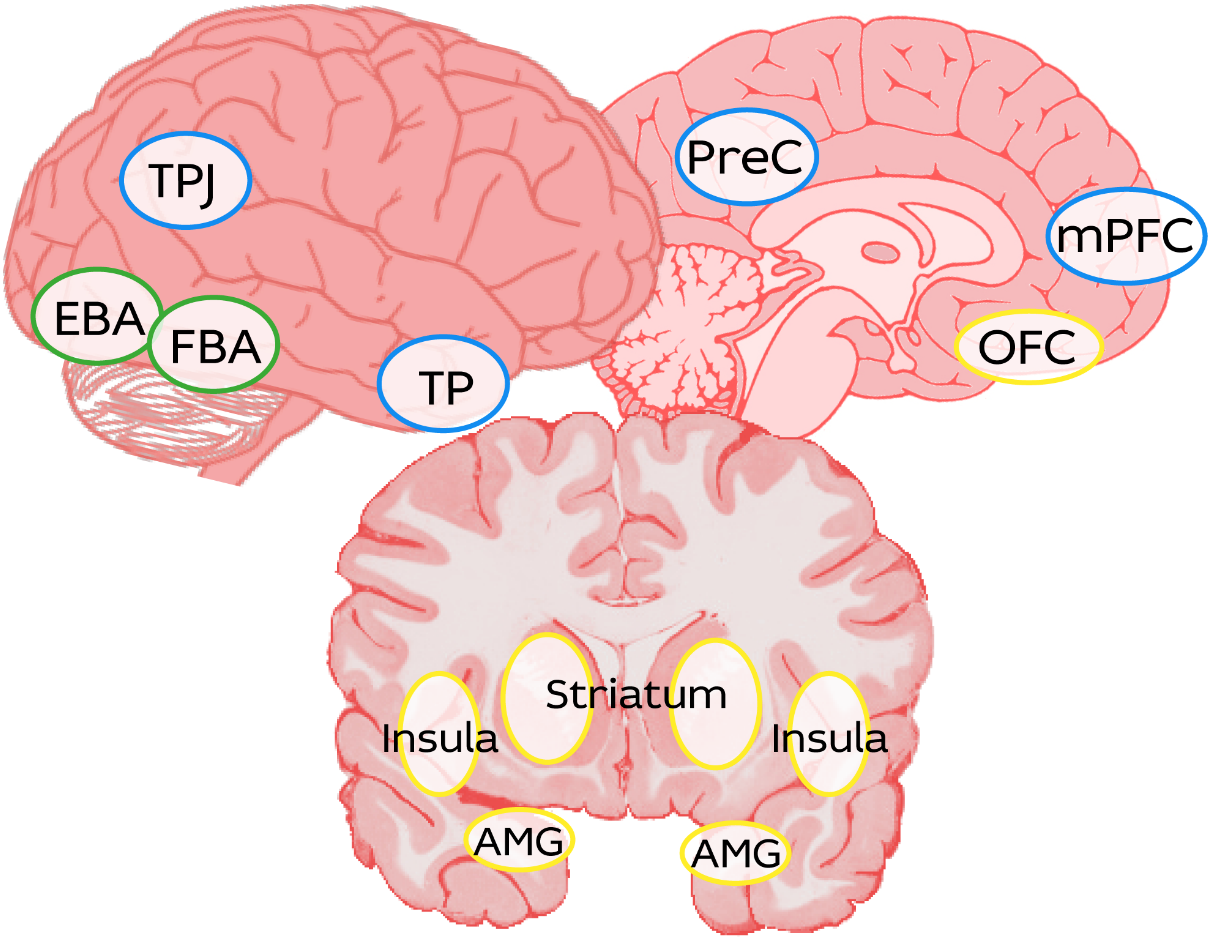

Figure 1.1. Neural networks involved in person perception (green), person knowledge (blue), and affective processing (yellow). Abbreviations: Extrastriate Body Area (EBA), Fusiform Body Area (FBA), TemporoParietal Junction (TPJ), Temporal Pole (TP), Precuneus (PreC), medial PreFrontal Cortex (mPFC), Amygdala (AMG), OrbitoFrontal Cortex (OFC).

1.2.4. Summary of functional segregation in the social brain

It is clear that different parts of the social brain are primarily focused on different mental operations, which span perceptual, inferential, and affective processes. The visual analysis of a person's body shape and posture occurs in dedicated areas in the occipitotemporal cortex and fusiform gyri, while reasoning about their traits and feeling empathy for another person arises from activity in temporoparietal, frontal, and limbic regions (Figure 1.1). Although evidence demonstrates that distinct social functions are at least partially segregated in the human brain, it is clear that everyday social interactions are typically complex and require us to quickly alternate between (or simultaneously perform) many mental operations; therefore, it is unlikely that these systems work in isolation (Sporns et al., 2005; Kanwisher, 2010). Instead, it is possible that anatomically and functionally distinct neural structures work together to form a coherent representation of another person (Georgieff and Jeannerod, 1998; Ramsey et al., 2011). However, it is currently not clear how distinct mental processes interact in general as well as in the social domain.

1.3. Functional integration in the social brain

Functional integration refers to context-dependent interactions between distinct groups of neurons (Friston, 1994; Friston and Price, 2001). From the evidence reviewed so far in this thesis, it is clear that neuroanatomically distinct brain circuits are involved in perceiving and reasoning about a person. However, behavioural research has provided evidence that inferences about other people's beliefs and traits can be made based on a person's physical features (Borkenau and Liebler, 1992; Rule and Ambady, 2008; Naumann et al., 2009; Kramer and Ward, 2010; Rojas et al., 2011; Thoresen et al., 2012). Therefore, signals from different brain circuits, such as those that are involved in processing body shape and posture and those that infer trait characteristics, appear to be integrated. To date, however, very little is known about how distinct neural systems exchange signals during social contexts. Before raising a number of outstanding questions, I will review current evidence for the interaction between perceptual, cognitive, and affective networks during social perception and cognition.

1.3.1. Current evidence

Several proposals have been put forward that describe functional integration in the human brain (Mesulam, 1990; Fuster, 1997; Friston and Price, 2001). Mesulam (1990) noted that complex behaviour does not arise from sequential processing, but from large-scale neural networks that are distributed across the brain and interact in parallel through reciprocal connections. Bruce and Young (1986) proposed a perceptual and cognitive model to account for different stages of face perception: the structural processing of a face leads to recognition, after which this information is fed to a cognitive system that allows to associate a name and other information to a face. Based on this model, Haxby and colleagues proposed a neural model for person perception with processes divided into core and extended systems (Haxby et al., 2000). The interaction between the core and extended systems have been thought to underlie the formation of identity representations (Haxby et al., 2000; Gobbini and Haxby, 2007; Ramsey et al., 2011; Collins and Olson, 2014; Blank et al., 2015).

Bidirectional connections between face-selective areas and amygdala were revealed when recognising or processing emotionally expressive faces, and with OFC when processing famous faces (Fairhall and Ishai, 2007; Herrington et al., 2011) or when forming a memory of a face (Xiu et al., 2015). Additionally, OFC and amygdala influence each other, depending on whether the perceived emotional expression of a face beckons the perceiver to approach or avoid the expressor of the emotions (Liang et al., 2009). While research investigating the interaction between core person perception nodes and an extended network has mostly focussed on face perception (Mechelli et al., 2004; Zhen et al., 2013; He et al., 2015; Hermann et al., 2015), the exchange of signals during body perception is limited to a few studies (Ewbank et al., 2011; Quadflieg et al., 2011; Zimmermann et al., 2013; Hutchison et al., 2014).

In the domain of body perception, functional links have been shown within the core body perception network, as well as between body patches and extended neural networks. One study has shown that when observing a series of bodies that all had the same identity, but changed in viewpoint, FBA modulated activity in EBA (Ewbank et al., 2011). As FBA has been shown to hold a holistic representation of bodies and EBA has been shown to be sensitive to body-parts (Taylor et al., 2007; Brandman and Yovel, 2016), it has been suggested that FBA might feed information about a body's identity in order to bias EBA and better predict what a person's body-parts would look like from a different angle.

Other studies have shown that body patches link with a wider network of brain regions also (Quadflieg et al., 2011; Zimmermann et al., 2013). Indeed, EBA has been shown to communicate with the intraparietal sulcus (Zimmermann et al., 2013), an area associated with the Action Observation Network (Kilner and Lemon, 2013; Caramazza et al., 2014). This suggests that increased activity in EBA when processing bodily actions might be the result of increased functional interaction with an extended network (Astafiev et al., 2004; Kable and Chatterjee, 2006; Marsh et al., 2010). In addition, Quadflieg and colleagues (2011) demonstrate links between body patches and the dorsolateral PFC while making social (gender) judgments about a person who defies gender norms. Therefore, the authors show that DLPFC is involved in limiting stereotypical thinking, and might exert influence on the person perception network. As this review demonstrates, to date, very little is known about relationships within the body network and between the body network and extended brain networks during person perception. In the next section, I outline some of the many remaining questions that relate to functional integration in person perception.

1.3.2. Outstanding questions

In general, much more is known about functional segregation in the human brain than integration, and the same is true for social perception research (Kanwisher, 2010; Sporns, 2014). Initial neuroimaging studies of body perception highlight that posterior brain circuits do not work in isolation during person perception (Downing and Peelen, 2011; Ramsey et al., 2011), but many questions remain unexplored. Indeed, the factors that govern interactions between core and extended networks remain largely unknown.

One open research question focuses on the extent to which the relationship between person perception and person knowledge neural networks underpins social perception. It has previously been demonstrated that trait-based information can be linked with a person's physical features, which involves the ToM-network (Mitchell et al., 2004, 2005; Gilron and Gutchess, 2012). Thus, it is possible that person perception nodes would interact with the ToM-network when linking a trait-based inference with physical features. However, it is still unknown how social knowledge is bound to body shape. Specifically, how is social knowledge (e.g., enthusiastic, intelligent) associated with physical features (e.g., tall, skinny)? In addition, once we associate social knowledge with someone, we can recall that knowledge at a later date. Todorov and colleagues (2007) demonstrated the involvement of the person perception and person knowledge network during the spontaneous retrieval of social information cued by a familiar face. A further fMRI study revealed that the fusiform gyrus and posterior cingulate (below the precuneus) were tuned to recognising faces that previously appeared hostile compared to friendly faces (Vrtička et al., 2009). While this informs us of the involvement of person perception and knowledge networks when observing faces that cue the recall of social knowledge, these studies did not investigate how these networks interact.

Social inferences about others can come in many forms other than solely from learning about someone's behaviour. For example, we can infer traits from body shape (Borkenau and Liebler, 1992; Naumann et al., 2009; Puhl and Heuer, 2009). In an experiment where participants were shown full-body photographs, personality traits such as extraversion and self-esteem could accurately be judged, even when the photographed targets had adopted a standardized pose (Naumann et al., 2009). However, it is unknown whether the activity in the neural systems supporting these inferences varies as a function of the observed body shape.

Another largely unexplored line of research is the extent to which affective neural systems interact with body perception and ToM networks during person perception. Perceptual, inferential, and affective neural networks respond differently in situations where we discern ‘us’ from ‘them’, which represents a so-called ‘group-bias’ (Molenberghs, 2013; Amodio, 2014). For instance, greater sensitivity in the anterior insula was found when participants observed faces of their own race experiencing pain compared to another race (Azevedo et al., 2013). Even when a group is created based on arbitrary criteria (Tajfel et al., 1971), simply determining whether someone is part of your group or the other group modulates activity in the person perception and affective networks (Van Bavel et al., 2008, 2011). However, no studies to date have investigated the relationship between these networks. It has previously been demonstrated that person perception and affective networks influence each other when processing a person’s facial expression, which differed in valence (Fairhall and Ishai, 2007; Xiu et al., 2015). Furthermore, person knowledge nodes are recruited when distinguishing between positive and negative individuals as well as social groups (Harris and Fiske, 2007; Vrtička et al., 2009). This raises the question how valence might influence the functional integration of perceptual, inferential, and affective neural networks.

In my thesis, I will investigate how these factors modulate functional integration. The following section will provide an overview of the thesis and the topics that each chapter covers.

1.4. Overview of thesis

The overarching aim that spans all empirical work in this thesis is to understand how functional integration between distinct cognitive and neural systems supports person perception.

In **Chapter 2** I will briefly describe the basic principles for the neuroimaging methodology that I have used to investigate functional connectivity throughout each empirical chapter.

Chapter 3 investigates how physical features are linked to social knowledge in order to investigate the neural systems that support the formation of first impressions. Participants were asked to form an impression of people (displayed as bodies or names) based on provided behavioural descriptions (trait-based or neutral). By including bodies and names, this study allows for the identification of neural systems that are specifically tied to linking social knowledge to physical features rather than other person-identifying knowledge such as a name.

Chapter 4 investigates how social signals are spontaneously extracted from the visual image of the body. It is still unclear whether the social judgments made based on body shape arises from functional integration between person perception and person knowledge networks. Chapter 4, therefore, can probe the relationship between person perception and person knowledge when there are no task instructions to form an impression. By doing so, the automaticity of the relationship is investigated.

In **Chapter 5**, I investigate functional integration under circumstances where seeing someone's familiar posture and shape (e.g., their broad shoulders and straight posture) will trigger the recall of stored trait-characteristics (e.g., patient and loyal). Remembering socially relevant knowledge, such as whether someone is friendly and generous or quarrelsome and easily annoyed, can help us decide whether to approach or avoid someone. Therefore, in Chapter 5, bodies are shown that prompt recall of social knowledge and compared to bodies that prompt recall of non-social knowledge.

Chapter 6 investigates group bias modulation in person perception. In a situation where there is no difference between either body shape and posture and all bodies had previously been paired with the same type of trait-based information (positive or negative), social judgments may still differ depending on whether the bodies belong to either the observer's in-group or out-group. To explore this difference in perception, we investigated valence-dependent group bias modulation of functional integration during person perception.

CHAPTER 2

GENERAL METHODS

Much has been learned about the functioning of the brain and its different regions during the last two centuries from anatomical, physiological, pharmacological, and psychological studies. Early psychological studies could not determine whether a certain brain region was responsible for a particular behaviour, but with a knowledge of the brain's anatomy, researchers gained information about several regions' functions from the analysis of brain lesions caused by disease or traumatic injuries. For instance, after a "rude missile had been shot through his brain", Phineas Gage displayed marked changes in behaviour, such as his temper, which sparked interest into whether social behaviour and personality depend on proper functioning of the frontal lobes (Eliot, 1911; Harlow, 1993; Damasio et al., 1994). Other, less drastic and widespread alterations to the brain resulted in the attribution of specific functional roles to particular brain areas. For example, the discovery of an area in the left frontal lobe responsible for speech production, known as Broca's area, was discovered after a lesion left a patient unable to clearly say any words other than "Tan" (Berker et al., 1986).

With the invention of magnetic resonance imaging, it became possible to non-invasively scan the body (Stoddart, 2008; Webb, 2008). The advent of functional imaging (fMRI) has provided information beyond morphology alone, allowing for the visualisation of activated brain areas during psychological tasks (Chao, 2008).

The two main techniques employed in this thesis are fMRI with univariate and functional connectivity analyses. As the analytical steps are described in the methods sections of each empirical chapter, I will use the current chapter to briefly outline the basic mechanisms that underlie fMRI with univariate and functional connectivity analyses. Additionally, I will summarise the steps that were taken to select the seed regions for the connectivity analyses.

2.1. Functional Magnetic Resonance Imaging

The brain, like all biological tissues, is abundant in hydrogen (H). The ^{1}H nucleus (proton) has a slightly uneven atomic mass, resulting in angular momentum, or spin, which induces a magnetic field. While normally the orientation of the magnetic dipoles of the hydrogen atoms is random, it can be aligned with a large, static magnetic field. However, such alignment is not perfect. Instead, the atoms will experience precession (i.e. rotate around the orientation, or axis, of the applied magnetic field) with a specific rate, or frequency, that depends on the strength of the magnetic field. The rate of precession (measured in megahertz) can be expressed as the angular momentum of the proton, multiplied by the strength of the magnetic field measured in Tesla (Philips Medical Systems, 1984; Narasimhan and Jacobs, 1996; Saper et al., 2000).

The alignment of the atoms can either be parallel or anti-parallel to the externally applied magnetic field. As the parallel alignment is more probable, there will be an imbalance between parallel and anti-parallel spins. The imbalance creates a net magnetisation oriented parallel to the external magnetic field. As the vector of the net magnetisation at equilibrium is static, it does not create a current that can be picked up by the receiver coil used in MR imaging. In order to get information from the spin of the protons, a second magnetic field is created through short bursts of radio frequency (RF pulses). The RF pulses cause the nuclei to precess at a different angle (excitation), which results in a net magnetisation with vectors in the longitudinal and transversal plane (Philips Medical Systems, 1984; Narasimhan and Jacobs, 1996; Saper et al., 2000). As the excited precess is tilted from its equilibrium state, it must return to this state. When returning to the equilibrium state (relaxation), the nuclei lose energy in the form of electromagnetic radiation, which can be received by the coil (Mansfield, 1977). Because of the differences in precession depending on whether the protons are embedded in grey or white matter, their relaxation times differ. By keeping a constant frequency of excitation and relaxation, grey matter can be distinguished from white matter (Saper et al., 2000).

A specific relaxation value, known as T2*, allows the coil to detect the release of energy immediately after termination of the RF pulse. Since the relaxation process occurs exponentially, this T2* measures a large loss of energy in a short period of time, which makes it more sensitive to detect inhomogeneous tissues that can change in their magnetic properties or magnetic susceptibility, such as blood. As blood flow to a particular brain area increases when active, T2* is used to visualise blood flow as an indirect correlate of neuronal activity in fMRI (Ogawa et al., 1992; Chao, 2008).

2.1.1. Blood Oxygen Level Dependent contrast imaging

The more neurons fire within a brain area, the larger the metabolic requirement of this area is. This leads to an increased consumption of oxygen carried by oxygenated blood, resulting in an increased ratio of deoxygenated to oxygenated blood (Philips Medical Systems, 1984; Narasimhan and Jacobs, 1996; Saper et al., 2000). Oxyhaemoglobin and deoxyhaemoglobin have different magnetic properties. The former is diamagnetic, which means that its magnetic field is opposite to the externally applied magnetic field. This results in a stronger MR signal. On the other hand, deoxyhaemoglobin is paramagnetic, resulting in an inhomogeneous magnetic field causing interferences with the MR signal. Blood flow will increase to replenish the active area with oxygen beyond what was actually consumed, as described by the haemodynamic response function (HRF). This overshoot causes a decrease in the concentration of deoxyhaemoglobin, leading to an increased MR signal, which is what the Blood Oxygen Level Dependent (BOLD) signal measures (Ogawa et al., 1990). It takes approximately 6 seconds for the HRF to reach its peak, after which it undershoots before returning to baseline.

2.2. Localisation and analysis

When participants perform a task while the BOLD signal is measured, it is possible to determine for each voxel in the brain how its activity changes over time (time course). A task typically consists of several different conditions that occur in a predetermined order and are repeated to gather enough data to investigate whether one brain region is more involved in one condition compared to another.

2.2.1. Univariate Analyses

To compare brain activity during different conditions, the times at which each condition starts and for how long it is presented are specified. This allows for the modelling of the time course in each voxel for each condition in the experiment.

Next, depending on the design of the experiment, subtraction analyses directly compare whether the magnitude of the response in a voxel is greater during one condition compared to another. For instance, when investigating whether body-selective areas are involved in distinguishing between different body-types, I can directly compare the magnitude of the response in these areas during the perception of muscular compared to slim bodies.

2.2.2. Localisation

Each empirical chapter has a different main task that is specifically designed to investigate the research question posed in that chapter. However, as the aim of this thesis is to investigate functional integration of person perception and person knowledge networks, two additional tasks were provided in each chapter. These tasks were independent to the main task and used to localise the specific brain circuits involved in body perception and mental state reasoning. To localise EBA and FBA, the time course when participants viewed blocks of images of bodies (without a head) was compared to the time course when viewing cars (Downing et al., 2007). To stay consistent with this localiser, the bodies in all main tasks were also presented without heads.

In the Theory of Mind (ToM) localiser, participants read “false-belief” stories, as described in the general introduction (Dodell-Feder et al., 2011). The time course extracted while reasoning about a person who has out-dated beliefs about a situation, is compared to the time course extracted during the presentation of “false-photograph” stories. In these control stories, false or out-dated information is still present, but does not require reasoning about another person’s beliefs.

To make sure that the functional integration measured is between brain regions associated with body perception and mental state reasoning, the data from the two localisers (Bodies > Cars; False-Belief > False-Photograph) will be used to constrain, or mask, the data from the contrasts in the main task. Both the univariate and the functional connectivity data are masked by the localisers. The cluster-level p-values reported in the tables have been corrected using the search volumes, i.e., the masks used to constrain the data.

2.2.3. Functional Connectivity

There are many different ways to test functional connectivity within the brain. In this thesis, I employed a generalized form of PsychoPhysiological Interaction (PPI) analysis. PPI enables the identification of brain regions whose activity correlates with the activity of a seed region as a function of a task (Friston et al., 1997; McLaren et al., 2012). For instance, as I will investigate functional integration between person perception and person knowledge networks, I can use a body-selective node as a seed region. After extracting the time course or activity from the seed region (the “physiological” element), I can see whether the time course from any voxels correlate with it stronger during one compared to another condition (the “psychological” element).

As I am interested in the specific coupling between brain regions that show magnitude-based sensitivity under the same psychological conditions (e.g., when forming an impression of a body paired with a trait-based statement), I will base the selection of my seed regions on the univariate analyses. Although this method of seed region selection may seem circular (i.e., using the same data for selection and subsequent analyses; Kriegeskorte et al., 2009), it is not. If two brain regions were active in the condition of interest, it does not necessarily follow that they interact. They could be independently active. Alternatively, the regions could work together interactively, either through the influence of one region on the other or through a bidirectional coupling. By including the regressors of the general linear model used for the univariate analyses as covariates of no interest, the PPI will only measure the correlation in time course between brain regions above and beyond the activation found in the main contrast (O'Reilly et al., 2012).

For the group-level analyses, I masked the results from the main task by both the body and ToM localisers. The resulting clusters would be used as seed regions. Once the seed regions of interest had been specified, they were identified in each individual participant by identifying clusters of overlap between 1) regions emerging from the univariate analyses in the main experiment, and 2) either body-selective or ToM-selective regions. If the main task did not yield statistically significant results, the seed regions would be defined based on the functional localiser data. In this case, the definition of the seed regions is independent of the main task. These seed regions include bilateral EBA and FBA for the body-localiser (Downing et al., 2007), and bilateral TPJ, bilateral temporal poles (TP), mPFC, and Precuneus for the ToM-localiser (Dodell-Feder et al., 2011).

CHAPTER 3

Linking person perception and person knowledge in the human brain

The study presented in the chapter examines whether the linking of traits to bodies works through a functional interaction between body-selective and Theory-of-Mind areas. All bodies were kept neutral and compared to names, which allows us to examine whether interaction is specific to the social agent of interest: bodies. By randomly pairing the social agents with trait-based or neutral information we further ensure that our results don’t reflect trait-inferences based on the body, but are driven by the behavioural descriptions presented. This is the first study to demonstrate functional links between perceptual and inferential networks during when observing bodies and simultaneously presented traits.

This chapter is published as it is in *Social Cognitive and Affective Neuroscience.*
DOI: 10.1093.scan.nsv148

Inez M. Greven, Paul E. Downing & Richard Ramsey
Wales Institute for Cognitive Neuroscience, School of Psychology, Bangor University,
Adeilad Brigantia, Penrallt Road, Bangor, Gwynedd, LL57 2AS Wales

Acknowledgements

The authors thank Andrew Fischer, Nia Goulden, Bronson Harry, Louise Kirsch, and Francesca Perini for providing scanning cover.

Abstract

Neuroscience research has examined separately how we detect human agents on the basis of their face and body (person perception) and how we reason about their thoughts, traits or intentions (person knowledge). Neuroanatomically distinct networks have been associated with person perception and person knowledge, but it remains unknown how multiple features of a person (e.g., thin and kind) are linked to form a holistic identity representation. In this fMRI experiment, we investigated the hypothesis that when encountering another person specialised person perception circuits would be functionally coupled with circuits involved in person knowledge. In a factorial design, we paired bodies or names with trait-based or neutral statements, and independent localiser scans identified body-selective and mentalizing networks. When observing a body paired with a trait-implying statement, functional connectivity analyses demonstrated that body-selective patches in bilateral fusiform gyri were functionally coupled with nodes of the mentalizing network. We demonstrate that when forming a representation of a person circuits for representing another person's physical appearance are linked to circuits that are engaged when reasoning about trait-based character. These data support the view that a "who" system for social cognition involves communication between perceptual and inferential mechanisms when forming a representation of another's identity.

Introduction

Appreciating the meaning of social interactions depends crucially on understanding others' identity. For example, one may react differently to an embrace offered from a romantic partner compared to a complete stranger. Attempts to understand the neurocognitive mechanisms that underpin identity processing have focused on two broad research topics: person perception and person knowledge. Person perception research investigates how sensory systems detect conspecifics in the environment on the basis of their face and body (Peelen and Downing, 2007), whereas person knowledge research investigates how inferential mechanisms represent others' mental states, such as beliefs, desires, and attitudes (Frith and Frith, 1999). However, little is currently known about the interaction between social perception and knowledge systems in the human brain. The current fMRI study uses functional connectivity analyses to investigate how distinct neural substrates are linked when perceiving and reasoning about others.

Human neuroimaging studies have provided clear evidence that the processes involved in person perception and person knowledge recruit distinct neural circuits (Adolphs, 2009). Fusiform gyri (FG) and occipitotemporal (OT) cortices respond more to the perception of social (faces and bodies) compared to non-social stimuli (Kanwisher et al., 1997; Downing et al., 2001; Spiridon et al., 2006), and the majority of evidence suggests that their contribution to understanding identity is restricted to the processing of physical appearance, such as facial features, body shape and posture (Downing and Peelen, 2011; Kanwisher, 2010). A distinct brain circuit comprising medial prefrontal cortex (mPFC), temporoparietal junction (TPJ), precuneus and temporal poles has been shown to respond when reasoning about others' thoughts as well as when making character judgments (Saxe and Kanwisher, 2003; Mitchell, 2009; Schiller et al., 2009; van Overwalle, 2009). The ability to draw inferences about underlying personal characteristics, such as whether someone is hardworking, honest, and friendly, also contributes to understanding another's identity (Ma et al., 2012; Macrae and Quadflieg, 2010).

Whilst it is clear that perceptual and inferential brain circuits contribute to forming an identity representation (Haxby et al., 2000; Mitchell et al., 2002; Todorov et al., 2007), and that trait information can be associated with a person's physical features, such as their face (Cloutier et al., 2011; Mende-Siedlecki et al., 2013), a fundamental question in neuroscience is how signals from such segregated neural systems are integrated (Friston et al., 2003). Indeed, how integration occurs between the neural representations of others' physical features and more elaborate cognitive processes remains unclear. For example, functional claims have been made regarding body-selective patches along the ventral visual stream that extend beyond visual analysis of body shape and posture, to include embodiment (Arzy et al., 2006), action goals (Marsh et al., 2010), and aesthetic perception (Calvo-Merino et al., 2010). However, the engagement of body-selective cortical patches in these more elaborate cognitive processes may, in part, index functional coupling within a distributed neural network, rather than local processing alone (Ramsey et al., 2011). Our primary focus in the current experiment, therefore, is to test the hypothesis that body patches along the ventral visual stream do not work alone when perceiving and reasoning about others, but interact with extended neural networks.

Prominent models of functional integration in the human brain involve distributed but reciprocally connected neural processing architectures (Mesulam, 1990; Fuster, 1997; Friston and Price, 2001). For example, extended brain networks involving forward and backward connections have been proposed for visual perception of faces (Fairhall and Ishai, 2007), bodies (Ewbank et al., 2011), and objects (Bar, 2004; Mechelli et al., 2004). Furthermore, when forming identity representations, person perception signals from posterior regions have been proposed to interact with person inference signals from a more anterior circuit (Haxby et al., 2000; Ramsey et al., 2011; Collins and Olson, 2014).

To date, however, there is little empirical evidence demonstrating interplay between brain systems for person perception and person knowledge. Thus, the current experiment investigates the hypothesis that the representation of identity comprises a distributed but connected set of brain circuits, spanning perceptual and inferential processes. To investigate this hypothesis, we collected functional imaging data while participants were observing two different depictions of an agent (bodies or names) paired with different types of social knowledge (trait-based or neutral). Participants were asked to form an impression of the people they observed. The manipulation of social knowledge replicated prior work that has compared descriptions of behaviour that imply specific traits to those where no trait-based inference can be made (Mitchell, 2009; Cloutier et al., 2011; Kuzmanovic et al., 2012; Ma et al., 2012). In addition, by including two forms of social agent, we are able to investigate the brain circuits that link person knowledge to a specific aspect of a person (physical bodily features), rather than other aspects of a person, which do not engage person perception neural networks, such as a name. By manipulating social agent stimuli and social knowledge information we test a model system of how person perception and person knowledge processes interact in the human brain. We hypothesise that brain circuits involved in person perception and person knowledge will show increased functional connectivity when seeing another person (rather than reading a name) and learning something about his or her trait-based character (rather than trait-neutral information). We expected such tuning to manifest in terms of 1) the magnitude of response observed in body-selective and ToM networks, and 2) the functional connectivity between these networks. This pattern of results would show that when trait inferences are linked to bodies, there is a functional connection between brain regions involved in the visual analysis of body shape and those that are involved in inferring trait inferences and attributing mental states more generally.

Materials and Methods

Participants

Twenty-three participants were recruited from the Bangor community and received a monetary reimbursement of £10. All participants had normal or correct-to-normal vision and reported no history of neurological damage. They gave informed consent according to the local ethics guidelines. One participant was excluded from data analysis because of a scanner malfunction whilst another was excluded due to difficulties understanding the task. The remaining 21 participants (13 females; mean ± SD age: 24.6 ± 5.7 years) were included in subsequent analyses. For 3 of these participants, 2 sessions from the main task had to be removed due to excessive head motion (displacement above 3 mm).

Stimuli and experimental procedure

Participants completed three tasks during scanning: the main experimental task, a body-localiser and a Theory-of-Mind (ToM) localiser (details of each task are provided below). Each participant's scanning session started with a run of the body-localiser (4.5 minutes), followed by two runs of the main task (6 minutes and 50 seconds each). This task sequence was then repeated a second time. The body-localiser was interspersed within runs of the main task to introduce a more varied experience for participants and offset boredom. Finally, participants completed two runs of the ToM-localiser (4.5 minutes each). The ToM-localiser was always presented after the main task, to ensure that participants were not primed towards making trait inferences during the main task. Stimuli were presented using a desktop PC and Matlab software with Psychtoolbox (www.psychtoolbox.org).

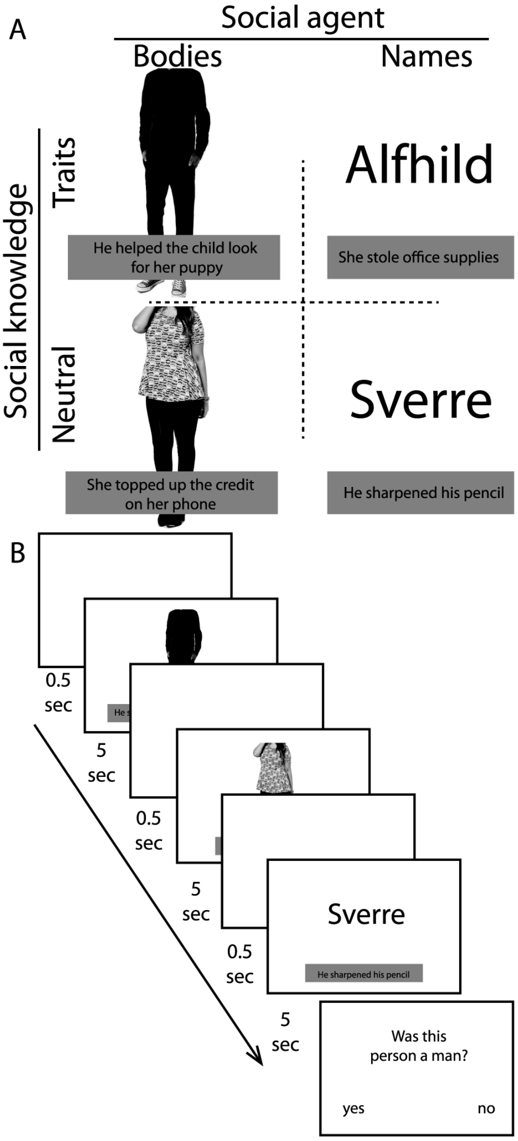

Figure 3.1. Design and presentation of the stimuli. **A)** A social agent (body or name) was paired with social knowledge (trait-based or neutral). **B)** In an event-related design, stimuli were presented for 5 s and separated by a fixation cross for 500 ms. Each block ended with a question about the last trial the participants saw.

Main experimental task: The main task comprised an event-related factorial design. In each trial, participants were presented concurrently with a social agent (body or name) and social knowledge (trait-based or neutral) (Figure 3.1). This resulted in four conditions: bodies paired with traits (BodiesTraits) or neutral statements (BodiesNeutral), and names paired with traits (NamesTraits) or neutral statements (NamesNeutral). For each participant, bodies and names were randomly assigned to the statements. Thus, there was no systematic relationship between particular bodies/names and statements across participants, which removes any coupling between low-level stimulus artefacts and any one condition in our design.

Each trial started with the presentation of a fixation cross for 500 ms, followed by the simultaneous presentation of an agent and a statement for 5 s. Participants were instructed to pay attention to both the person (body or name) as well as to the knowledge that they would receive about that person (trait or neutral). There were 256 trials within the entire experiment (64 per condition) that were spread over 4 separate functional runs of equal length. In each functional run, trials were presented in four segments containing a counterbalanced sequence of trials from all four experimental conditions. In order to help effectively model the influence of different events on BOLD signal, one can either introduce jitter between events, or counterbalance the conditions (Josephs and Henson, 1999). We counterbalanced the trial order so that within each segment, each condition was preceded equally often by all conditions (Wager and Nichols, 2003; Aguirre, 2007). To provide a completely balanced trial “history” across conditions, each segment of 16 trials began with a “starter trial”, which was not included in the data analysis. Subsequently, four further trials from each condition were presented in a counterbalanced manner. There was a 5 second rest period at the end of each segment.

To make sure participants paid attention to all aspects of the stimuli, at the end of each block they were asked a yes/no-question about the previous trial. Participants were given a response box, which they held with both hands. Within a maximum duration of 5 seconds, yes/no responses were made by pressing the left and right button, respectively. These questions could be about the agent's gender (was this person a man/woman?), body (was this person facing forward?), name (was there an a/o in this name?), as well as the person knowledge statements (did this person touch an object? did this person have a positive/negative attitude?). To ensure that participants remained alert to all elements of these stimuli, the content of questions could not be predicted. Accuracy was measured as the percentage of correct answers and compared to chance performance (50%) using 95% confidence intervals (CI.95; Cumming, 2014). Effect size was calculated using Cohen's d by dividing the mean difference from chance performance by the standard deviation pooled across conditions (Cohen, 1992; Lakens, 2013).

Social agent stimuli comprised images of bodies or names. The agent (body: full-colour picture, 300 x 750 pixels; name: black font colour, fontsize 60 pt) was presented in the middle of the screen with text (fontsize 30 pt) underneath (250 pixels below the centre of the screen). Pictures of 128 bodies (64 female) were selected that had an emotionally-neutral posture (i.e., crossed-arms or slouching postures were not included) but varied in terms of body shape, skin colour and clothing. Consistent with prior work (Downing et al., 2007), in order to target regions selective for images of bodies and not faces, images were cropped so the head was not visible. 128 Scandinavian names (64 female), such as Sverre and Alfhild, were selected to avoid associations with familiar names of people participants may know (Ma et al., 2012). Each body and name was only shown once during the entire experiment, to avoid any possible effects of combining the same person with different social knowledge statements over the course of the experiment.

Social knowledge stimuli comprised 128 statements that were adapted from Mitchell et al. (2006) to convey either trait-based (positive and negative) or neutral information. An example of a trait-implying statement is "He cut in front of the man in line", implying the person is inconsiderate, whereas a neutral example is "She walked through the swivel doors". Trait and neutral sentences did not differ (as tested with a paired-samples t-test) in the mean amount of words (t(63)=0.59, p=.56), nor in the amount of characters (t(63)=1.69, p=.09). Each statement (64 trait, 64 neutral) was presented twice during the experiment (once in female and once in male form; e.g., "She walked…" and "He walked…").

Functional localisers: To localise body-selective brain regions we used an established paradigm (Downing et al., 2007; http://pages.bangor.ac.uk/~pss811/page7/page7.html). We presented 12-sec blocks of cars and of whole bodies (without heads) that were not used in the main task. A run started with a blank screen for 14 seconds, followed by two alternations of each condition. This was repeated a second time, and followed by a final rest period of 14 seconds. Each image was presented for 600 ms, followed by a blank screen for 100 ms. Twice during each block, the same image was presented two times in a row. Participants had to press a button whenever they detected this immediate repetition (1-back task). The image location was slightly jittered (10 pixels around central fixation dot) to prevent participants from performing the 1-back task based on low-level after-effects from the previous image. Each participant completed two runs of this task, each with a complementary order of conditions (if run 1 started with bodies, run 2 would start with cars).

To localise brain regions that respond to mental state reasoning, we used an established ToM-localiser (Dodell-Feder et al., 2011; http://saxelab.mit.edu/superloc.php). Participants read 10 short false belief stories, in which the characters have false beliefs about the state of the world. Participants also read 10 false photograph stories, where a photograph, map, or sign has out-dated or misleading information. After reading each story, participants had to answer whether the subsequently presented statement was true or false. Each run started with a 12 second rest period, after which the stories and questions were presented for 14 seconds combined (stories: 10 seconds; questions: 4 seconds), and were separated by a 12 second rest period. The order of items and conditions is identical for each subject. In the first run, stimuli 1 – 5 from each condition were presented. The remaining stimuli were presented during the second run.

For both the body and ToM localiser, a design matrix was fitted for each participant with 3 regressors, two for each condition (bodies and cars; false beliefs and false photographs) and one for the rest periods. Body-selective regions were revealed by contrasting bodies and cars (Bodies > Cars). The ToM-network was revealed by contrasting false beliefs with false photographs (False Beliefs > False Photographs).

Data Acquisition

The experiment was conducted on a 3 Tesla scanner (Philips Achieva), equipped with an 8-channel SENSE-head coil. Stimuli were projected on a screen behind the scanner, which participants viewed via a mirror mounted on the head-coil. T2*-weighted functional images were acquired using a gradient-echo echo-planar imaging (EPI) sequence. An acquisition time of 2000 ms was used (image resolution: 3.03 x 3.03 x 4 mm^3, TE = 30, flip angle = 90°). After the functional runs were completed, a high-resolution T1-weighted structural image was acquired for each participant (voxel size = 1 x 1 x 1 mm^3, TE = 3.8 ms, flip angle = 8°, FoV = 288 × 232 × 175 mm^3). Four dummy scans (4 * 2000 ms) were routinely acquired at the start of each functional run and were excluded from analysis.

Data preprocessing and analysis

Data were preprocessed and analysed using SPM8 (Wellcome Trust Department of Cognitive Neurology, London, UK: www.fil.ion.ucl.ac.uk/spm/). Functional images were realigned, unwarped, corrected for slice timing, and normalized to the MNI template with a resolution of 3x3x3 mm and spatially smoothed using an 8 mm smoothing kernel. Head motion was examined for each functional run and a run was not analysed further if displacement across the scan exceeded 3 millimetres.

Univariate model and analysis: Each trial was modelled from the onset of the body/name and statement for a duration of 5 seconds. A design matrix was fitted for each participant with 6 regressors, one for each condition of the 2x2 factorial design (4 in total), one for the discarded starter trials and one for the question at the end of each block. Main effects of social agent (Bodies > Names: BodiesTraits + BodiesNeutral > NamesTraits + NamesNeutral) and social knowledge (Traits > Neutral: BodiesTraits + NamesTraits > BodiesNeutral + NamesNeutral) were evaluated to help demonstrate that our task engaged body-selective and ToM areas, respectively. We also evaluated the interaction of bodies and trait information to test our primary hypothesis [(BodiesTraits > BodiesNeutral) > (NamesTraits > NamesNeutral)].

Response magnitude analyses: To test the magnitude-based prediction, we calculated which brain regions showed a greater response for trait inferences (Traits > Neutral) when observing a body compared to reading a name. Two possible forms of interaction are predicted: 1) the effect of social knowledge (Traits > Neutral) will be present for both social agents, but be greater for bodies than names; 2) the effect of social knowledge (Traits > Neutral) will be present for bodies, but not names. To help distinguish among possible interaction patterns, we exclusively mask our interaction result by (NamesNeutral > NamesTraits). Exclusive masking in this manner makes sure that any interaction result is not produced by an unpredicted preference for neutral over trait-based information when paired with names.

Psychophysiological Interaction analysis: To test our hypothesis that body-selective cortical regions functionally couple with regions associated with mentalizing when one sees a body and also infers a trait from it, we assessed the relationship between these regions using a psychophysiological interaction (PPI) analysis (Friston et al., 1997). PPI enables the identification of brain regions whose activity correlates with the activity of a seed region as a function of a task. Here we used a generalized form of PPI, which allows for comparisons across the complete design space, including more than two conditions (McLaren et al., 2012). By doing so, it is possible to see whether any voxels across the brain show a correlation with activity in the seed region (the “physiological” element) as a function of the four conditions within the main task (the “psychological” element).

Our hypothesis was that the same parts of the person perception and person knowledge networks, which show a magnitude-based sensitivity to observing others and inferring traits (revealed in the univariate interaction analysis), would also show functional coupling with each other. As such, seed regions for the PPI analysis were defined based on results from the univariate analysis. Two steps were taken to define seed regions (Figure 3.2.A.). First, based on the group-level random-effects univariate analysis, we identified any clusters of overlap between 1) regions in which the type of social agent and social knowledge interacted in the predicted way (in the main experiment) and 2) either body-selective or ToM-selective regions as identified in the functional localisers. Second, where such clusters of overlap were identified at the group-level, we identified regions of overlap using the same approach in each individual participant. This approach allows us to identify with best possible resolution the key regions where these two phenomena concur. Therefore, regions identified in this manner respond to one of the localisers (Body or ToM), as well as the interaction term in the main task.

In the analyses performed at the single-subject level, we searched for overlap across a range of thresholds, which is common when identifying seed regions in individual’s data (Spunt and Lieberman, 2012; Klapper et al., 2014; Paulus et al., 2015). For each seed region, therefore, we report how many participants show overlap between the interaction term in the main task (across a range of thresholds) and functional localisers at a fixed threshold ($p<.005$, $k=10$). Volumes were generated using a 6 mm sphere, which were positioned on each individual’s seed-region peak.

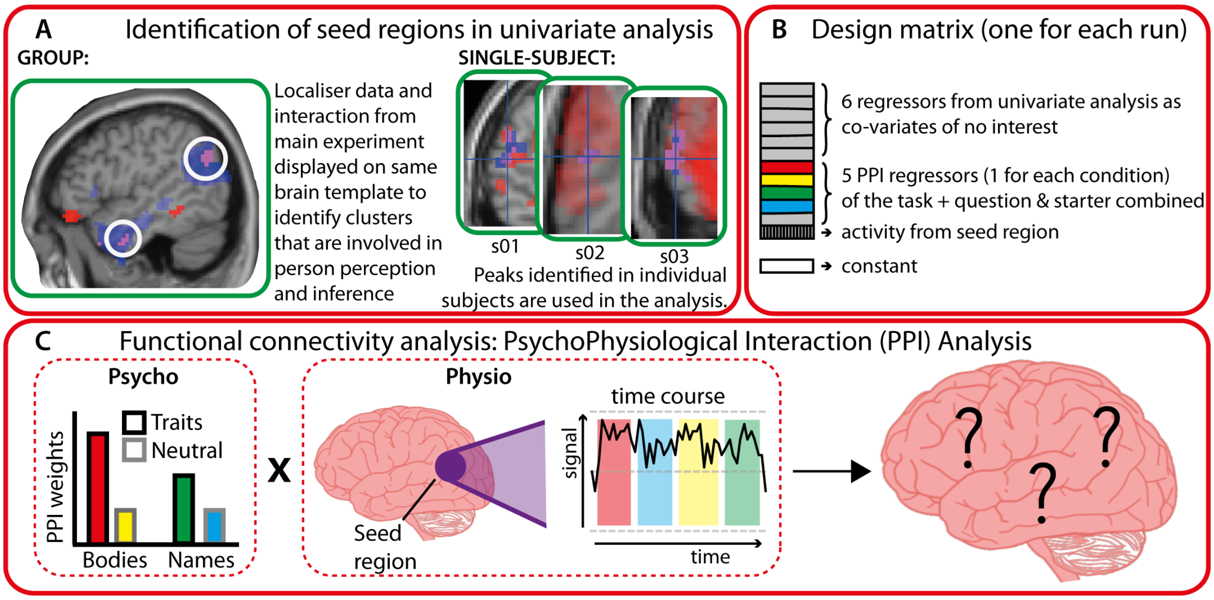

Figure 3.2. Flow chart illustrating the steps to define seed regions and run PsychoPhysiological Interactions (PPI) analyses. **A)** Identification of seed regions in the univariate analysis was done at group and single-subject level to allow for inter-individual differences in peak responses. **B)** An illustration of the design matrix (this was the same for each run), that was created for each participant. **C)** The "psychological" (task) and "physiological" (time course from seed region) inputs for the PPI analysis.

PPI analyses were run for all seed regions that were identified in each participant. PPI models included the 6 regressors from the univariate analyses, as well as 6 PPI regressors, one for each of the four conditions of the factorial design, one for the starter trial and question combined, and one that modelled seed region activity. Although we used clusters emerging from the univariate analysis to define seed regions for the PPI analysis, our PPI analysis is not circular (Kriegeskorte et al., 2009). Because all regressors from the univariate analysis are included within the PPI model as covariates of no interest (O'Reilly et al., 2012), the PPI analyses are only sensitive to variance in addition to that which is already explained by other regressors in the design (Figure 3.2.B.). Thus, the PPI analysis is statistically independent to the univariate analysis. Consequently, if clusters were only co-active as a function of the interaction term from the univariate task regressors, then we would not show any results using the PPI interaction term. Any correlations observed between a seed region and a resulting cluster explains variance above and beyond task-based activity as measured using a standard univariate General Linear Model (GLM).

To create these PPI regressors, the time series in the seed region was specified as the first eigenvariate, and was consequently deconvolved to estimate the underlying neural activity (Gitelman et al., 2003). Then, the deconvolved time series was multiplied by the predicted, pre-convolved time series of each of the five conditions (4 main task conditions plus the combined starter trial and question regressor). The resulting PPI for each condition in terms of predicted "neural" activity was then convolved with the canonical haemodynamic response function (HRF), and the time series of the seed region was included as a covariate of no interest (McLaren et al., 2012; Spunt and Lieberman, 2012; Klapper et al., 2014). At the second-level analysis, we examined the same social agent*social knowledge interaction term as described in the univariate analyses [(BodiesTraits > BodiesNeutral)>(NamesTraits > NamesNeutral)].

Names and neutral statements functioned as control conditions within our design. As such, names and neutral statements were included to allow comparisons to bodies and trait-diagnostic statements, and not because we had predictions for how names or neutral information are represented in terms of neural systems (see Discussion for more details). Consequently, the (Names > Bodies), (Neutral > Trait) and inverse interaction [(NamesTraits > NamesNeutral) > (BodiesTraits > BodiesNeutral)] contrasts did not address our main research question. Such contrasts, however, may be useful in future meta-analyses and we therefore report results from these contrasts in Appendix 1.

For all group-level analyses (univariate and connectivity-based), images were thresholded using a voxel-level threshold of p<.005 and a voxel-extent of 10 voxels (Lieberman and Cunningham, 2009). Based on our hypotheses for functional connections between person perception and person knowledge networks, contrasts from the main task were inclusively masked by the results from the functional localiser contrasts. The results from these analyses are presented in Table 3.1 and Table 3.2. Results that survive correction for multiple comparisons at the cluster level (Friston et al., 1994) using a family-wise error (FWE) correction (p<.05) are shown in bold font. To localise functional responses we used the anatomy toolbox (Eickhoff et al., 2005).

Results

Behavioural data

During the main task, participants' accuracy was assessed in order to see whether they had been paying attention to the task. Accuracy (percentage correct) in answering the yes/no-questions at the end of each block was above chance-level (M=87.2, CI.95 [82.75, 91.65], Cohen's d_z=3.81).

Neuroimaging data

Univariate analyses

Main effects: There was a main effect of social agent (Bodies > Names; Figure 3.3.A) in bilateral occipitotemporal cortices (overlapping with Extrastriate Body Area (EBA) and surviving FWE cluster correction) and bilateral fusiform gyri (overlapping with Fusiform Body Area (FBA) and surviving FWE cluster correction). There was also a main effect of social knowledge (Traits > Neutral; Figure 3.3.B) in mPFC, bilateral temporal poles, precuneus, and left TPJ, all of which overlapped with the ToM-localiser. The inverse contrasts for both main effects (Names > Bodies and Neutral > Trait) are reported in Appendix 1.

Interaction: For the interaction between social agent and social knowledge [(BodiesTraits > BodiesNeutral) > (NamesTraits > NamesNeutral)] clusters emerged in left TPJ, mPFC, and left temporal pole and all of these clusters overlapped with the ToM-localiser at the group-level (Table 3.1; Figure 3.3.C). The parameter estimates illustrate a greater difference between trait and neutral statements when bodies rather than names are presented. More specifically, the effect of social knowledge (Traits > Neutral) is present for both social agents, but it is greater for bodies than names. These results demonstrate that brain regions defined by being engaged in reasoning about others' mental states (social knowledge) emerge for the interaction term of the main task.

We also predicted that the person perception network would be engaged for the same interaction analysis, but we did not find this pattern of response at the initial threshold. To further explore this null result in EBA and FBA, we investigated the interaction term in body-selective regions at a more liberal threshold (p<.05, k=10). Using this less conservative threshold, right fusiform gyrus (FG) showed the predicted interaction pattern and this cluster overlapped with the body-localiser (Appendix 2 and Appendix Figure 1). In addition, there was a response in left middle temporal gyrus, but the location of this response was superior (z =19) to the typical location of EBA or FBA. Due to the chance of the univariate response in right FG being a false positive, any interpretation is necessarily cautious. However, the main reason for performing the univariate interaction analysis was to identify seed regions that can be used subsequently to test our primary hypothesis using functional connectivity analyses. If the result in right FG is a false positive and it does not reflect the linking of body and trait information, then we should expect no functional coupling between right FG and the ToM-network in the functional connectivity analyses. The inverse interaction contrast [(NamesTraits > NamesNeutral) > (BodiesTraits > BodiesNeutral)] is reported in Appendix 1.

Table 3.1. Results from the univariate analysis. The main effect of social agent (Bodies > Names) is masked by the body-localiser (Bodies > Cars); the main effect of social knowledge (Traits > Neutral) is masked by the ToM-localiser (False Beliefs > False Photographs); the social agent by social knowledge interaction [(BodiesTraits > BodiesNeutral) > (NamesTraits > NamesNeutral)] is masked by both the body and ToM localiser.

Region	Number of voxels	*T*	Montreal Neurological Institute coordinates		
			x	y	z
a) Main effect Social Agent: Bodies > Names					
Left occipitotemporal cortex	**498**	**11.12**	**-45**	**-82**	**-2**
		6.26	**-51**	**-70**	**16**
Right occipitotemporal cortex	**970**	**10.60**	**45**	**-82**	**-2**
extending into fusiform gyrus		**10.50**	**54**	**-70**	**4**
		9.92	**45**	**-76**	**10**
Left hippocampus	50	9.68	-18	-31	-5
Right hippocampus	100	9.01	18	-31	-2
Right inferior temporal gyrus	173	7.23	33	-4	-44
		5.87	30	-4	-35
		5.59	24	-4	-23
Right inferior frontal gyrus	37	6.87	48	35	4
Right cuneus	60	5.64	21	-79	43
		4.74	21	-61	58
Right inferior frontal gyrus	16	5.60	24	17	-26
Right calcarine gyrus	11	5.41	21	-94	22
Left fusiform gyrus	83	5.31	-39	-49	-26
		4.74	-36	-37	-29
		4.55	-39	-37	-20

Striatum	27	5.27	3	11	-17
Right inferior frontal gyrus	10	3.95	45	29	13
Left cerebellum	10	3.90	-9	-55	-50
b) Main effect Social Knowledge: Traits > Neutral					
Left temporal pole	**698**	**11.43**	**-51**	**11**	**-26**
		10.08	**-54**	**-1**	**-23**
		9.23	**-45**	**26**	**-14**
Right temporal pole	**510**	**10.88**	**51**	**11**	**-35**
		8.68	**60**	**-4**	**-20**
		7.63	**51**	**-13**	**-20**
Left medial prefrontal cortex (mPFC)	442	6.84	-3	53	31
		6.01	-12	53	43
		4.99	6	65	13
Left inferior frontal gyrus	68	6.40	-51	20	7
		5.52	-57	23	19
Right cerebellum	120	5.71	24	-82	-38
Left temporoparietal junction (TPJ)	211	5.06	-60	-58	19
		3.91	-48	-58	22
Right medial cerebellum	33	5.00	3	-58	-50
Right inferior frontal gyrus	46	4.97	48	23	-14
		4.49	60	26	7
Precuneus	101	4.74	-3	-52	28
		3.87	-3	-61	34
c) Interaction: Social agent * knowledge [(BodiesTraits > BodiesNeutral) > (NamesTraits > NamesNeutral)]					
Left temporal pole	24	4.16	-51	-1	-35
Right superior mPFC	33	4.04	9	50	28
Left superior mPFC	12	3.53	-9	32	55
Left TPJ	15	3.48	-48	-64	31

Note: Regions surviving a voxel-level threshold of $p<.005$ and 10 voxels are reported. Areas in bold survive FWE cluster correction for multiple comparisons. Subclusters at least 8 mm from the main peak are listed. The social agent by social knowledge interaction is exclusively masked by the NamesNeutral > NamesTraits contrast to make sure that any interaction result does not include (Neutral > Traits) when paired with names.

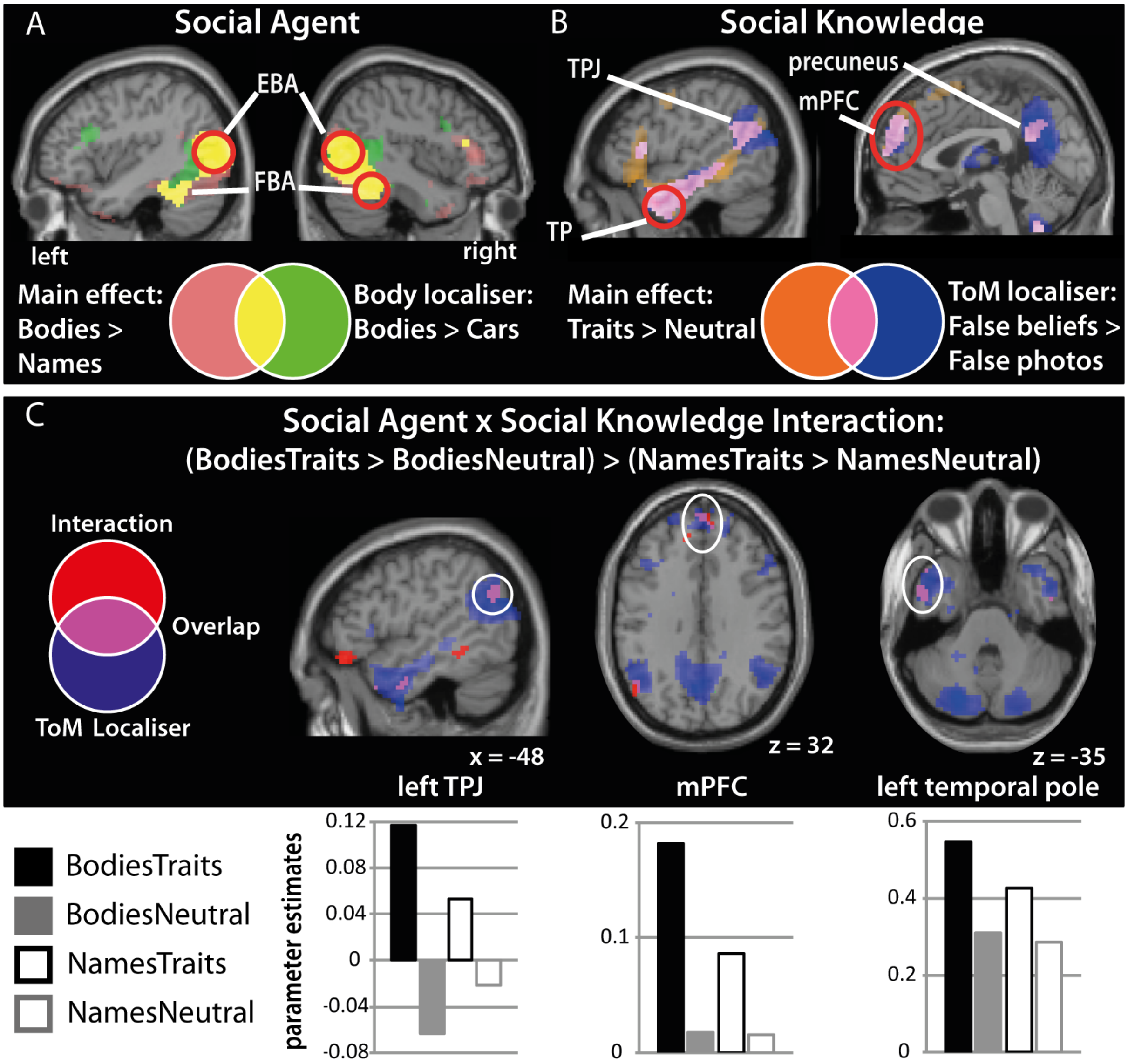

Figure 3.3. Results from the univariate analysis. **A)** The main effect of Social Agent (Bodies > Names) revealed clusters of activity in bilateral occipitotemporal cortices and bilateral fusiform gyri. The clusters overlapped with the extrastriate body area (EBA) and fusiform body area (FBA) as identified with the body-localiser (Bodies > Cars: green). Overlap is shown in yellow. **B)** The main effect for Social Knowledge (Traits > Neutral) revealed clusters of activity in medial prefrontal cortex (mPFC), bilateral temporal poles, precuneus and left temporoparietal junction (TPJ). These clusters overlapped with the ToM-network as identified with the ToM-localiser (False Beliefs > False Photographs: blue). Overlap is shown in pink. **C)** The Social Agent by Social Knowledge interaction ([BodiesTraits > BodiesNames] > [NamesTraits > NamesNeutral]) revealed a clusters in mPFC, left temporal pole, and left TPJ, which overlapped with the ToM-localiser (overlap is shown in pink). Parameter estimates were extracted from a 4 mm sphere around the peak coordinate.

Psychophysiological Interaction analyses: Coordinates of overlap within individual participants were identified in left TPJ (n=17), mPFC (n=17), left temporal pole (n=15), and right FG (n=19) (for more details, see Appendix 3). Our prediction was that person perception and person knowledge networks would show coupling as a function of our task. To test this prediction, for each seed region separately, we used the same interaction term for our PPI analysis as was previously used in the univariate analysis [(BodiesTraits > BodiesNeutral) > (NamesTraits > NamesNeutral)].

Both right fusiform gyrus and left temporal pole showed the predicted pattern of functional coupling with person perception or knowledge networks (Table 3.2; Figure 3.4). Figure 3.4.A shows that the response in left TPJ and bilateral temporal pole has greater functional coupling with right FG when social knowledge (Trait > Neutral) is present for bodies, but not names. Additionally, these clusters all overlapped with the ToM-localiser. As such, there is overlap between the clusters that show coupling with right FG when inferring a trait about a body and when reasoning more generally about others' mental states.

In addition, left temporal pole showed greater functional coupling with a region of left fusiform gyrus when social knowledge (Trait > Neutral) is present for bodies, but not names (Figure 3.4.B). Furthermore, this cluster in left fusiform gyrus overlapped with the body-localiser. As such, there is overlap between a cluster that shows coupling with left temporal pole when inferring a trait about a body and when perceiving bodies in general.

Table 3.2. Clusters revealed in the PsychoPhysiological Interaction (PPI) analysis for the social agent by social knowledge interaction [(BodiesTraits > BodiesNeutral) > (NamesTraits > NamesNeutral)], which is masked by both the body and ToM localiser.

Region	Number of voxels	*T*	Montreal Neurological Institute coordinates		
			x	y	z
Seed region: right fusiform gyrus					
Right temporal pole	11	4.23	51	11	-38
Left temporoparietal junction (TPJ)	17	3.79	-60	-52	19
		2.98	-60	-46	19
Left temporal pole	14	3.75	-45	20	-23
		3.28	-45	17	-32
Left temporal pole	12	3.53	-33	5	-26
		2.63	-42	2	-26
Seed region: left temporal pole					
Left fusiform gyrus	11	4.05	-45	-49	-26

Note: Regions surviving a voxel-level threshold of p<.005 and 10 voxels are reported. Subclusters at least 8 mm from the main peak are listed. These results are exclusively masked by the NamesNeutral > NamesTraits PPI contrast to make sure that any interaction result does not include (Neutral > Traits) when paired with names.

The other seed regions, left TPJ and mPFC, did not show the predicted pattern of functional coupling with person perception networks. Therefore, the pattern of functional coupling observed between person perception and person knowledge networks when linking a trait to a body is not a general one that applies to every region within these two networks; instead, it is specifically tied to bilateral FG and parts of the ToM-network (left TPJ and bilateral temporal poles).

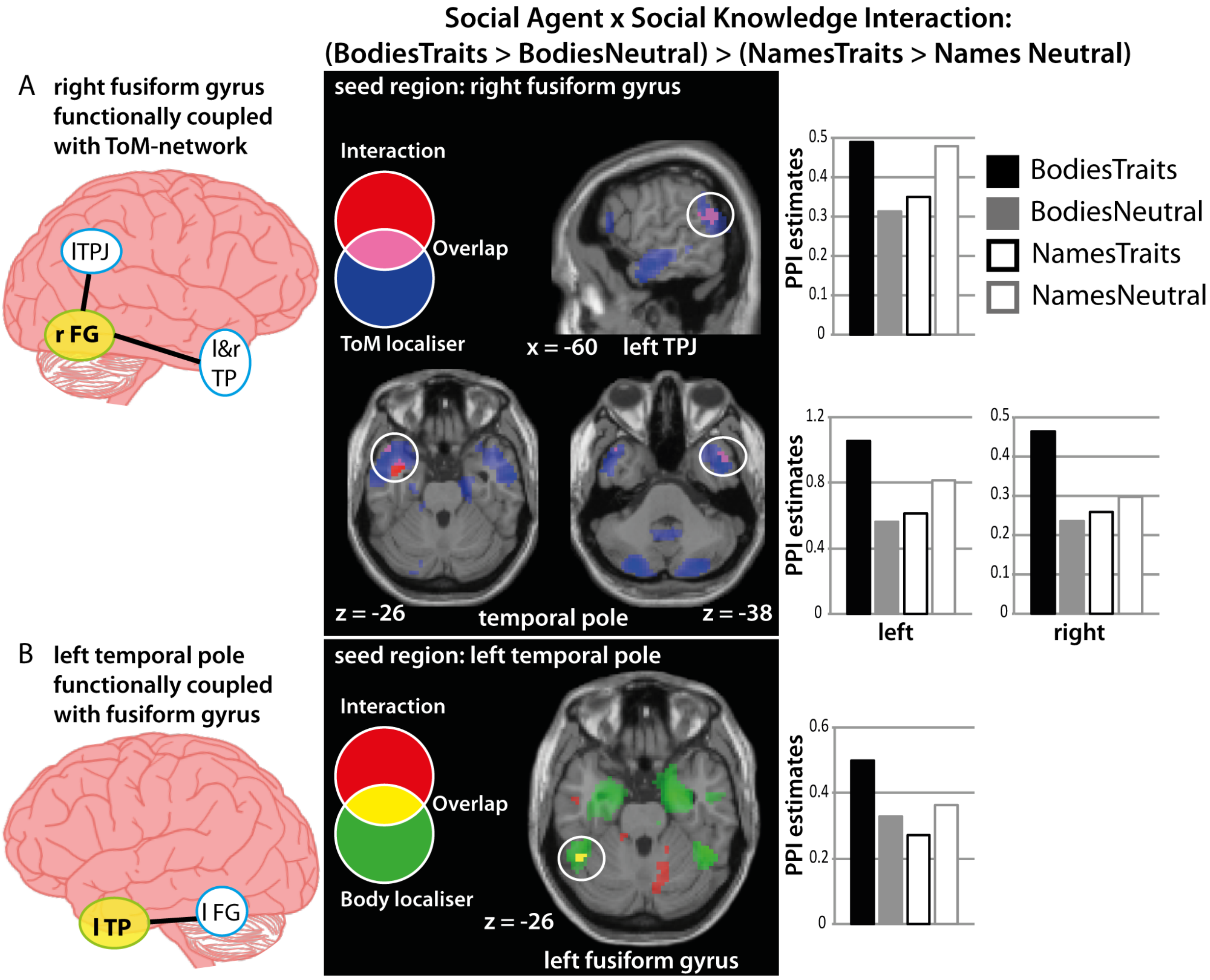

Figure 3.4. Results from the PsychoPhysiological Interaction (PPI) analysis. Seed regions were identified based on clusters emerging from the social agent by social knowledge interaction at the univariate level (including right fusiform gyrus – see supplementary table 1). These regions were either part of the person perception network (right fusiform gyrus) or person knowledge network (medial prefrontal gyrus (mPFC), left temporal pole (TP) and left temporoparietal junction (TPJ)) as defined by body and ToM localisers, respectively. In four separate PPI analyses, each identified region from the univariate analysis was used as a seed region with the social agent by social knowledge interaction term as the contrast of interest. Clusters emerging from these analyses reveal the strength of correlation over time between activity in that cluster and that in the seed region as a function of the task. These PPI parameter estimates are extracted from a 4 mm sphere around the peak coordinate. **A)** PPI analyses revealed that seed region right fusiform gyrus (solid yellow circle) showed functional coupling with nodes within the person knowledge network. Clusters in left temporoparietal junction and bilateral temporal pole showed greater functional coupling with right FG when inferring traits about bodies than names (shown in red). These areas overlapped with the ToM-localiser (shown in blue; overlap is shown in pink). **B)** PPI analyses revealed that seed region left temporal pole (solid yellow circle) showed functional coupling with left FG (shown in red). This area overlapped with the body-localiser (shown in green; overlap shown in yellow).

Discussion

When being introduced to someone, one forms an impression based on what you've heard about her character (e.g., "She volunteers in a hospital") as well as her physical appearance (e.g., tall and thin). Although much research has investigated the neural circuits involved in perceiving what another person looks like (person perception), as well as what one knows about that person (person knowledge), it is unclear how the human brain links these different pieces of information about a person's identity together. We demonstrate that anatomically and functionally distinct brain circuits exchange signals during the formation of identity representation. Specifically, brain circuits that represent aspects of another person's physical appearance, such as body shape and posture, are linked to brain circuits that engage when reasoning about another person's trait-based character, such as whether they are friendly, helpful or generous. These data support the view that a "who" system for social cognition spans perceptual and inferential mechanisms and that these mechanisms communicate to each other when forming a representation of another's identity.

Limitations and future directions

From our results we cannot infer whether the observed functional connectivity profile is tied to a particular person (i.e., person-specific) in addition to being tied to a particular form (i.e., body more than name). Given the trial-unique combinations of social agents and social knowledge, it is plausible that the results reflect person-specific representations. However, from our results alone, we cannot rule out the possibility that our results solely reflect a more generic category-level representation (i.e., body more than name). In addition, previous research has shown that mPFC is sensitive to person-specific information (Hassabis et al., 2014; Welborn and Lieberman, 2014). Future work, therefore, could adapt the methods developed here to directly test the degree to which person perception and knowledge networks interact at different levels of person-specificity.

One possible limitation to our interpretation relates to the familiarity of names that we used, which prior work has investigated (Sugiura et al., 2006). All names in the current study were unfamiliar to participants and as such it could have been more difficult to assign social knowledge to names than bodies. However, this difference is unlikely to explain our results for two reasons. Our main findings involve an interaction between agent and knowledge. Therefore, a greater difficulty assigning knowledge to names in general would apply to both types of knowledge (trait-based and neutral), rather than being preferentially tied to trait-based judgments more than neutral judgements. In addition, by using functional localisers, it becomes more difficult for a difference in difficulty alone to explain why body-selective patches were linked to the person knowledge network, unless body-selective areas are also involved for difficult of processing per se.

We also acknowledge limits to our methodology and design, which future work can build upon. First, functional connectivity analyses provide no direct insight into the underlying neural pathway that controls functional coupling between brain areas. As such, using measures of structural connectivity, it would be valuable for future research to investigate the neural pathways that underlie functional relationships between person perception and person knowledge systems. Second, it is conceptually possible that trait information is linked to names through functional links between the ToM-network and a neural representation of names. For instance, there may be functional links between ToM areas and a brain area processing words, such as the Visual Word Form Area (VWFA; Szwed et al. 2011). However, we do not have the same grounds for hypothesising links between the ToM-network and a "name" system, as we do for links with body patches. In contrast to EBA and FBA, which show category-selectivity for bodies, there is no evidence that the VWFA, or any other set of brain regions, shows the same category-selectivity for names (more than other words). In addition, we did not design the study to test for neural links between the ToM-network and a neural representation of names. To do so, we would have needed a relevant localiser in order to accurately locate the VWFA, for example, in each individual participant (Glezer and Riesenhuber, 2013). The current study, therefore, was not designed to address neural links between the representation of names and traits. These caveats aside, the interaction contrast that tests for clusters showing a greater response for trait inferences (Traits > Neutral) when reading a name compared to observing a body, showed no engagement of ToM-network or any clusters with coordinates near VWFA (Supplementary Table 1C). As such, the limited evidence we do have from the current study regarding this issue is not consistent with neural links between the ToM-network and the VWFA, but much more work is needed to pursue this line of research directly.

Implications for neural circuits subserving person perception and person knowledge

Coupling of functional responses between distinct brain circuits suggests that person perception and person knowledge networks are not completely encapsulated and resistant to influence from other brain systems. Downing and Peelen (2011) proposed that the primary function of EBA and FBA is to perform a visual analysis of bodies, but that these regions also exchange signals with other brain circuits. The current study, as well as others (Ewbank et al., 2011; Quadflieg et al., 2011; Zimmermann et al., 2013), are beginning to provide empirical support for this view by demonstrating that interactions between neural systems that are part of a broader cognitive landscape may upregulate or downregulate the response in body-selective cortex.

Linking person perception and person knowledge during social interactions

Neuroimaging research has identified patches of cortex selective for the perception of faces, bodies, and places as well as for thinking about other people's thoughts (Downing et al., 2001; Spiridon et al., 2006; Kanwisher, 2010). While these data have provided evidence for functional segregation within the human brain, it has not been clearly established how neural signals across multiple sites are integrated (Friston and Price, 2001; Friston et al., 2003). In the current experiment, we show that perceptual signals in the ventral visual stream are linked with inferential signals in the ToM-network. Specifically, we show that parts of the fusiform gyri, which are involved in processing body shape and posture (Downing and Peelen, 2011), exchange signals with TPJ and temporal poles, which form part of a circuit that is involved in making inferences about others' thoughts and traits (Frith & Frith, 1999; Saxe and Kanwisher, 2003; Mitchell, 2009; Van Overwalle, 2009). Moreover, we show that this exchange of signals is specifically tuned to situations when one is confronted with a combination of information that is relevant for both person perception and person knowledge networks (i.e., bodies, not names; traits, not neutral statements). As such, the pattern of functional connectivity is not generic to any form of social agent, such as someone we may read about in a novel; instead, it is tuned to an inference that is coupled to a body more than a name. On a broader level, these results provide empirical evidence to support the view that a "who" system for social cognition, which establishes and maintains a global representation of another's identity, comprises category-specific brain circuits that exchange signals (Haxby et al. 2000; Collins and Olson 2014; Ramsey et al. 2011; Ishai 2008; Moeller et al. 2008).

CHAPTER 4

Neural networks supporting social evaluation of bodies based on body shape

While in the previous chapter all the trait inferences came from the behavioural descriptions, in this chapter we wanted to investigate how social signals are extracted from the body based on differing shapes. Across two behavioural pilot experiments we selected a range of bodies that cued different social inferences based on three body-types: slim, muscular, and obese. By giving participants a purely perceptual task in the scanner, any trait inferences made would be task-independent and spontaneous.

Inez M. Greven, Paul E. Downing & Richard Ramsey
Wales Institute for Cognitive Neuroscience, School of Psychology, Bangor University,
Bangor, Gwynedd, Wales, LL57 2AS, United Kingdom

Acknowledgements
The authors thank Emily Butler, Dace Apšvalka, Louise Kirsch, Leah Johnstone, and David Carey for providing scanning cover.

Abstract

To date, neuroimaging studies have focused on characterising the function of segregated patches of cortex along the ventral visual stream during person perception. It remains largely unknown, however, how “body patches” in the ventral visual stream functionally couple with other brain regions during the visual detection of social signals. Using fMRI and functional connectivity analyses, we investigated the hypothesis that spontaneous social inferences based on body shape would involve functional interplay between the ventral visual stream and the Theory-of-Mind (ToM) network. Participants were presented with bodies selected to cue different social inferences. When comparing bodies that cue a salient social inference (muscular or overweight) to neutral bodies (slim), univariate analyses showed weak evidence for greater engagement of the left extrastriate body area and no evidence of activity within the ToM-network. Additionally, functional connectivity analyses showed no evidence for coupling between body patches and the ToM-network. Therefore, while the stimuli in this experiment were selected to cue different social judgments, we did not find any evidence that visually processing these bodies requires interplay between person perception and person knowledge neural networks. These results suggest that during passive observation (i.e., when intentional impression formation is not required), there is no interplay between body patches and the ToM-network, or such interplay is too subtle to detect using the present design. Future research should test this possibility by requiring participants to intentionally form an impression whilst observing similar body shapes.

Introduction

Social inferences are readily made based on body shape and posture. For instance, emotional states can be perceived from body posture (de Gelder, 2006), while health and personality judgments can be made based on body shape (Puhl and Heuer, 2009; Carels and Musher-Eizenman, 2010). Although social signals that guide behaviour can easily be recognised from physical features of others' bodies, the underlying neural architecture that underpins such social evaluations is far from clear. Using fMRI and functional connectivity analyses, the current study investigates how distinct brain circuits interact when social inferences are made from body shape.

Based on Bruce and Young's (1986) cognitive model of face perception, Haxby and colleagues proposed a neural model for person perception, which divided processes into core and extended systems (Haxby et al., 2000). The primary function of the core system is to detect physical features (face and body parts), while the extended system is engaged in additional processes relevant for person recognition such as attention, emotion and memory. Neuroimaging research to date has provided support for this model by demonstrating that patches of cortex along the ventral visual stream show selectivity for images of faces and bodies compared to non-social categories such as houses and cars (Kanwisher, 2010; Downing and Peelen, 2011). In addition, the extended network has been shown to span the amygdala, medial prefrontal cortex, dorsal frontoparietal systems and temporal poles (Ishai, 2008; Mende-Siedlecki et al., 2013; Collins and Olson, 2014). As such, brain regions within and beyond the ventral visual stream are engaged when recognising others and together they form a distributed neural network for person perception (Haxby et al., 2000).

As these prior studies demonstrate, there is compelling evidence for functional segregation in the neural architecture supporting person perception. However, less is known about functional integration between these anatomically distinct brain circuits. Interplay between discrete brain circuits is a growing consideration for understanding brain function (Sporns et al., 2005) and a fundamental question in neuroscience research is how signals from segregated neural systems are integrated (Friston et al., 2003). To date, research investigating functional integration in person perception has largely focussed on face recognition (Mechelli et al., 2004; Fairhall and Ishai, 2007; He et al., 2015; Hermann et al., 2015). These studies demonstrate that core and extended systems for person perception exchange signals as a function of facial information content (Ishai, 2008). However, bodies as well as faces can be used for person recognition, i.e. human identity processing (O'Toole et al., 2011; Rice et al.,

2013) and to make social inferences (de Gelder et al., 2010). For instance, particular body shapes (e.g., strong upper body: Sell et al. 2009; height: Stulp et al. 2015) and postures (Borkenau and Liebler, 1992; Naumann et al., 2009) cue judgments of health and personality. Moreover, in some social contexts, such as moments of intense joy, bodies offer unique social signals, which faces may hide (Aviezer et al., 2012). Whilst it is evident that social inferences are drawn from bodies, the underlying cognitive and neural architecture that supports such evaluations is still unclear.

Many proposals have suggested that detecting social information from bodies involves a distributed neural network, in a similar manner to face perception (de Gelder et al., 2010; Quadflieg and Rossion, 2011; Ramsey et al., 2011). To date, however, research that investigates how patches of cortex exchange signals during body perception is limited to a few studies (Figure 4.1). Neuroimaging research has shown functional coupling within core body perception nodes situated along the ventral visual stream (i.e., between fusiform and extrastriate body areas; FBA and EBA, respectively). Ewbank and colleagues suggest that as FBA may hold a more holistic representation of bodies (Peelen and Downing, 2007; Taylor et al., 2007), this information could help EBA to predict what a person’s body parts would look like from a different angle. Functional coupling has also been shown between core and extended networks in body perception (Quadflieg et al., 2011; Zimmermann et al., 2013; Greven et al., 2016). For instance, body patches link with dorsolateral prefrontal cortex (DLPFC) when making social judgments about bodies in stereotype-inconsistent contexts, such as a male nurse (Quadflieg et al., 2011). This suggests that DLPFC may modulate neural responses along the ventral visual stream during person perception (Baldauf and Desimone, 2014). In addition, brain regions associated with theory-of-mind (ToM) show stronger functional coupling with body-selective patches when observing a body and making a trait-based inference about the person compared to a neutral statement (Greven et al., 2016). Together, these initial functional connectivity studies of body perception provide empirical support for the view that a “who” system for social cognition involves functional interactions between distributed neural networks (Haxby et al., 2000), both within neural structures along the ventral visual stream, as well as with extended networks.

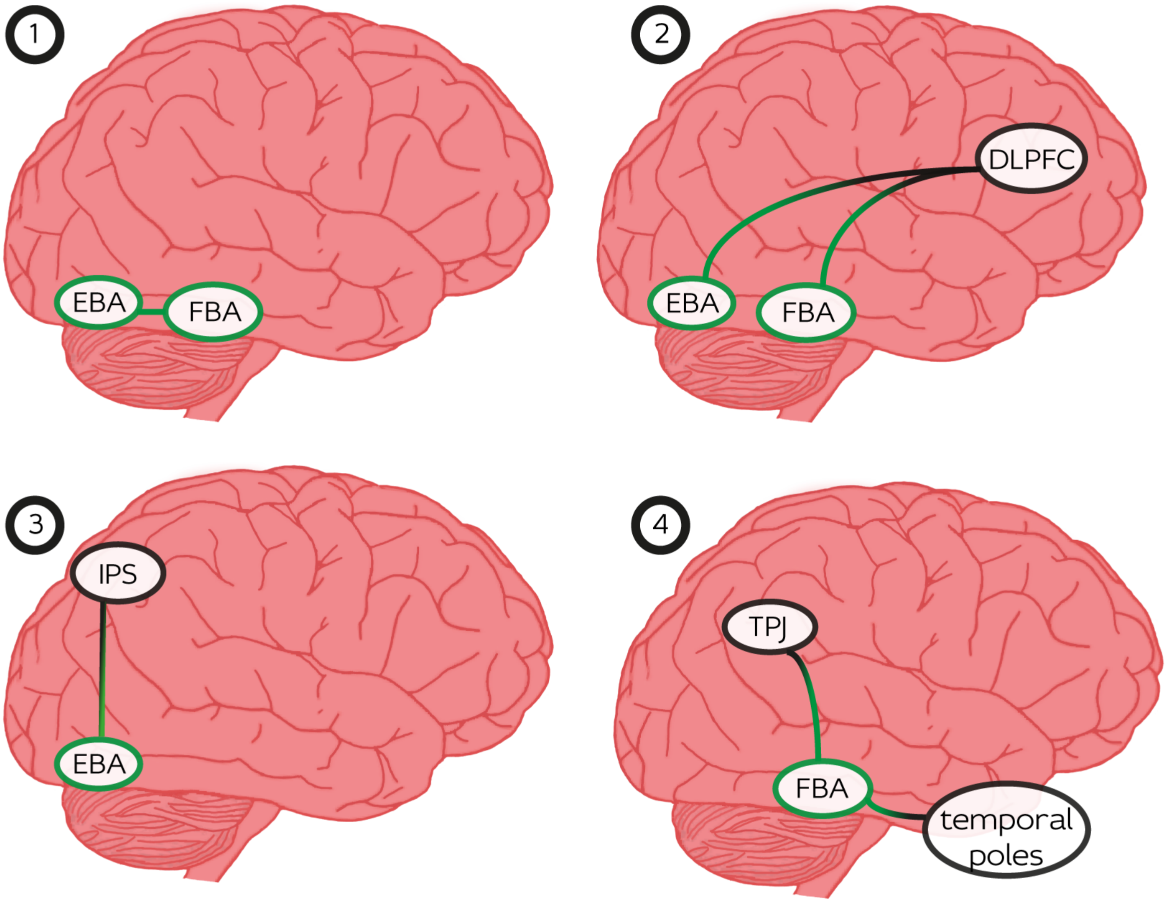

Figure 4.1. Evidence for effective and functional connectivity during body perception. Body network is presented in green, extended networks are presented in black. **1)** In Ewbank et al. (2011) blocks of bodies were presented that had the same or different identities. When a block of the same identity is presented, extrastriate and fusiform body areas (EBA and FBA, respectively) interact with each other. **2)** In Quadflieg et al. (2011) participants observed people in outfits that were consistent or inconsistent with gender stereotypes. When performing a sex categorization task, dorsolateral prefrontal cortex interacted with bilateral EBA and right FBA when the person's outfit was inconsistent with the gender stereotype. **3)** In Zimmerman et al. (2013) participants observed a hand performing two different actions. When observing an action that occurred less frequently, left intraparietal sulcus (IPS) interacted with EBA. **4)** In Greven et al. (2016), participants were instructed to form an impression of each person they saw (either presented as a body or name) based on the information that was provided (trait-based or neutral). When forming an impression about a body that was paired with trait-based information, right FBA interacted with bilateral temporal poles and left temporoparietal junction (TPJ), while left temporal pole was coupled with left FBA.

From these functional connectivity studies, it is clear that posterior brain circuits do not process social signals from bodies in isolation (Downing and Peelen, 2011; Ramsey et al., 2011). However, our understanding of functional integration in body perception is still rudimentary. Boundary conditions for interactions between neural networks for person perception are largely unknown. Indeed, there is a need to detail the types of social information that guide functional links between category-selective patches in the ventral visual stream, as well as between those regions and more extended brain circuits. For instance, Greven and colleagues (2016) showed that when seeing an image of a body and reading statements that are trait-diagnostic, such as “She gave money to charity”, functional links are formed between the ToM-network and body patches. But, social inferences regarding a person’s character are not only cued through written or verbal statements; they can also be drawn from body shape alone (Borkenau and Liebler, 1992; Naumann et al., 2009; Puhl and Heuer, 2009). From a neural network perspective, it is currently unclear how such social information is extracted from body shape.

In the current study, therefore, we used fMRI and functional connectivity analyses to investigate the neural circuits that support social inferences that are based on physical features alone (body shape). Here, body images that give rise to spontaneous social evaluations, such as muscular or obese individuals, were compared to images of slim individuals who elicit relatively neutral social inferences. Therefore, rather than a written statement being trait-diagnostic (Mitchell et al., 2005; Ma et al., 2012; Greven et al., 2016), it was the body itself that expressed social information. In addition, we wanted to investigate inferences that are spontaneously cued by body shape, rather than by an instruction to evaluate bodies on social parameters. As such, the task during scanning was to detect a repeated presentation of the same body, which ensured that social inferences were not cued by task instructions. Two possible functional relationships are hypothesised to underpin social inferences from bodies. First, coupling between body-selective patches in the ventral visual stream would show that EBA and FBA exchange signals during social evaluation of bodies (Ewbank et al., 2011). Second, extracting social inferences from bodies may result in greater coupling between core processing in the ventral visual stream and an extended network involved in ToM judgments (Greven et al., 2016). Finding such an interaction would reveal a multi-system mechanism by which social inferences about people are extracted from body shape and posture.

Materials and Methods

Participants

Twenty-six participants (13 females; mean ± SD age: 23.1 ± 5 years) were recruited from the Bangor community and received a monetary reimbursement of £15 for completing the fMRI experiment. All participants had normal or corrected-to-normal vision and reported no history of neurological damage. They gave informed consent according to the local ethics guidelines. Stimuli were selected and validated for the fMRI experiment in two behavioural pilot experiments, each with a different set of participants. Pilot Experiment 1 involved 14 participants (8 females; mean ± SD age: 19.2 ± 0.8 years) and pilot Experiment 2 involved 23 participants (17 females; mean ± SD age: 18.8 ± 0.7 years). None of the individuals in the pilot experiments participated in the fMRI study.

Stimuli and experimental procedure

Participants completed three tasks during scanning: the main experimental task, a body-localiser and a Theory-of-Mind (ToM) localiser (details of each task are provided below). Each participant's scanning session started with a run of the body-localiser, followed by two runs of the main task. A further body-localiser run and two runs of the main task then followed. Interspersing the body-localiser between runs of the main task was done to vary the experience for participants and offset boredom. Participants then completed two runs of the ToM-localiser. The ToM-localiser was always presented after participants had completed the main task, to ensure that participants were not primed towards making trait inferences during the main task. Stimuli were presented using a desktop PC and Matlab software with Psychtoolbox 3 (www.psychtoolbox.org).

Selection and validation of stimuli: To select and validate stimuli, we ran two behavioural pilot experiments (Appendix 4). Participants were required to make socially-relevant judgments about silhouettes either presented under unlimited viewing conditions (Pilot 1, n=14) or presented briefly (Pilot 2, n=23) by rating them on how well the statement matched the image of a body (with 1 being 'completely disagree' and 9 being 'completely agree'; Figure 4.2). Like prior work on the evaluation of faces (e.g., Kramer and Ward 2010), statements were taken from Big-5 personality measures (Extraversion, Conscientiousness, Agreeableness; Donnellan et al. 2006), as well as physical health (Ware et al., 1996). A series of body images were made that represented three different body shapes: muscular, obese, and slim. Because the focus of our research question was on body shape and posture only, we used body silhouettes with heads removed and neutral postures (e.g., no crossed-arms or slouching postures; see Figure 4.2). Slim bodies were selected from Greven et al. (2016), and images of muscular and obese bodies were gathered from various websites and converted into silhouettes and cropped using GIMP 2.8 (www.gimp.org). Stimuli were presented using an iMac computer and Matlab software using Psychtoolbox. Ratings for each condition were compared using a one-way Analysis of Variance and subsequent planned comparisons (slim vs. muscular and slim vs. obese). Therefore, for each judgment type (e.g., Extraversion), a one-way ANOVA was first computed and if this showed a difference between the body types, further planned contrasts were performed using paired t-tests. Cohen's d_z was calculated as a measure of standardised mean difference effect size by dividing the t-value by the square root of the sample size (Cohen, 1988; Lakens, 2013). This process was performed for each rating scale.

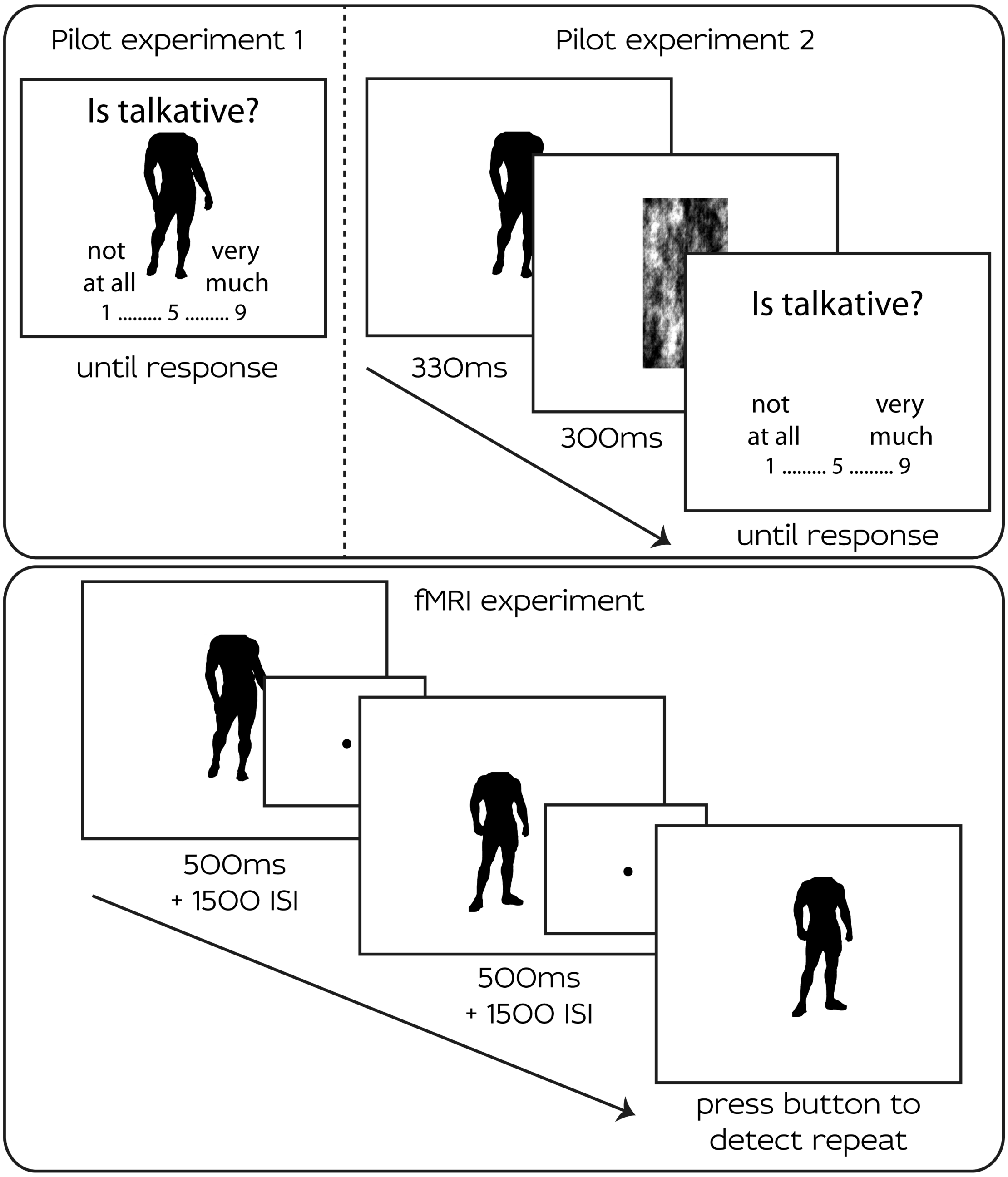

Figure 4.2. Methods for both pilot experiments and the fMRI experiment. Pilot experiment 1: Each body remained on screen until the participant had rated it on the statement displayed above the body. Pilot experiment 2: each body was displayed for 330 ms after which it was backward masked for 300 ms. After this the rating statement would appear on screen and remain there until the participant had provided the rating. fMRI experiment: to allow for spontaneous trait inferences, participants were not explicitly told to form an opinion of the bodies they saw, but instead performed a 1-back task where they had to detect a repeat.

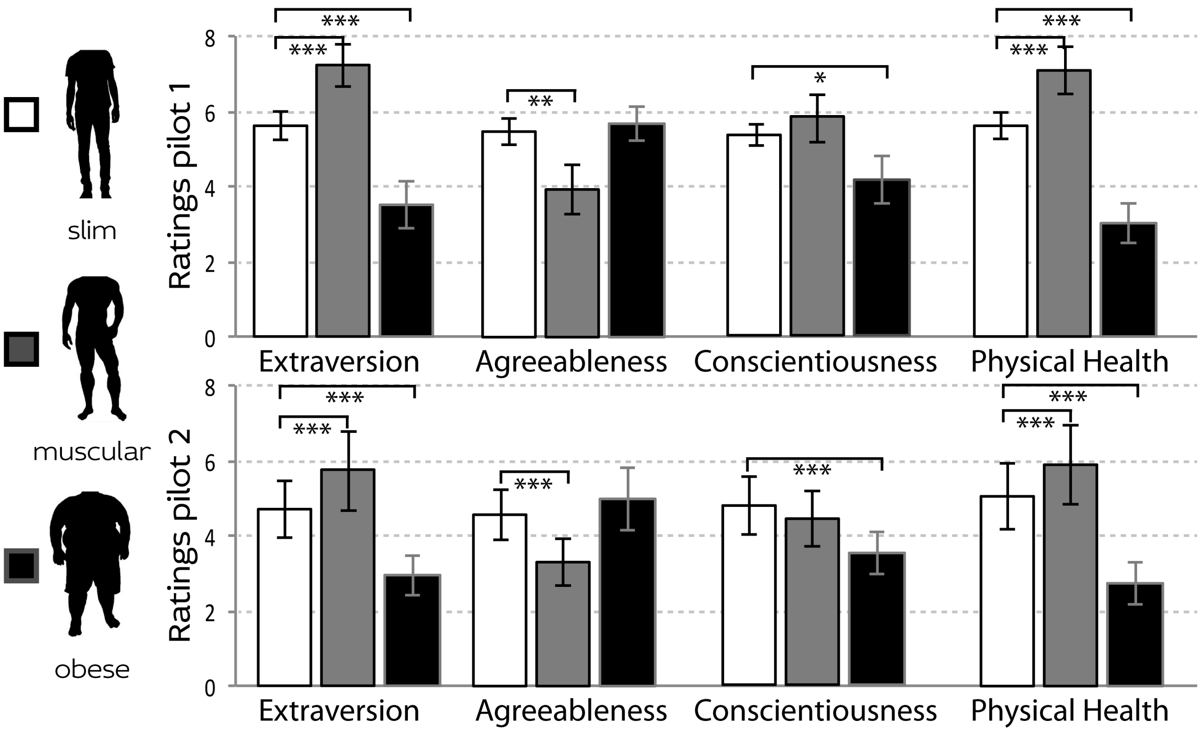

Figure 4.3. Ratings from pilot experiment 1 and 2. Participants rated muscular bodies as more extraverted and healthy, but less agreeable in comparison to slim bodies. Obese bodies were rated as less extraverted, conscientious, and healthy in comparison to slim bodies. *: p<.05, **: p<.01, ***: p<.001. Error bars show 95% confidence intervals.

Results from the first pilot Experiment (all $F \geq 5.11$, $p \leq .031$, $\eta_p^2 \geq .28$) showed that in comparison to neutral bodies, muscular bodies were rated as more extraverted and healthy, but less agreeable (all $t \geq 3.46$, $p \leq .004$, Cohen'$d_z \geq 0.92$, Figure 4.3.A). In addition, obese bodies were rated as less extraverted, conscientious, and healthy (all $t \geq 2.64$, $p \leq .02$, Cohen'$d_z \geq 0.71$,). Based on an item-analysis, we removed slim bodies that were rated more extreme (rating <3 and >7), as well as muscular and obese bodies that were rated more in mid range (rating >3 and <7), reducing the body database to 72 bodies. In the second pilot experiment (all $F \geq 12.60$, $p < .001$, $\eta_p^2 \geq .36$), relative to slim bodies, muscular bodies were rated as more extraverted and healthy, but less agreeable (all $t \geq 4.14$, $p < .001$, Cohen'$d_z \geq 0.86$, Figure 4.3.B), while obese bodies were rated as less extraverted, conscientious, and healthy (all $t \geq 4.75$, $p < .001$, Cohen'$d_z \geq 0.99$).

From the 72 bodies rated in the second pilot experiment, a further 18 images were removed in order have an equal number of bodies in each condition, resulting in a total of 54 unique bodies. To create more variety of stimuli, mirror-images of all 54 bodies were created by flipping along the y-axis. The mirror-reversed and original images were never shown together in the same functional run. Thus, 108 body images were used in the main task of the fMRI experiment.

Main experimental task: The main task used a block-design with blocks of bodies or a fixation cross, presented for 20 and 14 seconds, respectively. Three different body types were presented (Muscular, Obese and Slim), one body-type per block. These three body types formed two groups: Social evaluation (Muscular, Obese) and Neutral (Slim). In order to effectively model the influence of different events on BOLD signal, block order was counterbalanced so that within each run, each condition was preceded equally often by all conditions (Josephs and Henson, 1999; Wager and Nichols, 2003; Aguirre, 2007). To provide a completely balanced block "history" across conditions, each run began with a "starter block", which was not included in the data analysis as it was not preceded by anything. Subsequently, four further blocks from each condition were presented in a counterbalanced manner. Thus, there were 17 blocks per functional run. Each participant completed 4 runs of this task, with 16 Neutral blocks and 32 Social Evaluation blocks across the experiment.

Within body blocks, each image (300 x 650 pixels) was presented for 500 ms, followed by a blank screen for 1500 ms, resulting in a total of 9 bodies per block. Participants were given a 1-back recognition task (Downing et al. 2007; Figure 4.2). Once during each block, the same image was presented twice in a row and participants had to press a button whenever they detected this immediate repetition. The image location was slightly jittered (4 different locations that varied by 10 pixels around a central fixation dot) to prevent participants from performing the 1-back task based on low-level after-effects from the previous image. From the four options, the location of the image on each trial was randomly selected.

Functional localisers: To localise body-selective brain regions we used an established paradigm (Downing et al., 2007; http://pages.bangor.ac.uk/~pss811/page7/page7.html). We presented 12-sec blocks of cars and of whole bodies (without heads). A run started with a blank screen for 14 seconds, followed by two alternations of each condition. This was repeated a second time, and followed by a final rest period of 14 seconds. Each image was presented for 600 ms, followed by a blank screen for 100 ms. Twice during each block, the same image was presented twice in a row. Participants had to perform the same task as in the main task (1-back task). The image location was slightly jittered in the same way as in the main task. Each participant completed two runs of this task, counterbalancing the order of the stimulus presentation (Bodies or Cars).

To localise brain regions that respond to mental state reasoning, we used an established ToM-localiser (Dodell-Feder et al., 2011; http://saxelab.mit.edu/superloc.php). Participants read 10 short false belief stories, in which the belief characters have about the state of the world is false. Participants also read 10 false photograph stories, where a photograph, map, or sign has out-dated or misleading information. After reading each story, participants had to answer whether the subsequently presented statement is true or false. Each run started with a 12 second rest period, after which the stories and questions were presented for 14 seconds combined (stories: 10 seconds; questions: 4 seconds), and were separated by a 12 second rest period. The order of items and conditions was identical for each subject. In the first run, stimuli 1 – 5 from each condition were presented, and the remaining stimuli were presented during the second block.

Data Acquisition

The experiment was conducted on a 3 Tesla scanner (Philips Achieva), equipped with a 32-channel SENSE-head coil. Stimuli were displayed on a MR safe BOLD screen (Cambridge Research Systems: http://www.crsltd.com/) behind the scanner, which participants viewed via a mirror mounted on the head-coil. T2*-weighted functional images were acquired using a gradient echo echo-planar imaging (EPI) sequence. An acquisition time of 2000 ms was used (image resolution: 3.03 x 3.03 x 4 mm^3, TE = 30, flip angle = 90°). After the functional runs were completed, a high-resolution T1-weighted structural image was acquired for each participant (voxel size = 1 mm^3, TE = 3.8 ms, flip angle = 8°, FoV = 288 × 232 × 175 mm^3). Four dummy scans (4 * 2000 ms) were routinely acquired at the start of each functional run and were excluded from analysis.

Behavioural analysis

Performance on the 1-back task in the main experimental task was measured by calculating the d', i.e., the difference between the z-scores (raw data standardised to normal distribution) for hits and false alarms (Stanislaw and Todorov, 1999). This was compared against 0 for all body type conditions using a one-sample t-test, to see whether the targets (repetitions) could reliably be detected from the noise. A d' statistically indistinguishable from 0 signifies that participants pressed nearly every time they saw a body or barely responded at all. To assess whether repetition-detection differed between body types, a comparison across conditions was done using a one-way Analysis of Variance. When this ANOVA revealed a significance difference, post-hoc paired samples t-tests were performed.

Data preprocessing and analysis

Data were preprocessed and analysed using SPM8 (Wellcome Trust Department of Cognitive Neurology, London, UK: www.fil.ion.ucl.ac.uk/spm/). Functional images were realigned, unwarped, corrected for slice timing, and normalized to the MNI template with a resolution of 3x3x3 mm and spatially smoothed using an 8 mm smoothing kernel. Head motion was examined for each functional run and a run was not analysed further if displacement across the scan exceeded 3 millimetres. Three sessions of 1 participant and one session of 2 participants from the main task had to be removed due to excessive head motion.

Univariate model and analysis: Each condition was modelled from the onset of the first body for a duration of 18 seconds. A design matrix was fitted for each participant with 5 regressors in total; one for each body-type (3 in total), one for rest blocks, and one for the starter blocks. The main effect of body-type (Social Evaluation > Neutral) was evaluated by calculating ([Obese and Muscular] > Slim). This univariate analysis served two functions. The first was to identify independent seed regions for our critical connectivity-based analyses. The second was to test magnitude-based hypotheses regarding the role of person perception and ToM-network engagement when extracting social information from bodies. That is, we would be able to test if both body and ToM networks are preferentially involved when visually processing social evaluation compared to neutral bodies.

For the body and ToM localiser, a design matrix was fitted for each participant with 2 regressors, one for each experimental condition (bodies and cars; false beliefs and false photographs). Body-selective regions were revealed by contrasting bodies and cars (Bodies > Cars). The ToM-network was revealed by contrasting false beliefs with false photographs (False Beliefs > False Photographs).

Psychophysiological Interaction analysis: Our primary hypothesis was that the social evaluation of bodies based on body shape would involve functional coupling between distributed neural circuits. Specifically, coupling was predicted between body-selective patches in the ventral visual stream and between body patches and the ToM-network. To test this hypothesis, we used psychophysiological interaction (PPI) analysis (Friston et al., 1997). PPI enables the identification of brain regions whose activity correlates with the activity of a seed region as a function of a task. Here we used a generalized form of PPI, which allows for comparisons across the complete design space (McLaren et al., 2012). By doing so, it is possible to see whether any voxels across the brain show a correlation with activity in the seed region (the “physiological” element) as a function of the two conditions within the main task (the “psychological” element) (Figure 4.4.C).

Two steps were taken to define seed regions for the PPI analysis (Figure 4.4.A). First, based on the group-level univariate analysis, we identified any clusters of overlap between the Social Evaluation > Neutral contrast of the main experiment, and the body and ToM functional localisers. After clusters of overlap were identified at the group-level, we identified subject-specific coordinates for regions of overlap at the single-subject level, allowing for inter-individual differences in peak responses. In order to include as many participants’ data as possible, we searched for overlap across a range of thresholds, which is common when identifying seed regions in individual data (Spunt and Lieberman, 2012; Klapper et al., 2014; Paulus et al., 2015). For each seed region, therefore, we report how many participants show overlap between the main task contrast (across a range of thresholds) and the functional localisers at a fixed threshold ($p<.005$, $k=10$). Volumes were generated using a 6 mm sphere, which was positioned on each individual’s seed-region peak. PPI analyses were run for all seed regions that were identified in this manner.

PPI models for each participant included the 5 regressors from the univariate analyses, as well as 6 PPI regressors. PPI regressors included one for each of the four conditions of the design (Slim, Muscular, Obese, fixation), one for the starter block, and one that modelled seed region activity (Figure 4.4.B). Although we used clusters emerging from the univariate analysis to define seed regions for the PPI analysis, our PPI analysis is not circular (Kriegeskorte et al., 2009), because all regressors from the univariate analysis are included within the PPI model as covariates of no interest (O’Reilly et al., 2012). Therefore, the PPI analyses explain variance in addition to that which is already explained by other regressors in the design and is statistically independent to the univariate analysis.

To create the PPI regressors, the time series in the seed region was specified as the first eigenvariate, and was consequently deconvolved to estimate the underlying neural activity (Gitelman et al., 2003). Then, the deconvolved time series was multiplied by the predicted, pre-convolved time series of each of the five conditions (4 main task conditions and one for the starter). The resulting PPI for each condition in terms of predicted “neural” activity was then convolved with the canonical haemodynamic response function (HRF), and the time series of the seed region was included as a covariate of no interest (McLaren et al., 2012; Spunt and Lieberman, 2012; Klapper et al., 2014). At the second-level analysis, we examined the same contrast as in the univariate analyses (Social Evaluation > Neutral).

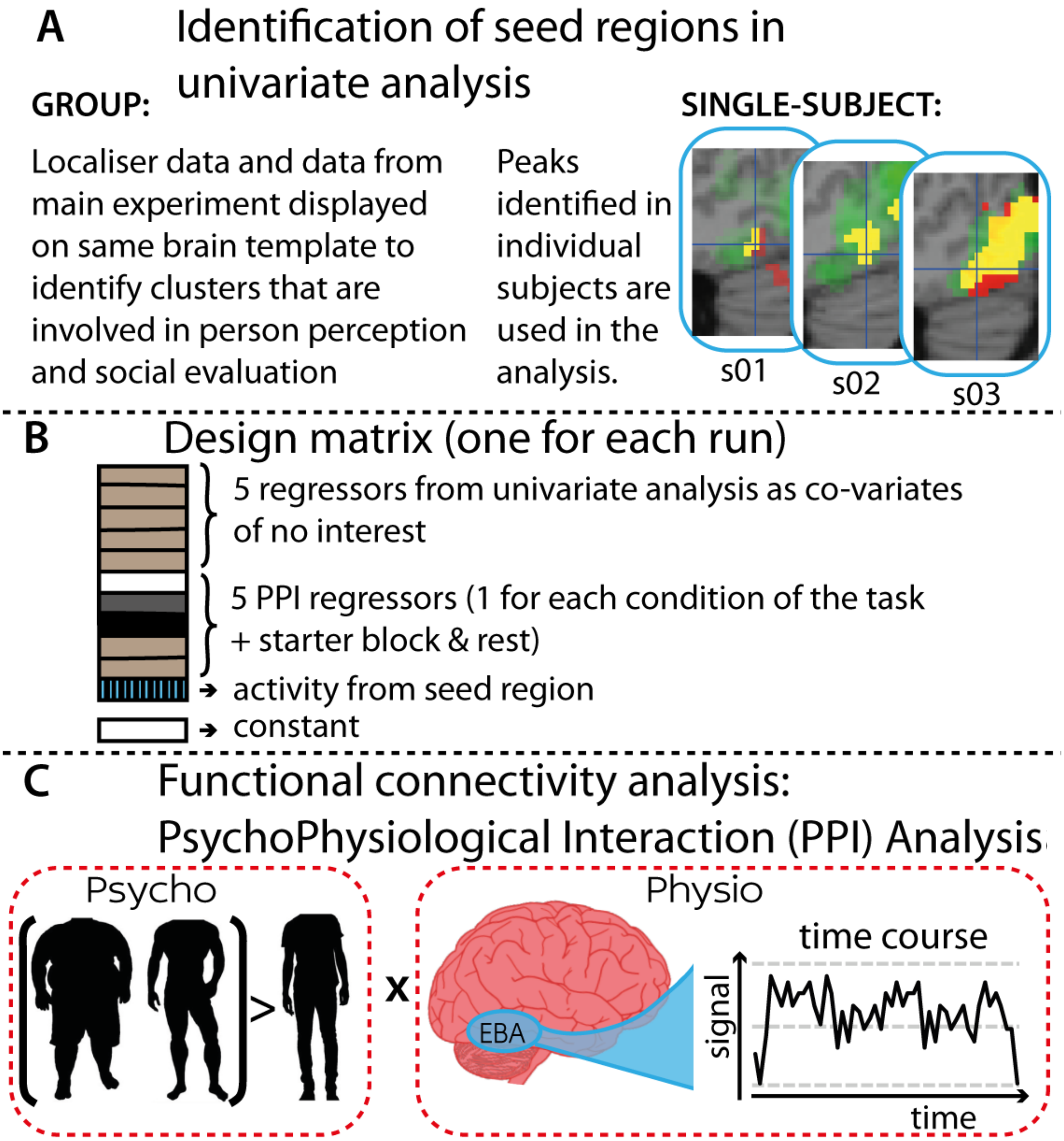

Figure 4.4. Set-up of the PsychoPhysiological Interaction (PPI) analysis. **A)** Identification of seed regions in the univariate analysis was done at group and single-subject level (Social Evaluation > Neutral) to allow for inter-individual differences in peak responses. **B)** An illustration of the design matrix (identical for each run), created for each participant. **C)** The “psychological” (task) and “physiological” (time course from seed region) inputs for the PPI analysis.

For all group-level analyses (univariate and connectivity-based), images were thresholded using a voxel-level threshold of p<.005 and a voxel-extent of 10 voxels (Lieberman and Cunningham, 2009). Based on our hypotheses for functional connections in and between core and extended person perception networks, we inclusively mask the contrasts from the main task by body and ToM localisers (Bodies>Cars and False Beliefs>False Photographs at p<.005, k=10). Inclusive masking in this manner makes sure that only body-selective areas and areas involved in mentalizing are revealed from our analyses. Any results that survive correction for multiple comparisons at the cluster level (Friston et al., 1994) using a family-wise error (FWE) correction ($p<.05$) will be identified. To localise functional responses we used the anatomy toolbox (Eickhoff et al., 2005).

Results

Behavioural data

Performance on the 1-back task was analysed by comparing the sensitivity index (d') of all conditions to 0 with a one-sample t-test, as well as between conditions using a one-way ANOVA. D' differed significantly from 0 for all body types (Slim: M=2.68, CI.95 [2.33, 3.02], Cohen's d_z=3.15; Muscular: M=2.81, CI.95 [2.44, 3.17], Cohen's d_z=3.08; Obese: M=2.50, CI.95 [1.94, 3.06], Cohen's d_z=1.81), revealing that participants could reliably detect the repetition. Additionally, there was no significant difference in performance across different body types ($F(2,50)=0.62$, $p=.27$, $\eta_p^2=.051$).

Neuroimaging data

Univariate analyses: The Social Evaluation > Neutral contrast revealed no suprathreshold clusters in either the body or the ToM network. To explore this null-result, we performed a set of exploratory analyses. First, we removed the voxel extent and a cluster emerged in left inferior occipital gyrus, which overlapped with the body localiser (Appendix 5.A). Second, we explored the same contrast at a more liberal voxel-wise threshold of $p<.05$, $k=10$ (Appendix 5.B, Appendix Figure 2). At this more liberal threshold two clusters emerged, one in left occipitotemporal cortex and one in left fusiform gyrus. At such a liberal threshold, we do not interpret these results as they could reflect false positives. Instead, we used these univariate analyses to guide the location of seed region specification in subsequent PPI analyses. In line with the PPI analyses in chapter 3, we will only use the cluster that emerged at $p<.005$, $k=0$ as a seed region.

Psychophysiological Interaction analyses: Coordinates of overlap between the Social Evaluation > Neutral contrast and the body-localiser were identified within individual participants in left EBA (n=24; for more details, see Appendix 6). We hypothesized that body-selective areas could interact with each other, as well as with areas within the ToM-network when processing bodies about which more extreme social judgments could be made.

To test this hypothesis, one PPI analysis (Social Evaluation > Neutral) was performed using the body-selective cluster that was identified in the univariate analysis. No suprathreshold clusters emerged from this analysis within the person perception network, nor within the person knowledge network.

To further interrogate these null-findings, we defined seed-regions in a different manner, based on coordinates from the body and ToM localiser (details of the localisers, including number of participants included, in Appendix 7). These regions included bilateral EBA and FBA as defined by the body-localiser, as well as bilateral TPJ and temporal poles (TP), precuneus, and mPFC as defined by the ToM-localiser. These ten separate PPI analyses showed no evidence of functional coupling when visually processing muscular and obese in contrast to neutral bodies within the person perception network, nor with the person knowledge network.

Exploratory analyses: We had no a prior predictions regarding neural sensitivity to the differences between muscular and obese bodies. For completeness and to aid future meta-analyses, in Appendix 8, we include univariate and PPI analyses for Muscular > Slim and Obese > Slim. Although univariate analyses show that Muscular bodies engage FBA and EBA more compared to Slim, there is no evidence of functional coupling with body areas or between the body circuit and the ToM network for either body-type. Furthermore, Obese > Slim does not reveal suprathreshold clusters in either the univariate or the PPI analyses when masked by the body and ToM localisers.

Discussion

While behavioural research has investigated social inferences based on body shape (Puhl and Heuer, 2009; Sell et al., 2009; Stulp et al., 2015), the neural underpinnings of such inferences are unclear. Here, we find weak evidence that body-selective patches along the ventral visual stream are engaged more when perceiving bodies that cue inferences about personality and health than neutral bodies. In addition, we find no evidence for increased functional coupling within the body-network or between body-selective patches and the ToM-network when bodies cue such salient social inferences. Therefore, while the stimuli used in this experiment were selected because they cued different social judgments, we did not find any evidence that visually processing these bodies requires interplay between person perception and person knowledge neural networks. Implications for these null-results as well as future directions are discussed.

Implications for neural circuits subserving person perception

Contrary to our hypothesis, we did not find any evidence for functional coupling between the body and ToM network, or within the body network, when social inferences are cued by body shape. In a previous experiment (Greven et al., 2016), we demonstrated that fusiform gyri were functionally coupled with parts of the ToM-network (temporal poles and left TPJ) when trait-implying sentences were paired with bodies. Thus, body patches can interact with extended neural networks, which are engaged when reasoning about another person's trait characteristics. Furthermore, our pilot experiments demonstrated that, when prompted to do so, participants reliably judged the different body types differently on personality measures (extraversion, agreeableness, conscientiousness) and physical health. Moreover, our selection of silhouettes for the fMRI experiment was based on an item-analysis where only bodies that gave rise to distinctly different judgments were included. As such, the bodies used in the current experiment cued distinct judgments when explicitly instructed to evaluate other people on social parameters. Therefore, the current results suggest that when not explicitly forming an impression of a person, there is limited to no evidence for engagement of body or ToM networks, as well as interplay between these networks.

The lack of functional interplay between person perception and person knowledge could have several implications, which future research will need to address. First, as PPI does not allow for an investigation of functional connectivity that is present during all conditions, it may be that participants spontaneously made trait-inferences to the same degree about all body-types. If this is true, body-selective areas could exchange information with ToM nodes every time a body is processed. Secondly, if there is a difference in spontaneous inference between conditions, it could be evidence of a type-II error. Indeed, it may be that links between person perception and person knowledge networks, which are based on body shape cues alone, are subtle and our study was not sensitive enough to detect such links. A way in which this could have been made less subtle is by telling the participants that after completing the experiment in the scanner they would be asked to rate each body on several adjectives. This way participants would be primed to pay more attention to the body shape without being told explicitly to form an impression of the bodies.

Finally, the results may suggest that interplay between person perception and person knowledge neural circuits underpins intentional social inferences more reliably than spontaneous or task-independent inferences. The current study employed a spontaneous traitcueing paradigm, whereby the task was independent to the inference that was cued by body shape. Indeed, the task only involved detecting a repeat presentation of a body. Two prior studies showed functional interplay between body and extended neural networks with tasks that were focussed more directly on social components of the observed stimuli. For instance, Greven and colleagues (2016) showed links between body and ToM networks when participants read a statement that cued a trait inference whilst concurrently observing a body. In addition, Quadflieg et al. (2011) asked participants to categorise, based on gender, people who wore gender-stereotype consistent or inconsistent clothes. Functional connectivity analyses revealed increased connectivity between the person perception network and dorsolateral prefrontal cortex (DLPFC), and the authors concluded that this area was likely to be involved in limiting stereotypical thinking. As such, future work that requires an explicit social judgment may be useful to examine the conditions under which perceptual and extended neural networks may interact during person perception.

CHAPTER 5

Neural networks supporting recall of person knowledge during person perception

This chapter follows up on chapter 3 by examining the functional integration of body- and ToM-networks when recalling trait-based and neutral information about bodies when the first impression has been made previously. Participants formed an impression of people in the same way as in chapter 3 outside the scanner. Inside the scanner, they saw all the bodies again and were asked to form an impression based on what they learned about them previously. After completing all tasks in the scanner, participants performed a recognition task.

This approach allows us to add to the findings from the previous two chapters, using neutral bodies with trait-based text and bodies alone that cue different social evaluations, by allowing us to contrast traits with neutral individuals while only presenting the body.

The neuroimaging data presented in this chapter and the following chapter are the same, but analysed differently. The pilot experiment are post-scanning recognition task are unique to this chapter.

Inez M. Greven, Paul E. Downing & Richard Ramsey

Wales Institute for Cognitive Neuroscience, School of Psychology, Bangor University, Bangor, Gwynedd, Wales, LL57 2AS, United Kingdom

Acknowledgements

The authors thank Emily Butler, Dace Apšvalka, Louise Kirsch, Leah Johnstone, and David Carey for providing scanning cover.

Abstract

Seeing someone we know triggers spontaneous trait inferences, such as ‘friendly’, ‘considerate’ or ‘selfish’, which guides social behaviour. Many studies have revealed the involvement of both perceptual and inferential neural networks when encoding and recalling social information about a person. For example, seeing a person again who had previously appeared hostile instead of friendly differentially engages body-selective and ToM nodes. Using fMRI and functional connectivity analyses we investigated the degree to which these distinct neural networks interact in a task where participants observed bodies that had previously been associated with trait-based (positive and negative) or neutral information. We demonstrate that when the observed person has been associated trait-based rather than neutral information, several body-selective nodes along the ventral visual stream interact with each other and are coupled with areas within the ToM-network. The current experiment adds to previous research suggesting that person perception circuits are not completely encapsulated, but instead interact with other brain systems in a manner that is tied to the type of knowledge associated with the person (i.e., trait-based more than neutral). It suggests that functional integration between neuroanatomically distinct circuits is necessary to establish and maintain a global representation of another’s identity.

Introduction

As you walk through a crowd of people, you recognise a person with a tall frame and broad shoulders and begin to wave at your Dad. Not only can we recognise a person's identity based on physical features, but bodily appearance also cues the recall of trait inferences, such as whether the person is friendly, kind, and generous (Uleman et al., 2008; Sugiura, 2014). Many neural networks have been associated with person recognition and trait inference processes (van Overwalle, 2009; Kanwisher, 2010), but little is known about how these distributed neural circuits interact and influence each other. The current fMRI experiment investigates the hypothesis that recall of social knowledge prompted by seeing others involves functional coupling between a distributed set of neural networks that spans perceptual and inferential processes.

Two neuroanatomically distinct brain circuits have been associated with detecting physical features and reasoning about social traits. Research on person perception investigates how sensory systems detect and visually analyse conspecifics on the basis of their face and body (Kanwisher et al., 1997; Downing et al., 2001; Downing and Peelen, 2011). These studies have revealed that brain areas located along the ventral visual stream, including occipitotemporal cortices and fusiform gyri, show category-selective responses for social compared to non-social items (e.g., faces and bodies vs. objects). In parallel, person knowledge research has identified a brain network that is engaged when representing others' mental states, such as beliefs, desires, and attitudes (Theory of Mind (ToM) network: Frith and Frith 1999; Saxe and Kanwisher 2003; Mitchell 2009; van Overwalle et al. 2009; Ma et al. 2012). The ToM-network comprises temporoparietal junction (TPJ), medial prefrontal cortex (mPFC), temporal poles, and precuneus, and has been shown to be active when inferring traits, such as whether someone is helpful and kind or cheats and lies (Ma et al., 2012). Together, both person perception and knowledge processes have been argued to form a network that contribute to understanding who someone is and how we might expect them to behave (Haxby et al., 2000).

To have a meaningful understanding of who someone is and be able to use this knowledge during social interactions, it is important to bind together different pieces of social information, as well as access this information during social exchanges. For example, when we interact with others, we are able to associate someone's physical appearance with social knowledge about their character, and then recall that information at a later time point (Uleman et al., 2008; Hirst and Echterhoff, 2012). Therefore, binding and recall of social information are key processes that guide social interactions. Neuroimaging research, to date, has shown that binding social information together engages nodes of the ToM-network (Mitchell et al., 2004; Cloutier et al., 2011; Gilron and Gutchess, 2012). For example, Mitchell and colleagues (2004) paired different faces with trait-diagnostic behavioural descriptions (e.g., “he lied on his CV”). When comparing instances where participants had to form an impression to when they remembered the order in which the behaviours happened, activity was greater in mPFC. Moreover, activity in mPFC was enhanced when the person and associated behaviour were later recognised, suggesting that mPFC is involved in encoding person-specific social information.

Other neuroimaging work has investigated which neural networks are involved in the recall of social knowledge (Todorov et al., 2007; Vrtička et al., 2009; Bayliss et al., 2012). For example, Todorov and colleagues showed participants a sequence of faces, which had previously been paired with trait-based (e.g., “Jessica threw a chair at her classmate”) or neutral information (e.g., “Jason read a book in the cafe”). When observing faces associated with behaviours (trait-based and neutral) compared to faces that had not been seen before, both person perception and person knowledge networks were engaged. Furthermore, a node within the person knowledge circuit, which borders left TPJ, was engaged more if the face had previously been paired with social compared to non-social information. In addition, a further fMRI study revealed that the fusiform gyrus and posterior cingulate (below the precuneus) were tuned to recognising faces that previously appeared hostile compared to friendly faces (Vrtička et al., 2009). Together, these studies show that person perception and knowledge networks are involved when observing faces that cue the recall of social knowledge.

As discussed above, neuroimaging research has so far shown that networks associated with person perception and person knowledge are active when binding social knowledge to a person’s physical identity, as well as when the detection of physical features prompts the recall of social knowledge. It remains unclear, however, to what extent functional integration between person perception and knowledge networks contribute to the binding and recall of social information. While the magnitude-based studies presented above have demonstrated the engagement of separate neural circuits in associating and recalling multiple features of a person’s identity, it remains unclear whether or how these networks interact during social perception. Moreover, complex mental operations, such as those that underlie social perception and interaction, are unlikely to be underpinned by cognitive processes and neural networks that function in isolation (Sporns et al., 2005; Kanwisher, 2010). Indeed, recent research has demonstrated that person perception and knowledge networks interact with each other when associating trait-based information with a person's body shape and posture (Greven et al., 2016). However, it has yet to be explored how links between person perception and person knowledge contribute to the recall of trait information based on physical features. Therefore, the current fMRI study uses functional connectivity analyses to investigate how the relationship between these two networks contributes to recall social information during person perception.

The study was designed to investigate neural network integration during recall of social knowledge, which is prompted by seeing others. Therefore, prior to entering the scanner, participants associated different bodies with positive, negative, or neutral information. We used bodies as they generally receive less attention in the literature compared with faces, even though, like faces, they convey a plethora of social signals, and even reveal information that faces may hide (Slaughter et al., 2004; Aviezer et al., 2012). Then, inside the scanner, all the bodies were shown again and participants had to form an impression based on what they learned previously about that person. In situations where participants could recall trait-based (positive or negative) information in comparison to neutral information, we hypothesise that brain circuits involved in person perception and person knowledge will show increased functional coupling. Such increased coupling is hypothesised to reflect integration of perceptual and inferential signals, which are triggered during social perception. Two possible functional relationships are proposed. First, as participants will only observe bodies, coupling within body-selective patches in the ventral visual stream could be expected (Ewbank et al., 2011). This would reveal that EBA and FBA exchange signals when recalling social information about bodies. Second, greater coupling between nodes in the person perception network and in the person knowledge network would support the view that a "who" system for social cognition involved communication between perceptual and inferential mechanisms (Haxby et al., 2000; Ramsey et al., 2011; Greven et al., 2016).

Methods

Participants

Twenty-four participants (15 females; mean ± SD age: 22.6 ± 4.7 years) were recruited from the Bangor community and received a monetary reimbursement of £15 for completing the fMRI experiment. All participants had normal or corrected-to-normal vision and reported no history of neurological damage. They gave informed consent according to the local ethics guidelines. Stimuli were selected and validated for the fMRI experiment in a behavioural pilot experiment. The behavioural pilot experiment involved 73 participants (56 females; mean ± SD age: 20 ± 2.9 years). No participants completed both pilot and fMRI experiments.

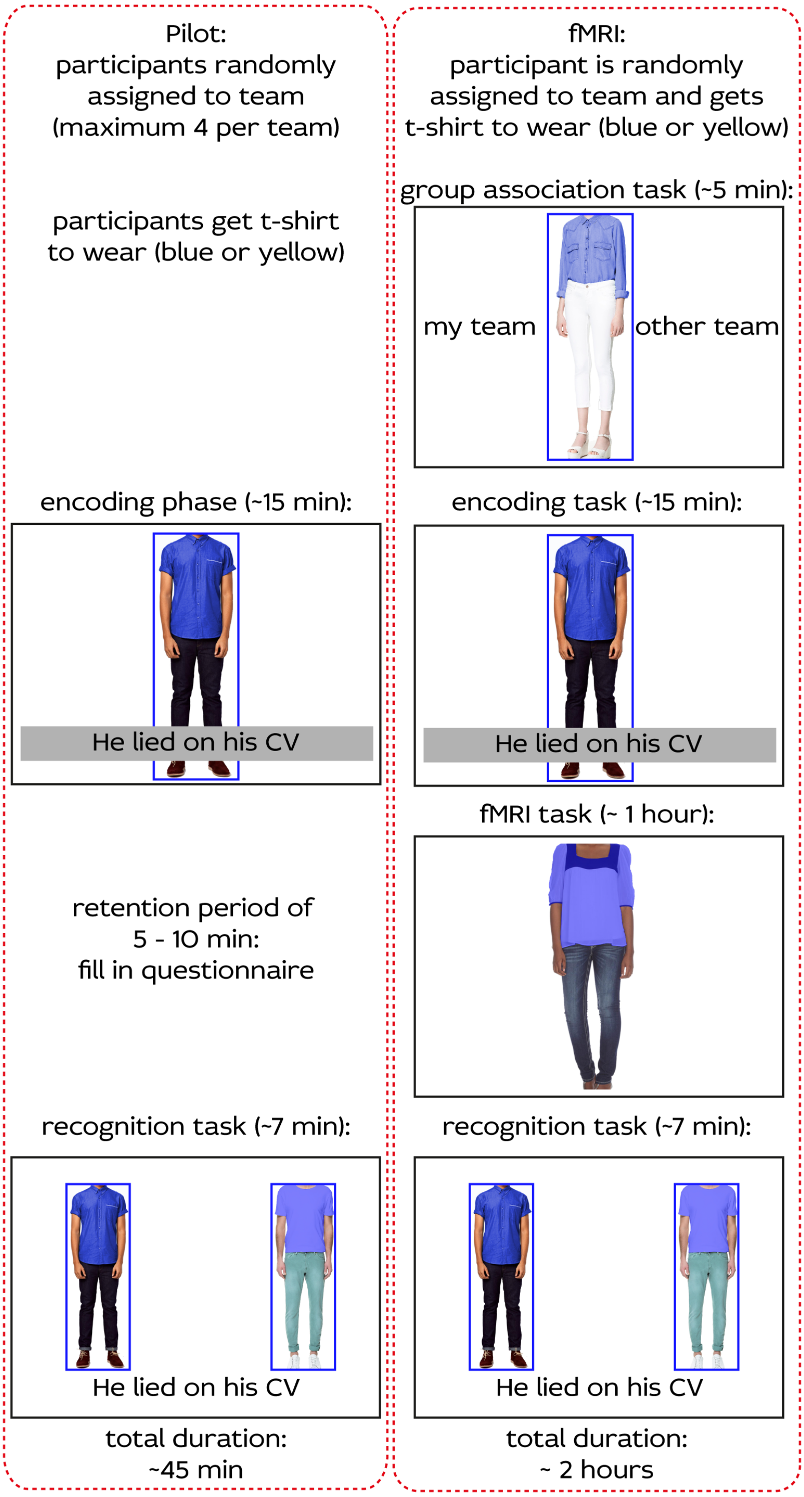

Figure 5.1. Methods and procedure for the pilot and fMRI experiment separately. All analyses are collapsed across group. The group assignment and association task are thus not relevant here, but are included for transparency. The analyses of group bias are reported in chapter 6.

Experimental design overview

This experiment was designed to address two separate questions. The first question relates to social knowledge retrieval from body perception and is reported here. The second question focussed on neural mechanisms of group-bias and is reported in chapter 4. The experiment involved a pilot phase and an fMRI experiment, which were very similar in content and structure. To assess ability to recall information about people, this experiment consisted of several stages (Figure 5.1): 1) Group assignment to team yellow or blue, 2) Encoding phase, where participants were asked to form an impression about unique body-statement pairs, 3) Retention phase in the pilot experiment and several tasks detailed below in the fMRI experiment,

4) Recognition phase, where participants had to judge which of the two bodies presented in each trial was previously paired with the shown statement. Details of each task are provided below. During scanning, three tasks were completed (the main experimental task, a body-localiser and a Theory-of-Mind (ToM) localiser). The two recognition tasks completed after the scanning session tap into different questions. Within each team (blue and yellow), which had an equal number of male and female participants, half first completed recognition task 1, followed by number 2, while the other half first received task 1, then 2. This was done to counteract order effects.

Stimuli

Pictures of 128 bodies (64 female) were adapted from Greven et al. (2016) that had been selected to convey an emotionally-neutral posture (i.e., crossed-arms or slouching postures were not included) but varied in terms of body shape, skin colour and clothing. Consistent with prior work (Downing et al., 2007), in order to target regions selective for images of bodies and not faces, images had been cropped so the head was not visible. For the pre-scanning experiment, 16 extra pictures (8 female) were added to the 128 pictures for a total of 144 bodies. The bodies were edited using GIMP 2.8 software (www.gimp.org) to give them a blue and a yellow shirt (each body could be part of either team). Participants would never see the same body in both a yellow and a blue shirt. Instead, half the participants would see bodies 1 – 64 (1 – 72 for pre-scanning) in blue and 65 – 128 (73 – 144 for pre-scanning) in yellow, and the other participants would see the opposite combination. Each body was only shown once during the encoding experiment, to avoid any possible effects of combining the same person with different social knowledge statements over the course of the experiment.

Social knowledge stimuli comprised 128 statements that were adapted from Mitchell et al. (2006) to convey either trait-based (positive and negative) or neutral information. For the pre-scanning task, 16 statements were removed from the 64 original neutral statements, and 32 extra statements were created for the Trait condition (16 positive, 16 negative). This resulted in a total of 144 statements. An example of a trait-implying statement is “He cut in front of the man in line”, implying the person is inconsiderate, whereas a neutral example is “She walked through the swivel doors”. Each statement (64 traits, 64 neutral for the pilot experiment, 48 positive, 48 negative, 48 neutral for the pre-scanning experiment) was presented once during the experiment.

Each participant's scanning session started with a run of the body-localiser, followed by two runs of the main task. A further body-localiser run and two runs of the main task then followed. Interspersing the body-localiser between runs of the main task was done to vary the experience for participants and offset boredom. Participants then completed two runs of the ToM-localiser. The ToM-localiser was always presented after participants had completed the main task, to ensure that participants were not primed towards making trait inferences during the main task. Stimuli were presented using a desktop PC and Matlab software with Psychtoolbox (www.psychtoolbox.org).

Behavioural tasks

Group assignment: In the pilot experiment, participants were divided into two teams (blue and yellow), given a t-shirt of their team's colour to wear, and the two teams completed the experiments in separate rooms. For the fMRI experiment, each participant was assigned to one of two teams upon arrival. They believed this happened randomly as they picked one of two coins (blue or yellow) out of an opaque bag. In fact, it was ensured that there were an equal number of females and males in each team. For this purpose, the coins were occasionally both of the same colour when required, unbeknownst to the participant. After being assigned to a team, participants wore the t-shirt and completed a group association task in order to enforce their association with their team members. In the group association task, participants were presented with every single body they would later see in the fMRI experiment. They had to answer as fast and accurately as possible to which team this person belonged by pressing 'F' for their team and 'J' for the other team.

Encoding phase: In the encoding task participants were told that they would see lots of different bodies about whom they would learn something, and later on they would be asked a number of questions about the bodies. In each trial, participants were presented concurrently with a body (from team blue or yellow) and social knowledge (trait-based [positive or negative] or neutral). For each participant, bodies were randomly assigned to the statements. Thus, there was no systematic relationship between particular bodies and statements across participants, which removes any coupling between low-level stimulus artefacts and any one condition in our design.

The body (full-colour picture, 300 x 750 pixels) was presented in the middle of the screen with text (fontsize 30 pt) underneath (250 pixels below the centre of the screen). Each trial started with the presentation of a fixation cross for 500 ms, followed by the simultaneous presentation of an agent and a statement for 5000 ms. Participants were instructed to pay attention to both the person as well as to the knowledge that they would receive about that person (Traits or Neutral).

There were 128 trials within the pilot experiment (32 per condition; Traits and Neutral for Blue and Yellow). Trials were presented in 8 blocks containing a random sequence of 16 trials from all four experimental conditions. There were 144 trials in the pre-scanning experiment (24 per condition; Positive, Negative, and Neutral for Blue and Yellow teams). Trials were presented in 8 blocks containing a random sequence of 18 trials from 3 valence conditions. Blocks alternated between a presentation of team yellow and team blue. To make sure participants paid attention to all aspects of the stimuli, at the end of each block they were asked a yes/no-question about the previous trial. Within a maximum duration of 5 seconds, yes/no responses were made by pressing the ‘F’ and ‘J’ button, respectively. These questions could be about the agent’s gender (was this person a man/woman?), or body (was this person facing forward?), as well as the person knowledge statements (did this person touch an object? did this person have a positive/negative attitude?). To ensure that participants remained alert to all elements of these stimuli, the content of questions could not be predicted.

Retention period: Following the encoding phase, participants in the pilot experiment would take a short break (~10 min) during which they filled in a questionnaire. This was done to ensure that recency effects (performance on recognition is better for bodies that were presented last during encoding phase; Gershberg and Shimamura, 1994) did not influence the performance on the subsequent recognition test. The fMRI experiment served as a retention period for the other participants.

Recognition phase: After the retention period, participants performed a recognition task where all the bodies and statements were presented again. In each trial, two bodies appeared on the screen (both of the same team and gender) together with a statement. One of the two bodies was previously paired with that statement. During this task, each body was presented twice, once as the correct and once as the incorrect answer. There were two conditions: Traits and Neutral. For Traits, the correct answer was a body that was previously paired with a trait (either both bodies or only the correct body were previously paired with a trait-based [positive or negative] statement). On neutral trials, the correct answer was a body that was previously paired with neutral information (both bodies or only the correct body were previously paired with a neutral statement).

Behavioural analysis

A trial was considered an outlier if the reaction time was below 200 ms, ensuring that participants had taken enough time to read the statement and observe the bodies. Including outliers, participants had a median response time of 2.81 s (interquartile range (IQR): 1.59) in the pilot experiment, and 2.76 s (IQR: 1.69) in the post-scanning task. This resulted in no rejected trials in the pilot experiment, and 0.94% of trials rejected in data collection after scanning. In both the pilot experiment as well as the fMRI experiment, participants' performance on the two conditions (Traits and Neutral) of the recognition task was compared against chance performance (50%), as well as across the two conditions. Cohen's d_z was calculated as a measure of effect size by dividing the t-value by the square root of the sample size (Cohen, 1992; Lakens, 2013). 95% confidence intervals are reported (Cumming, 2014).

Pilot experiment: 9 participants who performed at or below chance (50% correct) for both conditions (Traits and Neutral) were considered outliers and removed from analysis. Performance on the recognition task revealed that participants, after an average retention period of 7.45 +/- 1.80 minutes, recognised bodies above chance-level performance (Figure 5.2) for trait-based information (M=66.58, CI.95 [63.96, 69.25], Cohen's d_z=1.55) and neutral information (M=61.79, CI.95 [59.28, 64.46], Cohen's d_z=1.17). In addition, trait-based information was recalled more accurately than neutral (Mean difference=4.79, CI.95 [2.05, 7.52], Cohen's d_z=0.44).

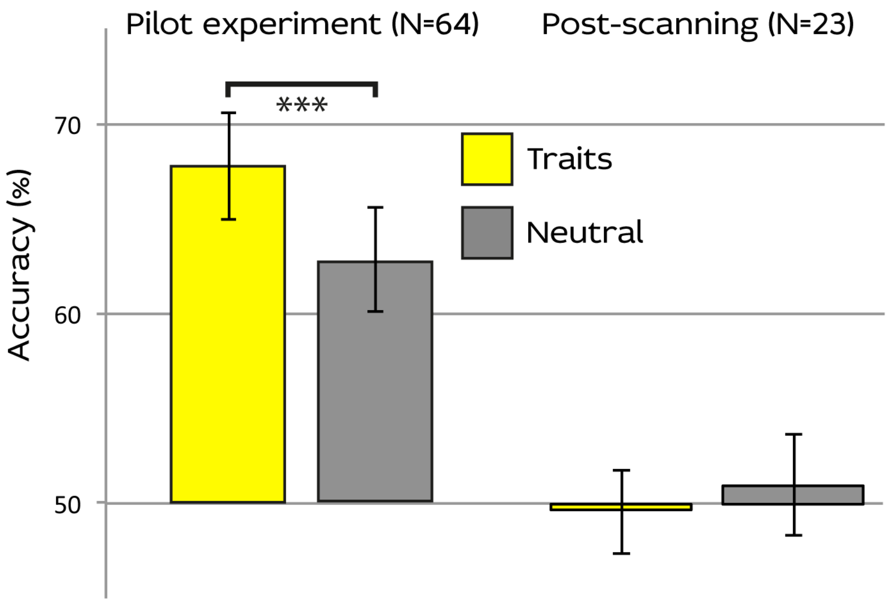

Figure 5.2. Behavioural results for the pilot and fMRI experiment separately. ***: p<.001. Error bars show 95% confidence intervals.

fMRI experiment: Main experimental task. The main task used a block-design with blocks of bodies presented for 16 seconds. Each image (300 x 650 pixels) was presented for 1800 ms, followed by a blank screen for 200 ms, resulting in a total of 8 bodies per block. The same bodies presented in the encoding task were now presented during scanning and grouped together in a block according to their assigned social knowledge (positive, negative, and neutral). Each functional run consisted of two sequences, each presenting only one team (blue or yellow.) The order of presenting team blue and yellow was counterbalanced across participants. Each sequence presented a counterbalanced order (details provided below) of 10 blocks from each of the three social knowledge conditions. Blocks were separated by a jittered rest block with an average duration of 7 seconds (which varied between 5 and 9 seconds with 500 ms steps).

In order to help effectively model the influence of different events on BOLD signal, the block order was counterbalanced so that within each sequence, each condition was preceded equally often by all conditions (Josephs and Henson, 1999; Wager and Nichols, 2003; Aguirre, 2007). To provide a completely balanced block "history" across conditions, each sequence began with a "starter block", which was not included in the data analysis. Subsequently, three further blocks from each condition were presented in a counterbalanced manner. Thus, there were 10 blocks per sequence and 20 per functional run. Each participant completed 4 runs of this task, with 24 Neutral blocks and 48 Trait blocks across the experiment.

Participants were given the instruction to form an impression of each body, based on the information they learned about that body during the encoding phase. At the end of each block, participants were asked a question about the previous body relating to their gender (was this person a woman/man?) or their team (was this person part of your/other team?). From trial-to-trial, the image location was slightly jittered (4 different locations that varied by 10 pixels around a central fixation dot). From the four options, the location of the image on each trial was randomly selected.

Functional localisers: To localise body-selective brain regions we used an established paradigm (Downing et al., 2007; http://pages.bangor.ac.uk/~pss811/page7/page7.html). We presented 12-sec blocks of cars and of whole bodies (without heads). A run started with a blank screen for 14 seconds, followed by two alternations of each condition. This was repeated a second time, and followed by a final rest period of 14 seconds. Each image was presented for 600 ms, followed by a blank screen for 100 ms. Twice during each block, the same image was presented two times in a row. Participants had to press a button whenever they detected this immediate repetition (1-back task). The image location was slightly jittered in the same way as in the main task. Each participant completed two runs of this task, counterbalancing the order of the stimulus presentation (Bodies or Cars).

To localise brain regions that respond to mental state reasoning, we used an established ToM-localiser (Dodell-Feder et al., 2011; http://saxelab.mit.edu/superloc.php).

Participants read 10 short false belief stories, in which the belief characters have about the state of the world is false. Participants also read 10 false photograph stories, where a photograph, map, or sign has out-dated or misleading information. After reading each story, participants had to answer whether the subsequently presented statement is true or false. Each run started with a 12 second rest period, after which the stories and questions were presented for 14 seconds combined (stories: 10 seconds; questions: 4 seconds), and were separated by a 12 second rest period. The order of items and conditions is identical for each subject. In the first run, stimuli 1 – 5 from each condition were presented, and the remaining stimuli were presented during the second block.

Data Acquisition

The experiment was conducted on a 3 Tesla scanner (Philips Achieva), equipped with a 32-channel SENSE-head coil. Stimuli were displayed on a MR safe BOLD screen (Cambridge Research Systems: http://www.crsltd.com/) behind the scanner, which participants viewed via a mirror mounted on the head-coil. T2*-weighted functional images were acquired using a gradient echo echo-planar imaging (EPI) sequence. An acquisition time of 2000 ms was used (image resolution: 3.03 x 3.03 x 4 mm^3, TE = 30, flip angle = 90°). After the functional runs were completed, a high-resolution T1-weighted structural image was acquired for each participant (voxel size = 1 mm^3, TE = 3.8 ms, flip angle = 8°, FoV = 288 × 232 × 175 mm^3). Four dummy scans (4 * 2000 ms) were routinely acquired at the start of each functional run and were excluded from analysis.

Data preprocessing and analysis

Data were preprocessed and analysed using SPM8 (Wellcome Trust Department of Cognitive Neurology, London, UK: www.fil.ion.ucl.ac.uk/spm/). Functional images were realigned, unwarped, corrected for slice timing, and normalized to the MNI template with a resolution of 3x3x3 mm and spatially smoothed using an 8 mm smoothing kernel. Head motion was examined for each functional run and a run was not analysed further if displacement across the scan exceeded 3 millimetres.

Univariate model and analysis: Each condition was modelled from the onset of the first body for a duration of 16 seconds. A design matrix was fitted for each participant with 3 regressors in total; one for Traits (positive and negative combined), one for Neutral, and one for the starter blocks. The main effect of social knowledge was evaluated (Traits > Neutral).

This univariate analysis served two functions. As our primary research question could only be addressed by functional connectivity analyses, the first function of univariate analysis was to identify seed regions for subsequent connectivity-based analyses. The second function enabled the test of magnitude-based hypotheses regarding the role of person perception and ToM network engagement when recalling social information from bodies. That is, we will be able to test if both body and ToM networks are preferentially involved when visually processing bodies about which trait-based information could be recalled compared to neutral bodies.

For the body and ToM localiser, a design matrix was fitted for each participant with 2 regressors, two for each condition (bodies and cars; false beliefs and false photographs). Body-selective regions were revealed by contrasting bodies and cars (Bodies > Cars). The ToM-network was revealed by contrasting false beliefs with false photographs (False Beliefs > False Photographs).

Psychophysiological Interaction analysis: Our primary hypothesis was that recalling social information about bodies involved functional coupling between distributed neural circuits. Specifically, coupling was predicted between body-selective patches in the ventral visual stream and between body patches and the ToM-network. To test this hypothesis, we used psychophysiological interaction (PPI) analysis (Friston et al., 1997). PPI enables the identification of brain regions whose activity correlates with the activity of a seed region as a function of a task. Here we used a generalized form of PPI, which allows for comparisons across the complete design space (McLaren et al., 2012). By doing so, it is possible to see whether any voxels across the brain show a correlation with activity in the seed region (the “physiological” element) as a function of the two conditions within the main task (the “psychological” element) (Figure 5.3.C).

Two steps were taken to define seed regions for the PPI analysis (Figure 5.3A). First, based on the group-level univariate analysis, we identified any clusters of overlap between the Traits > Neutral contrast and the functional localisers (i.e., body and/or ToM localiser) at the group-level. This group-level analysis can identify clusters showing body or ToM selectivity as well as sensitivity to the main task’s contrast. Second, if clusters of overlap were identified at the group-level, we identified subject-specific coordinates for regions of overlap at the single-subject level, thus allowing for inter-individual differences in peak responses.

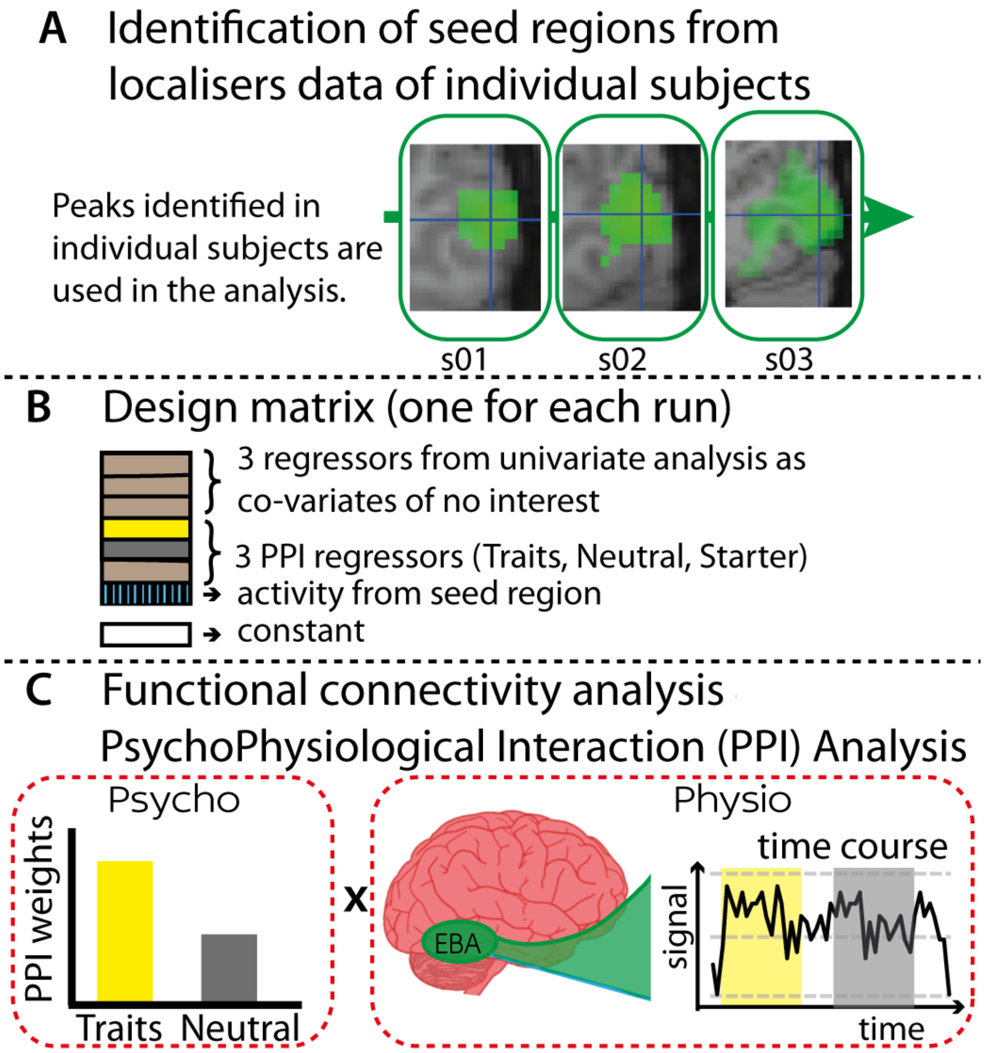

Figure 5.3. Flow chart illustrating the steps to define seed regions and run PsychoPhysiological Interactions (PPI) analyses. **A)** Identification of seed regions was done based on single-subject peak coordinates in the body and ToM localisers to allow for inter-individual differences in peak responses. **B)** An illustration of the design matrix (this was the same for each run), that was created for each participant. **C)** The "psychological" (task) and "physiological" (time course from seed region) inputs for the PPI analysis.

In the case of null-results in our univariate analysis, we would use functional localiser data to define seed regions within the body and ToM networks. These seed regions will include bilateral EBA and FBA for the body-localiser, and bilateral TPJ, bilateral temporal poles (TP), mPFC, and Precuneus for the ToM-localiser. Volumes were generated using a 6 mm sphere, which was positioned on each individual's seed-region peak. PPI analyses were run for all seed regions that were identified.

PPI models for each participant included the 3 regressors from the univariate analyses, as well as 4 PPI regressors. PPI regressors included one for the traits and one for the neutral condition, one for the starter block, and one that modelled seed region activity (Figure 5.3.B).

To create the PPI regressors, the time series in the seed region was specified as the first eigenvariate, and was consequently deconvolved to estimate the underlying neural activity (Gitelman et al., 2003). Then, the deconvolved time series was multiplied by the predicted, pre-convolved time series of each of the 3 conditions (2 main task conditions plus the starter). The resulting PPI for each condition in terms of predicted "neural" activity was then convolved with the canonical haemodynamic response function (HRF), and the time series of the seed region was included as a covariate of no interest (McLaren et al., 2012; Spunt and Lieberman, 2012; Klapper et al., 2014). At the second-level analysis, we examined the same contrast as in the univariate analyses (Traits > Neutral).

For all group-level analyses (univariate and connectivity-based), images were thresholded using a voxel-level threshold of p<.005 and a voxel-extent (k) of 10 voxels (Lieberman and Cunningham, 2009). Based on our hypotheses for functional connections in and between core and extended person perception networks, we inclusively mask the contrasts from the main task by body and ToM localisers (Bodies>Cars and False Beliefs>False Photographs at p<.005, k=10). Inclusive masking in this manner makes sure that only body-selective areas and areas involved in mentalizing are shown. The results from these analyses are presented in Tables 5.1, 5.2, and 5.3. Results that survive correction for multiple comparisons at the cluster level (Friston et al., 1994) using a family-wise error (FWE) correction (p<.05) are shown in bold font. To localise functional responses we used the anatomy toolbox (Eickhoff et al., 2005).

Results

Behavioural data

Performance on the recognition task completed after the scanning sessions showed that information was recalled at chance-level performance (Figure 5.2) for both trait-based and neutral information (Traits: M=49.57, CI.95 [47.41, 51.85], Cohen's $d_{z=}0.08$; Neutral: M=51.02, CI.95 [48.37, 53,64], Cohen's d_z=0.16), nor did it differ between Traits and Neutral (Mean difference=1.46, CI.95 [-2.83, 5.74], Cohen's d_z=0.15).

Neuroimaging data

Univariate analyses: The Traits > Neutral contrast revealed no suprathreshold clusters when masked by either the body or the ToM localiser. To explore this null result further, we removed the voxel extent. At this threshold, we still found no engagement within the body or ToM network.

Psychophysiological Interaction analyses: We hypothesized that body-selective areas would interact with each other, as well as with parts of the ToM-network. Because of the null-results in the univariate analysis, we used localiser-defined seed regions in order to test this hypothesis. For details of the localiser data, see Appendix 9.

For the body-selective seed regions (Table 5.1, Figure 5.4), we looked at connectivity both within the body-network as well as with the ToM-network that was stronger when recalling trait-based in comparison to neutral information about bodies. Left EBA revealed connectivity with other body patches, specifically with bilateral EBA and right FBA (Figure 5.4.A). Right EBA and bilateral FBA did not show suprathreshold clusters within the body-network.

Additionally, right FBA showed greater functional coupling with areas within the ToM-network, specifically left temporal pole and precuneus, when recalling trait-based rather than neutral information about bodies (Figure 5.4.B). Left FBA and bilateral EBA did not show suprathreshold clusters within the ToM-network.

ToM seed regions (Table 5.2, Figure 5.5) were hypothesised to be functionally connected with body-selective areas when recalling trait-based information about bodies. Both left temporal pole and mPFC showed stronger functional coupling under this condition with bilateral EBA and right FBA (Figure 5.5.A). Additionally, both right temporal pole and precuneus were functionally coupled with EBA, specifically right and left EBA, respectively (Figure 5.5.B).

Table 5.1. Clusters revealed in the PsychoPhysiological Interaction (PPI) analysis for the Traits > Neutral contrast masked by **A)** the body-localiser, and **B)** the ToM-localiser. Seed regions are defined by the body-localiser (Bodies > Cars; bilateral EBA and FBA).

Region	Number of voxels	Cluster P_{FWE}	Peak T	Montreal Neurological Institute coordinates		
				x	y	z
a) Masked by body-localiser (EBA and FBA)						
Seed regions: right EBA & bilateral FBA						
No suprathreshold clusters						
Seed regions: left EBA						
Left inferior occipital gyrus (EBA)	26	.76	4.75	-45	-82	1
Right inferior occipital gyrus extending into middle occipital gyrus (EBA)	46	.57	4.68	48	-82	1
			3.84	45	-73	-8
			3.16	48	-79	10
Right fusiform gyrus (FBA)	10	.92	3.70	48	-58	-17
b) Masked by ToM-localiser						
Seed regions: bilateral EBA and left FBA						
No suprathreshold clusters						
Seed region: right FBA						
Left precuneus	47	.39	3.97	-9	-43	40
Right precuneus	24	.59	3.87	6	-55	28
Left temporal pole	10	.76	3.83	-54	5	-26

Note: Regions surviving a voxel-level threshold of $p<.005$ and 10 voxels are reported. Cluster-level p-values are corrected for the search volume, i.e., the mask created from the localisers. Subclusters at least 8 mm from the main peak are listed.

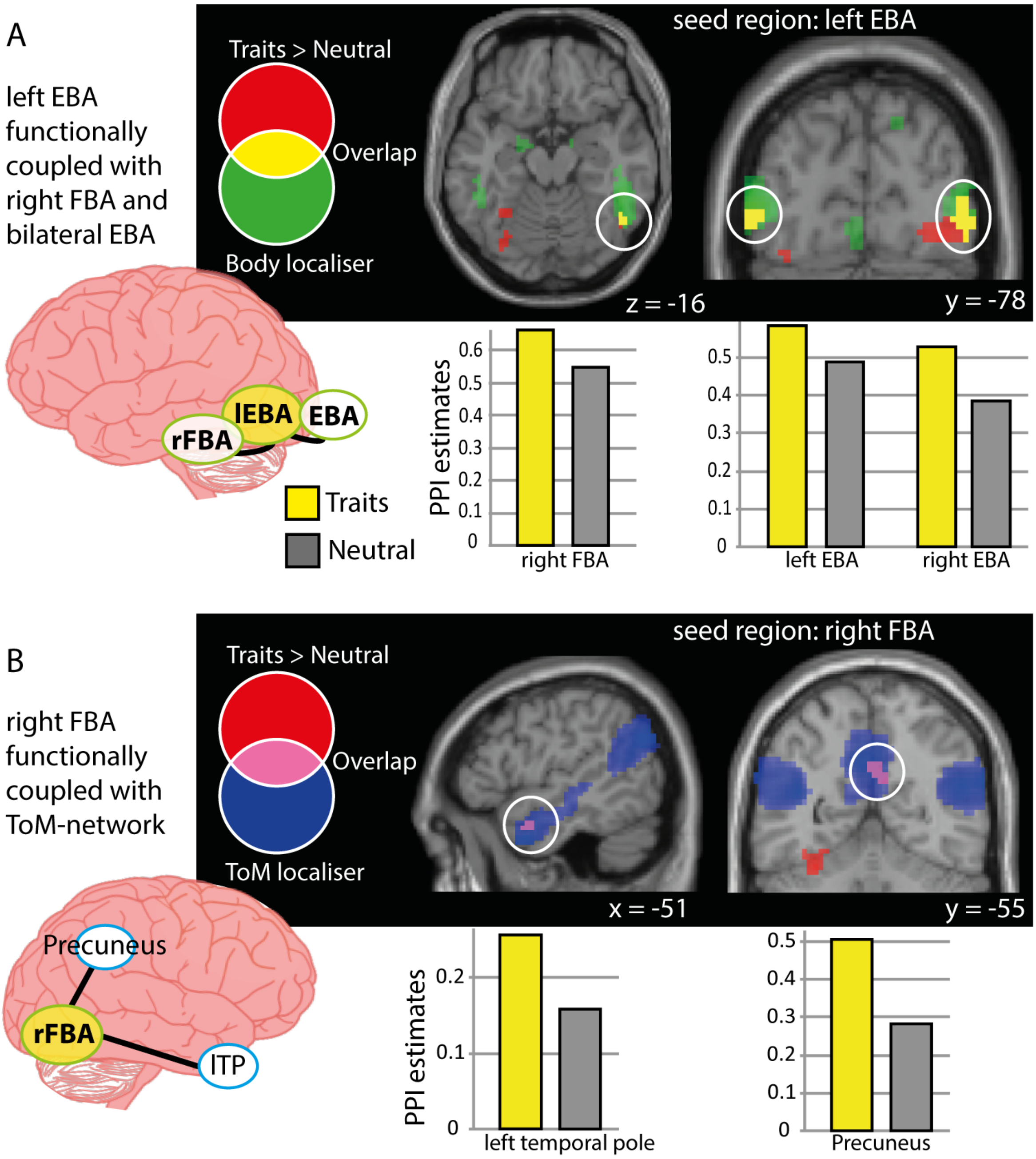

Figure 5.4. Results from the PsychoPhysiological Interaction (PPI) analysis. Seed regions were defined by the localisers (see Appendix 9). In this figure, the body-selective seed regions (bilateral extrastriate and fusiform body areas; EBA and FBA) are presented. In four separate PPI analyses, each identified seed region was used with the Traits > Neutral term as the contrast of interest. Clusters emerging from these analyses reveal the strength of correlation over time between activity in that cluster and that in the seed region as a function of the task. These PPI parameter estimates are extracted from a 4 mm sphere around the peak coordinate. **A)** PPI analyses revealed within body-network connectivity for seed region left EBA (solid yellow circle). Clusters in bilateral EBA and right FBA (shown in red) showed greater functional connectivity with left EBA when recalling traits about bodies. These areas overlapped with the body-localiser (shown in green; overlap is shown in yellow). **B)** PPI analyses revealed connectivity between person perception and person knowledge networks. Seed regions right FBA (solid yellow circle) showed greater functional coupling with left temporal pole (TP) and precuneus when recalling traits about bodies. These areas overlapped with the ToM-localiser (shown in blue; overlap is shown in pink).

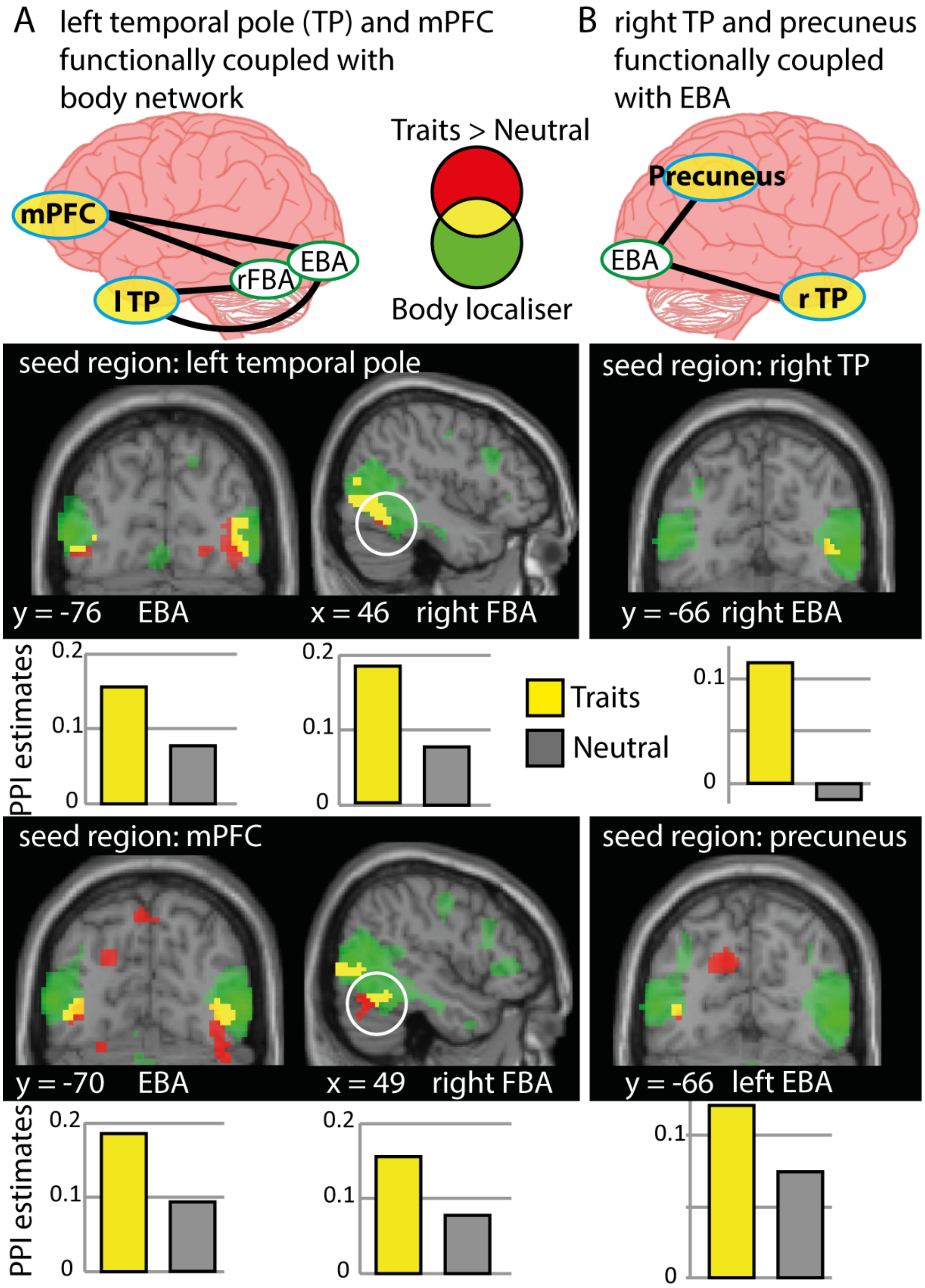

Figure 5.5. Results from the PsychoPhysiological Interaction (PPI) analysis. Seed regions were defined by the localisers (see Appendix 9). In this figure, the ToM seed regions (bilateral temporal poles (TP) and temporoparietal junctions (TPJ), medial prefrontal cortex (mPFC), and precuneus) are presented. In six separate PPI analyses, each identified seed region was used with the Traits > Neutral term as the contrast of interest. Clusters emerging from these analyses reveal the strength of correlation over time between activity in that cluster and that in the seed region as a function of the task. These PPI parameter estimates are extracted from a 4 mm sphere around the peak coordinate. PPI analyses revealed connectivity between person perception and person knowledge networks. **A)** Seed regions mPFC and left TP (solid yellow circles) showed greater functional coupling with bilateral extrastriate body area (EBA) and right fusiform body area (FBA) when recalling traits about bodies (shown in red). These areas overlapped with the body-localiser (shown in green; overlap is shown in yellow). **B)** Seed regions right TP and precuneus (solid yellow circles) both had stronger functional connectivity with EBA (shown in red). Specifically, right TP was functionally coupled with right EBA, and precuneus was functionally coupled with left EBA. These areas overlapped with the body-localiser (shown in green; overlap is shown in yellow).

Table 5.2. Clusters revealed in the PsychoPhysiological Interaction (PPI) analysis for the Traits > Neutral contrast masked by the body-localiser. Seed regions are defined by the ToM-localiser (False Beliefs > False Photographs; bilateral temporoparietal junction (TPJ) and temporal poles (TP), Precuneus, and mPFC).

Region	Number of voxels	Cluster P_{FWE}	Peak T	Montreal Neurological Institute coordinates		
				x	y	z
Seed region: bilateral TPJ						
No suprathreshold clusters						
Seed region: right TP						
Right middle occipital gyrus (EBA)	19	.84	3.21	39	-64	1
Seed region: left TP						
Right middle occipital gyrus (EBA)	164	.10	5.75	39	-64	-2
extending into fusiform gyrus (FBA)			4.43	39	-73	-2
and inferior occipital gyrus			3.80	39	-73	10
			3.63	45	-55	-14
			3.18	51	-61	-20
Seed region: mPFC						
Left middle occipital gyrus (EBA)	41	.64	4.55	-39	-67	4
Right cerebellum extending into	53	.54	3.81	51	-64	-20
fusiform gyrus (FBA)			3.74	48	-49	-17
			3.59	54	-52	-20
Right middle occipital gyrus extending	85	.34	3.53	39	-67	4
into inferior occipital gyrus (EBA)			3.41	42	-70	-2
			3.28	45	-79	1
Seed region: Precuneus						
Left middle occipital gyrus (EBA)	13	.90	3.69	-39	-67	4

Note: Regions surviving a voxel-level threshold of p<.005 and 10 voxels are reported. Cluster-level p-values are corrected for the search volume, i.e., the mask created from the localisers. Subclusters at least 8 mm from the main peak are listed.

Discussion

Seeing someone we know triggers spontaneous trait inferences that allow us to select the appropriate behaviour in order to interact with them (Uleman et al., 2008). While many studies have revealed the involvement of both perceptual and inferential neural networks when encoding and recalling social information about a person (Mitchell et al., 2004; Todorov et al., 2007; Vrtička et al., 2009; Cloutier et al., 2011; Gilron and Gutchess, 2012), the degree to which these distinct neural networks interact is still unclear. By using functional connectivity analyses we investigated the interplay between these networks when recalling trait-based information about people. We demonstrate that several body-selective nodes along the ventral visual stream (extrastriate and fusiform body areas) interact with each other and are coupled with areas within the ToM-network (temporal poles, mPFC, and Precuneus), with the strongest connection between left temporal pole and right EBA. These data extend previous work by showing that recall of social knowledge that is triggered by seeing others is subserved by functional connections between neural systems for person perception and person knowledge.

Neural network integration during person perception when recalling person knowledge

The functional interplay between distinct brain circuits shown in the current experiment adds to previous research suggesting that person perception circuits are not completely encapsulated and resistant to influence from other brain systems (Ewbank et al., 2011; Quadflieg et al., 2011; Zimmermann et al., 2013; Greven et al., 2016). Specifically, we show that body-selective nodes, which are involved in visual analysis of body shape and posture (Peelen and Downing, 2007; Downing and Peelen, 2011), exchange signals with each other as well as with temporal poles, mPFC, and precuneus, which form part of a circuit that is involved in making inferences about others' thoughts and traits (Frith & Frith, 1999; Saxe and Kanwisher, 2003; Mitchell, 2009; Van Overwalle, 2009). This exchange of signals is specifically tied to seeing others that are associated with a particular type of social knowledge. Indeed, functional coupling is greater when the observed person has been associated with trait-based information, which pertains to their character (e.g., "She gave money to charity"), rather than neutral information (e.g., "He put a bowl in the cupboard"). These results suggest that neural networks that have previously been associated with distinct functions, such as person recognition and trait inference, also cooperate when social inferences are prompted by person recognition (Greven et al., 2016). More generally, these results provide empirical evidence to support the existence of a “who” system for social cognition, which comprises category-specific brain circuits that establish and maintain a global representation of another’s identity (Haxby et al. 2000; Collins and Olson 2014; Ramsey et al. 2011; Ishai 2008; Moeller et al. 2008).

For any complex social process, such as recalling stored social knowledge based on body shape, there are likely to be contributions made from many functional processes. Our data show that such complex processing involves interactions between a set of functionally and anatomically distinct neural circuits. Based on our data, however, we cannot distinguish between different connections in terms of the functional processes that they may underpin. Instead, we can only propose functional divisions that future research will need to test directly. For instance, linking person-specific information to a person’s physical features has been associated with activity in mPFC (Mitchell et al., 2004; Gilron and Gutchess, 2012; Welborn and Lieberman, 2014). Furthermore, mPFC aids the selection of accurate social knowledge from semantic memory (Satpute et al., 2013). Thus, the interaction between mPFC and body patches shown in the current study could represent the recollection of person-specific knowledge. The temporal poles have also been implicated in the recall of social knowledge (Simmons and Martin, 2009; Simmons et al., 2010; Drane et al., 2013). Olson and colleagues (2007, 2013) have argued that the temporal poles bind complex information from different modalities (e.g., body and name, profession, character) together in order to represent and retrieve social knowledge. In the current study, the temporal poles may be integrating person recognition input from body patches with stored person knowledge. By contrast, the temporal poles have been implicated in the recall of *general* conceptual knowledge (Rogers et al., 2004, 2006; Patterson et al., 2007). In this light, the temporal poles could function as an intermediate step between category-selective body areas and parts of the ToM-network. Future work will need to distinguish between these possibilities.

The process of recalling traits based on body shape is not resolved solely by functional links between neural networks subserving person perception and person knowledge. In addition, our data suggest that links within the body-network also make a contribution. The connection between EBA and FBA was stronger when observing bodies associated with trait-based rather than neutral information. Previous research demonstrated that when observing a series of bodies with the same identity, but changing in viewpoint, FBA modulated activity in EBA (Ewbank et al., 2011). The information on the holistic representation of bodies held in FBA (Taylor et al., 2007; Brandman and Yovel, 2016) could help EBA to predict what a person's body-parts would look like from a different angle. The functional interaction in the current study could thus reveal a reciprocal exchange of visual information that contributes to determining a person's identity. Currently, however, functional divisions between different links remain speculative and future research would need to directly test such hypotheses.

Limitations and future directions

Our pilot data showed recognition performance was above chance-level and better for trait-based compared to neutral information. However, performance on the post-scanning recognition task for bodies paired with both trait-based and neutral information did not differ from chance-level or from each other. Therefore, although we interpret our neuroimaging results as evidence for a neural network supporting recall of person knowledge, based on the scanner recognition data alone, this interpretation may be hard to justify. However, two factors are worth noting. First, compared to the fMRI data, the pilot data had approximately a threefold larger sample (N=23 vs. N=64), which makes it a considerably more precise estimate of the effect and replicates prior work that trait-based information is recalled better compared to neutral information (Mitchell et al., 2004; Gilron and Gutchess, 2012). Second, the time between the encoding and recognition phase was longer in the fMRI experiment (>1 hour) than it was in the pilot experiment (~7.5 minutes), which may have reduced recall ability due to the more challenging demands on memory systems. Based on our pilot data, therefore, it would be expected that soon after encoding, when participants were being scanned, recall would more closely reflect our pilot behavioural data. Therefore, when the scanner data was being collected, we feel that it is likely that recall was enhanced for traits compared to neutral person knowledge.

Apart from the connection between left temporal pole and right EBA, the connectivity reported here does not survive FWE correction. As such, these results should be taken with caution. Furthermore, we acknowledge that functional connectivity analyses provide no direct insight into the underlying neural pathway that controls functional coupling between brain areas. Previous research using diffusion MRI (Le Bihan, 2012) has provided evidence for a direct white matter pathway between occipital and anterior temporal regions (Catani et al., 2003; Saygin et al., 2012; Gomez et al., 2015; Hodgetts et al., 2015), thus making it plausible that the functional connectivity between body patches and bilateral temporal poles are the result of direct connection. However, other areas such as mPFC are unlikely to be directly anatomically connected to body patches, as the human brain has greater local interconnectivity with a short mean distance between connected brain regions (small-world brain network; Bassett and Bullmore 2006; Gong et al. 2009; Vaessen et al. 2010). Instead, the functional connectivity between body-selective nodes and mPFC could reflect an indirect pathway through, for instance, precuneus, which has been shown to be interconnected with the frontal lobes (Cavanna and Trimble, 2006). Future research using measures of structural connectivity can build upon this.

CHAPTER 6

Neural networks integration during the perception of in- and out-group members

While the previous chapters all compared trait-implying to neutral statements or bodies, this chapter diverges from this by comparing bodies associated with positive and negative information. As the neuroimaging data presented in this chapter are the same as in the previous chapter, the methodological set up is the same, but the analyses differed. The pilot experiment and post-scanning recognition task are unique to this chapter.

Participants were assigned to the blue or the yellow team, making each body they formed an impression of either part of their in- or out-group. By comparing brain activity, functional connectivity, and post-scanning recognition for positive and negative in-group and out-group members, we were able to detect that group-bias modulation was valence-dependent.

Inez M. Greven, Paul E. Downing & Richard Ramsey
Wales Institute for Cognitive Neuroscience, School of Psychology, Bangor University,
Bangor, Gwynedd, Wales, LL57 2AS, United Kingdom

Acknowledgements

The authors thank Emily Butler, Dace Apšvalka, Louise Kirsch, Leah Johnstone, and David Carey for providing scanning cover.

Abstract

Neuroscience research has shown that a distributed set of brain circuits involved in perceptual, affective, and cognitive processing give rise to seeing in-group and out-group members as “us” and “them” during social interactions. The current fMRI study uses functional connectivity analyses to investigate whether these widespread neural circuits interact and influence each other as a function of group membership. Participants were assigned to an arbitrary (minimal) group, which was denoted by the colour of a t-shirt. In addition, before scanning, participants associated positive and negative traits with images of in-group and out-group members. In the scanner, participants observed bodies with an in-group or out-group affiliation that cued the recall of positive or negative social knowledge that had previously been associated with each body. The results showed that functional coupling between perceptual, affective, and cognitive neural networks is dependent both on valence and group membership, i.e., strongest when seeing a person that had previously been paired with information consistent with their biases (positive for in-group and negative for out-group). The valence and group dependent modulation of neural network integration during person perception found in the current experiment provides evidence that perceptual, cognitive, and affective neural networks do not work in isolation, but bias each other to give rise to a representation of another person’s identity.

Introduction

On your way to an important football match, an opposition supporter cuts in front of you and takes the last seat on the bus. The observed behaviour itself triggers trait-inferences (e.g., ‘rude’, ‘unfriendly’), but on top of this, the person’s group membership also influences how we perceive the person. Indeed, group-biases are prevalent in daily social interactions and typically involve in-group favouritism and dislike of out-group members (Allport, 1954; Brewer, 1999; Stangor, 2014). To date, neuroscience research has shown that a distributed set of brain circuits are sensitive to perceiving, reasoning, and responding to interactions with others from different groups (Molenberghs, 2013; Amodio, 2014). However, little to no research has shown how these widespread neural circuits interact and influence each other as a function of group membership. The current fMRI experiment investigates group bias modulation of person perception using functional connectivity analyses.

Among the features used to (implicitly or explicitly) categorize individuals as members of an in-group or out-group, race is commonly studied (Ito and Bartholow, 2009; Kubota et al., 2012; Azevedo et al., 2013; Molenberghs, 2013). For example, it has been demonstrated that the ability to recognise members of another race is impaired compared to own-race recognition (Malpass and Kravitz, 1969). Besides such pre-existing social categories, group biases can also be elicited by assigning individuals to a group based on arbitrary rules, such as the toss of a coin; a procedure known as minimal group assignment (Tajfel et al., 1971). Such an arbitrary categorisation also leads to better recognition of in-group members (Bernstein et al., 2007), as well as more favourable judgments of in-group compared to out-group members (Tajfel et al., 1971; Otten and Moskowitz, 2000; Hertel and Kerr, 2001). As such, even a temporary group assignment based on arbitrary criteria biases the way others are perceived and judged. In short, group membership has a powerful influence on the mental operations that underpin and guide social interactions.

Over the last 15 years, neuroscience research has started to investigate the neural correlates of group-bias. Several brain circuits that span perceptual, affective, and cognitive systems have been shown to be tuned to group-membership (for reviews, see Molenberghs 2013; Amodio 2014). For example, patches of cortex along the ventral visual stream involved in person perception show a response bias for in-group compared to out-group members based on racial and minimal group assignment (Golby et al., 2001; Van Bavel et al., 2008, 2011; Azevedo et al., 2013). As the person perception network is involved, in part, in person recognition and identity processing (McKone et al., 2007; Peelen and Downing, 2007), reduced activity for out-group compared to in-group members has been associated with diminished motivation to process and individuate out-group members (Malpass and Kravitz, 1969; Golby et al., 2001).

Categorising others based on group membership also has an affective component, such that we "feel" differently about members of an in-group compared to an out-group. An "affective network" of brain regions comprising amygdala, insula, medial prefrontal and orbitofrontal cortex (mPFC and OFC, respectively), and striatum, has been found to be involved in affective empathy (the ability to feel what someone else might feel), as well as emotion and reward processing more generally (Keysers and Gazzola, 2009; Fan et al., 2011; Bartra et al., 2013; Eres and Molenberghs, 2013). These brain areas have also been shown to be sensitive to group biases (Golby et al., 2001; Wheeler and Fiske, 2005; Harris and Fiske, 2007; Van Bavel et al., 2008; Molenberghs, 2013; Amodio, 2014; Azevedo et al., 2014; Molenberghs et al., 2016). For instance, left OFC was more active when participants saw an out-group member inflict harm to an in-group member compared to an out-group member (Molenberghs et al., 2016). Moreover, this area was functionally coupled with left insula and amygdala under these conditions, revealing a bias in the affective network to preferentially process in-group suffering.

The third neural network to show sensitivity to group membership is the Theory-of-Mind (ToM) network (Harris and Fiske 2007; Volz et al. 2009; Contreras et al. 2012; Eres and Molenberghs 2013; Molenberghs and Morrison 2014). The ToM-network is engaged when making self-other distinctions, when reasoning about others' mental states (cognitive empathy), as well as when inferring traits about others (van Overwalle, 2009). The ToM-network includes mPFC, temporal poles, temporoparietal junction (TPJ), and precuneus (Frith and Frith 1999; Mitchell, 2009; Saxe and Kanwisher 2003; van Overwalle 2009). When categorising individuals as in-group members, several ToM nodes are also involved (Volz et al., 2009; Molenberghs and Morrison, 2014). For example, in a task where participants had to divide money between in- and out-group members, they gave significantly more money to their in-group members (Volz et al., 2009). In addition, the decision to favour the in-group over the out-group was accompanied by greater activation of mPFC and left TPJ. The authors suggest that ToM-network engagement also reflects the need to make evaluative self-other distinctions in a social group setting.

Together, neuroimaging and behavioural data suggest that conceptual, perceptual, and emotional responses give rise to seeing "us" and "them" during social interactions

(Molenberghs, 2013). A key question from a neuroscience perspective, however, is how distributed neural circuits interact to support mental processes (Sporns et al., 2005). More specifically with regard to group bias, it is currently unclear to what extent and in what ways distributed neural circuits interact as a function of group membership. Recent work has started to uncover functional links between perceptual and extended neural networks during person perception (Quadflieg et al., 2011; Zimmermann et al., 2013; Greven et al., 2016). For example, when linking trait-based information to body shape, body patches in the ventral visual stream show increased coupling with the ToM network (Greven et al., 2016). These results suggest that brain areas typically subserving perceptual functions do not work in isolation during person perception, but communicate with extended neural networks. Using a similar approach, the current fMRI study uses functional connectivity analyses to investigate whether perceptual, affective and cognitive circuits show functional coupling as a function of group bias.

The design of the current study was based on evidence that information that confirms group biases is remembered better than bias-inconsistent information (Snyder and Swann, 1978; Fyock and Stangor, 1994; Leichtman and Ceci, 1995). Indeed, positive information about in-groups and negative information about out-groups are remembered better than bias-inconsistent information (Heider et al., 2007). Before scanning, therefore, participants were assigned to an arbitrary group (blue or yellow) and then asked to form an impression of different bodies. Each body was either an in-group or out-group member and appeared alongside a statement detailing positive or negative information about the person. Then, inside the scanner, all the bodies were shown again without a statement and participants were instructed to form an impression of the person, based on what they had learned previously about that person. We hypothesise increased functional coupling between perceptual, affective, and cognitive neural networks when seeing a person that had previously been paired with information consistent with their biases (positive for in-group and negative for out-group).

Two possible functional relationships are proposed. First, greater coupling between nodes in the person perception and person knowledge network would support the view that a “who” system for social cognition involves communication between perceptual and inferential mechanisms, rather than these nodes acting in isolation (Ramsey et al., 2011; Greven et al., 2016). Second, as we vary both the valence of information (positive vs. negative) and group membership (in vs. out), which have both been shown to engage brain regions associated with affective responses, we expect parts of the affective network to couple more with nodes of the person perception and person knowledge networks. Specifically, we expect to observe increased functional coupling in situations where the person's behavioural descriptions 'fit' the social categorisation (Oakes et al., 1991; Otten and Moskowitz, 2000), i.e., positive for in- and negative for out-group members. This would suggest that recalling trait-based information while merely seeing the body of an in- or out-group members not only engages distinct neural networks, but that they also communicate to each other as a function of valence and group bias.

Methods

Participants

Twenty-four participants (15 females; mean ± SD age: 22.6 ± 4.7 years) were recruited from the Bangor community and received a monetary reimbursement of £15 for completing the fMRI experiment. All participants had normal or corrected-to-normal vision and reported no history of neurological damage. They gave informed consent according to the local ethics guidelines. Stimuli were selected and validated for the fMRI experiment in a behavioural pilot experiment. The pilot experiment involved 31 participants (24 females; mean ± SD age: 20.8 ± 6 years). No participants completed both the pilot and fMRI experiments.

Experimental design overview

This experiment was designed to address two separate questions. The first question relates to social knowledge retrieval from body perception and is reported in chapter 5. The second question focussed on neural mechanisms of group-bias and is reported here. The experiment involved a pilot phase and an fMRI experiment, which were very similar in content and structure. To assess difference in ability to recall positive and negative information about in- and out-group members, this experiment consisted of several stages (Figure 6.1): 1) Group assignment to team yellow or blue, 2) Encoding phase, where participants were asked to form an impression about unique body-statement pairs, 3) Retention phase in the pilot experiment and several tasks detailed below in the fMRI experiment, 4) Recognition phase, where participants had to judge which of the two bodies presented in each trial was previously paired with the shown statement.

Details of each task are provided below. During scanning, three tasks were completed (the main experimental task, a body-localiser and a Theory-of-Mind (ToM) localiser). The two recognition tasks completed after the scanning session tap into different questions. Within each team (blue and yellow), which had an equal number of male and female participants, half completed first recognition task 1, followed by number 2, while the other half first received task 2, then 1. This was done to counteract order effects.

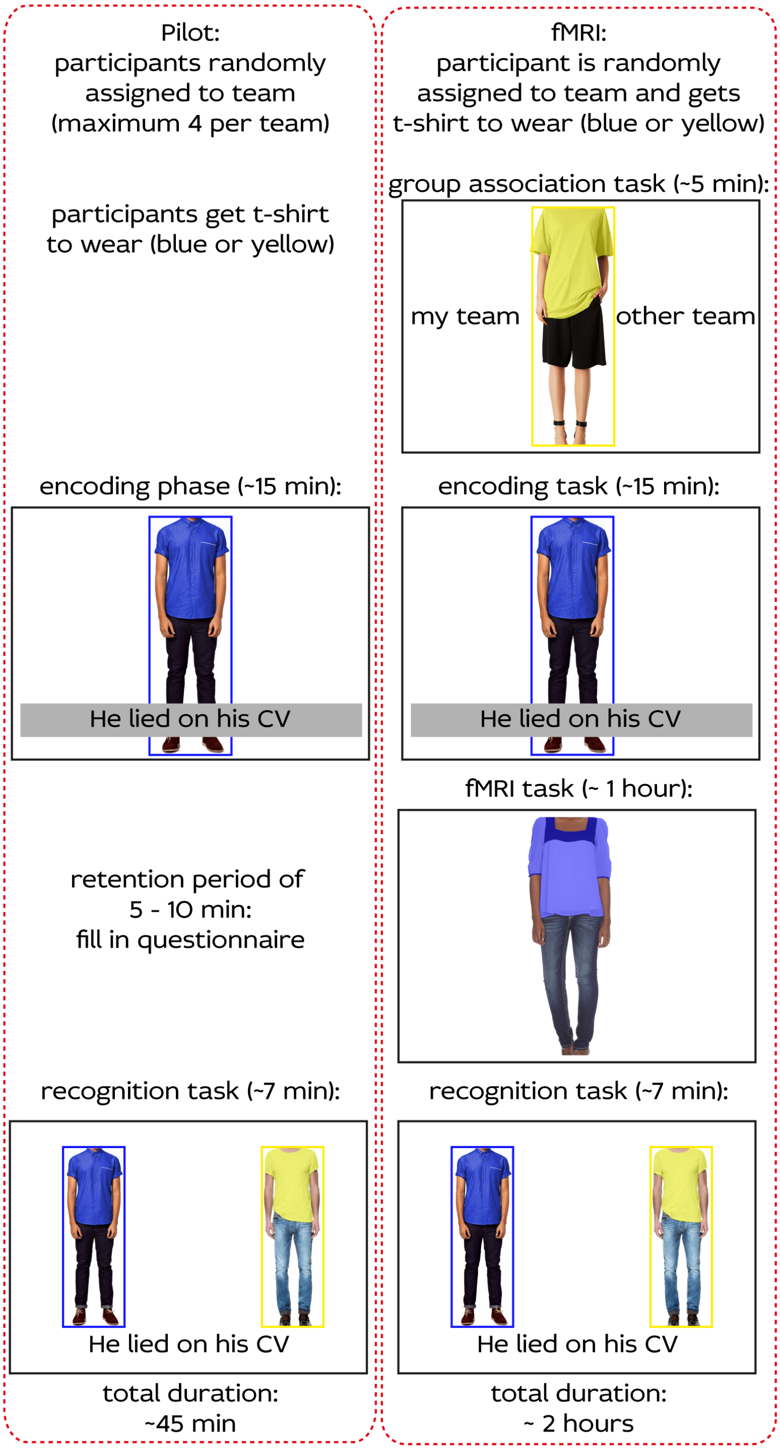

Figure 6.1. Methods and procedure for the pilot and fMRI experiment separately.

Stimuli

Pictures of 128 bodies (64 female) were adapted from Greven et al. (2016) that had been selected to convey an emotionally-neutral posture (i.e., crossed-arms or slouching postures were not included) but varied in terms of body shape, skin colour and clothing. Consistent with prior work (Downing et al., 2007), in order to target regions selective for images of bodies and not faces, images had been cropped so the head was not visible. For the pre-scanning experiment, 16 extra pictures (8 female) were added to the 128 pictures for a total of 144 bodies. The bodies were edited using GIMP 2.8 software (www.gimp.org) to give them a blue and a yellow shirt (each body could be part of either team). Participants would never see the same body in both a yellow and a blue shirt. Instead, half the participants would see bodies 1 – 64 (1 – 72 for pre-scanning) in blue and 65 – 128 (73 – 144 for pre-scanning) in yellow, and the other participants would see the opposite combination. Each body was only shown once during the encoding experiment, to avoid any possible effects of combining the same person with different social knowledge statements over the course of the experiment.

Social knowledge stimuli comprised 128 statements that were adapted from Mitchell et al. (2006) to convey either trait-based (positive and negative) or neutral information. For the pre-scanning task, 16 statements were removed from the 64 original neutral statements, and 32 extra statements were created for the Trait condition (16 positive, 16 negative). This resulted in a total of 144 statements. An example of a trait-implying statement is "He cut in front of the man in line", implying the person is inconsiderate, whereas a neutral example is "She walked through the swivel doors". Each statement (64 traits, 64 neutral for the pilot experiment, 48 positive, 48 negative, 48 neutral for the pre-scanning experiment) was presented once during the experiment.

Each participant's scanning session started with a run of the body-localiser, followed by two runs of the main task. A further body-localiser run and two runs of the main task then followed. Interspersing the body-localiser between runs of the main task was done to vary the experience for participants and offset boredom. Participants then completed two runs of the ToM-localiser. The ToM-localiser was always presented after participants had completed the main task, to ensure that participants were not primed towards making trait inferences during the main task. Stimuli were presented using a desktop PC and Matlab software with Psychtoolbox (www.psychtoolbox.org).

Behavioural tasks

Group assignment: In the pilot experiment, participants were divided into two teams (blue and yellow), given a t-shirt of their team's colour to wear, and the two teams completed the experiments in separate rooms. For the fMRI experiment, each participant was assigned to one of two teams upon arrival. They believed this happened randomly as they picked one of two coins (blue or yellow) out of an opaque bag. In fact, it was ensured that there were an equal number of females and males in each team. For this purpose, the coins were occasionally both of the same colour when required, unbeknownst to the participant. After being assigned to a team, participants wore the t-shirt and completed a group association task in order to enforce their association with their team members. In the group association task, participants were presented with every single body they would later see in the fMRI experiment. They had to answer as fast and accurately as possible to which team this person belonged by pressing ‘F’ for their team and ‘J’ for the other team.

Encoding phase: In the encoding task participants were told that they would see lots of different bodies about whom they would learn something, and later on they would be asked a number of questions about the bodies. In each trial, participants were presented concurrently with a body (from team blue or yellow) and social knowledge (trait-based (positive or negative) or neutral). For each participant, bodies were randomly assigned to the statements. Thus, there was no systematic relationship between particular bodies and statements across participants, which removes any coupling between low-level stimulus artefacts and any one condition in our design.

The body (full-colour picture, 300 x 750 pixels) was presented in the middle of the screen with text (fontsize 30 pt) underneath (250 pixels below the centre of the screen). Each trial started with the presentation of a fixation cross for 500 ms, followed by the simultaneous presentation of an agent and a statement for 5000 ms. Participants were instructed to pay attention to both the person as well as to the knowledge that they would receive about that person (Traits or Neutral).

There were 128 trials within the pilot experiment (32 per condition; Traits and Neutral for Blue and Yellow). Trials were presented in 8 blocks containing a random sequence of 16 trials from all four experimental conditions. There were 144 trials in the pre-scanning experiment (24 per condition; Positive, Negative, and Neutral for Blue and Yellow teams). Trials were presented in 8 blocks containing a random sequence of 18 trials from 3 valence conditions. Blocks alternated between a presentation of team yellow and team blue. To make sure participants paid attention to all aspects of the stimuli, at the end of each block they were asked a yes/no-question about the previous trial. Within a maximum duration of 5 seconds, yes/no responses were made by pressing the ‘F’ and ‘J’ button, respectively. These questions could be about the agent’s gender (was this person a man/woman?), or body (was this person facing forward?), as well as the person knowledge statements (did this person touch an object? did this person have a positive/negative attitude?). To ensure that participants remained alert to all elements of these stimuli, the content of questions could not be predicted.

Retention period: Following the encoding phase, participants in the pilot experiment would take a short break (~10 min) during which they filled in a questionnaire. This was done to ensure that recency effects (performance on recognition is better for bodies that were presented last during encoding phase; Gershberg and Shimamura, 1994) did not influence the performance on the subsequent recognition test. The fMRI experiment served as a retention period for the other participants.

Recognition phase: After the retention period, participants performed a recognition task where all the bodies and statements were presented again. In each trial, two bodies appeared on the screen (both of the same gender, one of each team) together with a statement. One of the two bodies was previously paired with that statement. During this task, each body was presented twice, once as the correct and once as the incorrect answer. There were six different conditions, three where team blue was the correct answer, and three where team yellow was the correct answer. The two bodies could both have previously been paired with a positive, negative, or neutral statement.

Behavioural analysis

A trial was considered an outlier if the reaction time was below 200 ms, ensuring that participants had taken enough time to read the statement and observe the bodies . Including outliers, participants had a median response time of 2.80 s (interquartile range (IQR): 1.60) in the pilot experiment, and 2.84 s (IQR: 1.80) in the post-scanning task. This resulted in 0.10% rejected trials in the pilot experiment, and 0.67% rejected trials in the fMRI experiment. In both the pilot experiment as well as the fMRI experiment, participants' performance on the recognition task was first compared for all conditions against chance-level performance (50%). To do so, 95% CIs were calculated for each condition compared to 50% and Cohen's d was calculated as a measure of effect size by dividing the t-value by the square root of the sample size (Cohen, 1992; Lakens, 2013).

In addition, a 2 (Valence: Positive, Negative) x 2 (Group: in-group, out-group) ANOVA compared performance between conditions. We expected an interaction between Valence and Group, whereby recognition was better for positive compared to negative in-group members and vice versa for out-group members. A significant interaction would be followed-up with two paired-samples t-tests, where recognition for positive and negative bodies was compared for in- and out-group members separately. We would expect a similar difference in accuracy on the positive and negative conditions, but in opposite direction for in- and out-group members.

Pilot Experiment: Four participants were removed as outliers as their performance on all conditions was at or below chance. Performance on the recognition task (Figure 6.2) revealed that, after an average retention time of 9 +/- 2.08 and 8.77 +/- 1.88 minutes for team yellow and team blue respectively (which did not significantly differ from each other:

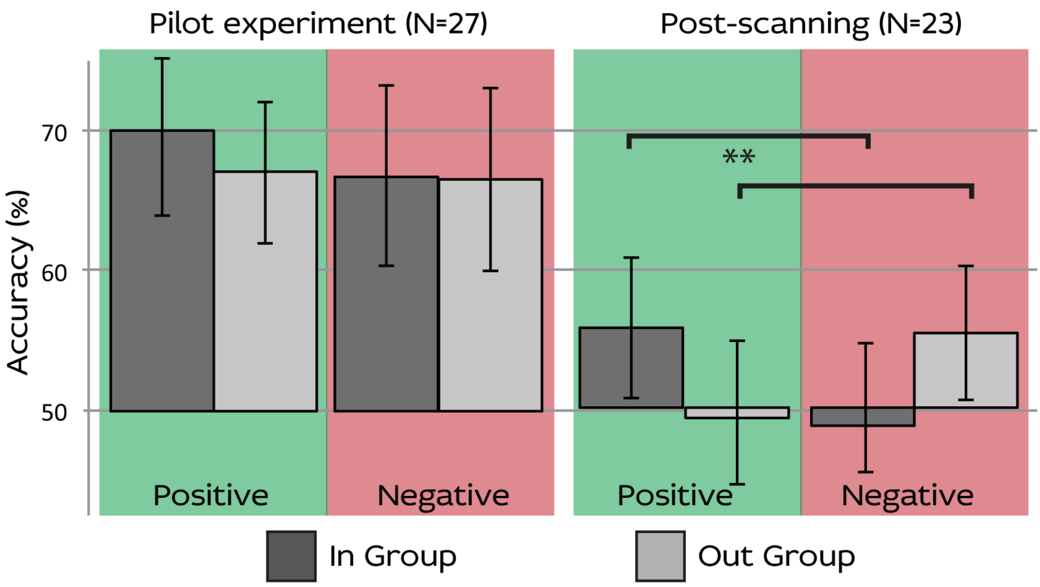

Figure 6.2. Behavioural results for the pilot and fMRI experiment separately. **: p<.01. Error bars show 95% confidence intervals.

Mean difference=0.23, CI.95 [-1.80, 1.34], Cohen's d=0.12), there was no main effect of Valence or Group (Valence: F(1,26)=0.50, p=.49, η_p^2=.02; Group: F(1,26)=0.60, p=.45, η_p^2=.02), nor a significant Valence*Group interaction (F(1,26)=0.55, p=.46, η_p^2=.02). Participants performed above chance on all conditions (PosIn: M=70.07, CI.95 [63.92, 75.20], Cohen's d_z=1.54; PosOut: M=67.13, CI.95 [62.06, 72.20], Cohen's d_z=1.23; NegIn: M=66.67, CI.95 [60.23, 73.10], Cohen's d_z=1.01; NegOut: M=66.59, CI.95 [60.01, 73.17], Cohen's d_z=1.00).

fMRI experiment:

Main experimental task: The main task used a block-design with blocks of bodies presented for 16 seconds. The same bodies presented in the encoding task were now presented during scanning and grouped together in a block according to their assigned social knowledge (positive, negative, and neutral). In each functional run, these three conditions were presented in two sequences (each sequence presenting only one team) of ten blocks. The order of presenting team blue and yellow was counterbalanced across participants. Blocks were separated by a jittered rest block with an average duration of 7 seconds (varied between 5 and 9 seconds with 500 ms steps). In order to help effectively model the influence of different events on BOLD signal, the block order was counterbalanced so that within each sequence, each condition was preceded equally often by all conditions (Josephs and Henson, 1999; Wager and Nichols, 2003; Aguirre, 2007). To provide a completely balanced block "history" across conditions, each sequence began with a "starter block", which was not included in the data analysis. Subsequently, three further blocks from each condition were presented in a counterbalanced manner. Thus, there were 10 blocks per sequence and 20 per functional run. Each participant completed 4 runs of this task, with 24 Neutral blocks and 48 Trait blocks across the experiment.

Within body blocks, each image (300 x 650 pixels) was presented for 1800 ms, followed by a blank screen for 200 ms, resulting in a total of 8 bodies per block. Participants were given the instruction to form an impression of each body, based on the information they learned about that body during the encoding phase. At the end of each block, participants were asked a question about the previous body relating to their gender (was this person a woman/man?) or their team (was this person part of your/other team?). From trial-to-trial, the image location was slightly jittered (4 different locations that varied by 10 pixels around a central fixation dot). From the four options, the location of the image on each trial was randomly selected.

Functional localisers: To localise body-selective brain regions we used an established paradigm (Downing et al., 2007; http://pages.bangor.ac.uk/~pss811/page7/page7.html). We presented 12-sec blocks of cars and of whole bodies (without heads). A run started with a blank screen for 14 seconds, followed by two alternations of each condition. This was repeated a second time, and followed by a final rest period of 14 seconds. Each image was presented for 600 ms, followed by a blank screen for 100 ms. Twice during each block, the same image was presented two times in a row. Participants had to press a button whenever they detected this immediate repetition (1-back task). The image location was slightly jittered in the same way as in the main task. Each participant completed two runs of this task, counterbalancing the order of the stimulus presentation (Bodies or Cars).

To localise brain regions that respond to mental state reasoning, we used an established ToM-localiser (Dodell-Feder et al., 2011; http://saxelab.mit.edu/superloc.php). Participants read 10 short false belief stories, in which the belief characters have about the state of the world is false. Participants also read 10 false photograph stories, where a photograph, map, or sign has out-dated or misleading information. After reading each story, participants had to answer whether the subsequently presented statement is true or false. Each run started with a 12 second rest period, after which the stories and questions were presented for 14 seconds combined (stories: 10 seconds; questions: 4 seconds), and were separated by a 12 second rest period. The order of items and conditions is identical for each subject. In the first run, stimuli 1 – 5 from each condition were presented, and the remaining stimuli were presented during the second block.

Data Acquisition

The experiment was conducted on a 3 Tesla scanner (Philips Achieva), equipped with a 32-channel SENSE-head coil. Stimuli were displayed on a MR safe BOLD screen (Cambridge Research Systems: http://www.crsltd.com/) behind the scanner, which participants viewed via a mirror mounted on the head-coil. T2*-weighted functional images were acquired using a gradient echo echo-planar imaging (EPI) sequence. An acquisition time of 2000 ms was used (image resolution: 3.03 x 3.03 x 4 mm^3, TE = 30, flip angle = 90°). After the functional runs were completed, a high-resolution T1-weighted structural image was acquired for each participant (voxel size = 1 mm^3, TE = 3.8 ms, flip angle = 8°, FoV = 288 × 232 × 175 mm^3). Four dummy scans (4 * 2000 ms) were routinely acquired at the start of each functional run and were excluded from analysis.

Data preprocessing and analysis

Data were preprocessed and analysed using SPM8 (Wellcome Trust Department of Cognitive Neurology, London, UK: www.fil.ion.ucl.ac.uk/spm/). Functional images were realigned, unwarped, corrected for slice timing, and normalized to the MNI template with a resolution of 3x3x3 mm and spatially smoothed using an 8 mm smoothing kernel. Head motion was examined for each functional run and a run was not analysed further if displacement across the scan exceeded 3 millimetres.

Univariate model and analysis: Each condition was modelled from the onset of the first body for a duration of 16 seconds. A design matrix was fitted for each participant with 7 regressors in total; one for each condition (PosIn, PosOut, NegIn, NegOut, NeutralIn, NeutralOut), and one for the starter blocks. Main effects of Valence [Pos > Neg; Neg > Pos] and Group [In > Out; Out > In] were calculated first for completeness.

The main analysis of interest, however, was the Valence by Group interaction [(PosIn > PosOut) > (NegOut > NegIn)]. This univariate interaction analysis served two functions. As our primary research question could only be addressed by functional connectivity analyses, the first function of univariate analysis was to identify seed regions for subsequent connectivity-based analyses. The second function enabled the test of magnitude-based hypotheses regarding the role of person perception, affective, and ToM networks during the perception of bodies as a function of group bias. That is, we will be able to test if body, affective and ToM networks are preferentially involved when visually processing bodies about which particular trait and group-based information is known.

For the body and ToM localiser, a design matrix was fitted for each participant with 2 regressors, two for each condition (bodies and cars; false beliefs and false photographs). Body-selective regions were revealed by contrasting bodies and cars (Bodies > Cars). The ToM-network was revealed by contrasting false beliefs with false photographs (False Beliefs > False Photographs).

Psychophysiological Interaction analysis: Our primary hypothesis was that recalling social information about bodies involved functional coupling between distributed neural circuits when it fit their stereotype. Specifically, coupling was predicted between body-selective patches in the ventral visual stream and the ToM-network, as well as between the body patches and the ToM-network with the affective network. To test this hypothesis, we used psychophysiological interaction (PPI) analysis (Friston et al., 1997). PPI enables the identification of brain regions whose activity correlates with the activity of a seed region as a function of a task. Here we used a generalized form of PPI, which allows for comparisons across the complete design space (McLaren et al., 2012). By doing so, it is possible to see whether any voxels across the brain show a correlation with activity in the seed region (the "physiological" element) as a function of the two conditions within the main task (the "psychological" element) (Figure 6.3.C).

Two steps were taken to define seed regions for the PPI analysis (Figure 6.3.A). First, based on the group-level univariate analysis, we identified any clusters of overlap between the interaction contrast and the functional localisers (i.e., body and/or ToM localiser) at the group-level. This group-level analysis can identify clusters showing body or ToM selectivity as well as sensitivity to the main task's contrast. Second, if clusters of overlap were identified at the group-level, we identified subject-specific coordinates for regions of overlap at the single-subject level, this allowing for inter-individual differences in peak responses. Separately for each individual participant we searched for overlap between the interaction contrast and the functional localisers (body and/or ToM localiser at the single-subject level). In order to include as many participant's data as possible, we searched for overlap across a range of thresholds, which is common when identifying seed regions in individual's data (Spunt and Lieberman, 2012; Klapper et al., 2014; Paulus et al., 2015). For each seed region, therefore, we report how many participants show overlap between the main task's contrast (across a range of thresholds; reported in Supplementary Table 2) and functional localisers at a fixed threshold ($p<.005$, voxel extent = 10). Volumes were generated using a 6 mm sphere, which was positioned on each individual's seed-region peak. PPI analyses were run for all seed regions that were identified in this manner.

PPI models for each participant included the 7 regressors from the univariate analyses, as well as 8 PPI regressors. PPI regressors included one for each condition (6 in total), one for the starter block, and one that modelled seed region activity (Figure 6.3.B). Although we use clusters emerging from the univariate analysis to define seed regions for the PPI analysis, our PPI analysis is not circular (Kriegeskorte et al., 2009), because all regressors from the univariate analysis are included within the PPI model as covariates of no interest (O'Reilly et al., 2012). The PPI analyses, therefore, explain variance in addition to that which is already explained by other regressors in the design and is statistically independent to the univariate analysis.

To create the PPI regressors, the time series in the seed region was specified as the first eigenvariate, and was consequently deconvolved to estimate the underlying neural activity (Gitelman et al., 2003). Then, the deconvolved time series was multiplied by the predicted, pre-convolved time series of each of the seven regressors (6 conditions, and 1 starter block). The resulting PPI for each condition in terms of predicted "neural" activity was then convolved with the canonical haemodynamic response function (HRF), and the time series of the seed region was included as a covariate of no interest (McLaren et al., 2012; Spunt and Lieberman, 2012; Klapper et al., 2014). At the second-level analysis, we examined the same contrast as in the univariate analyses [(PosIn > PosOut) > (NegOut > NegIn)]. We expected an the same type of Valence by Group interaction as in the behavioural analyses, whereby functional coupling was stronger for positive compared to negative in-group members and vice versa for out-group members.

For all group-level analyses (univariate and connectivity-based), images were thresholded using a voxel-level threshold of $p<.005$ and a voxel-extent of 10 voxels (Lieberman and Cunningham, 2009). Based on our hypotheses for functional connections in and between core and extended person perception networks, we inclusively mask the contrasts from the main task by body and ToM localisers (Bodies>Cars and False Beliefs>False Photographs at $p<.005$, $k=10$). The affective network mask included amygdala, insula, striatum and orbital frontal cortex (full details of all masks are reported in Table 6.1). Inclusive masking in this manner makes sure that only body-selective, affective and areas involved in mentalizing are shown. The results from these analyses are presented in Tables 2 and 3. Results that survive correction for multiple comparisons at the cluster level (Friston et al., 1994) using a family-wise error (FWE) correction ($p<.05$) are shown in bold font. To localise functional responses we used the anatomy toolbox (Eickhoff et al., 2005).

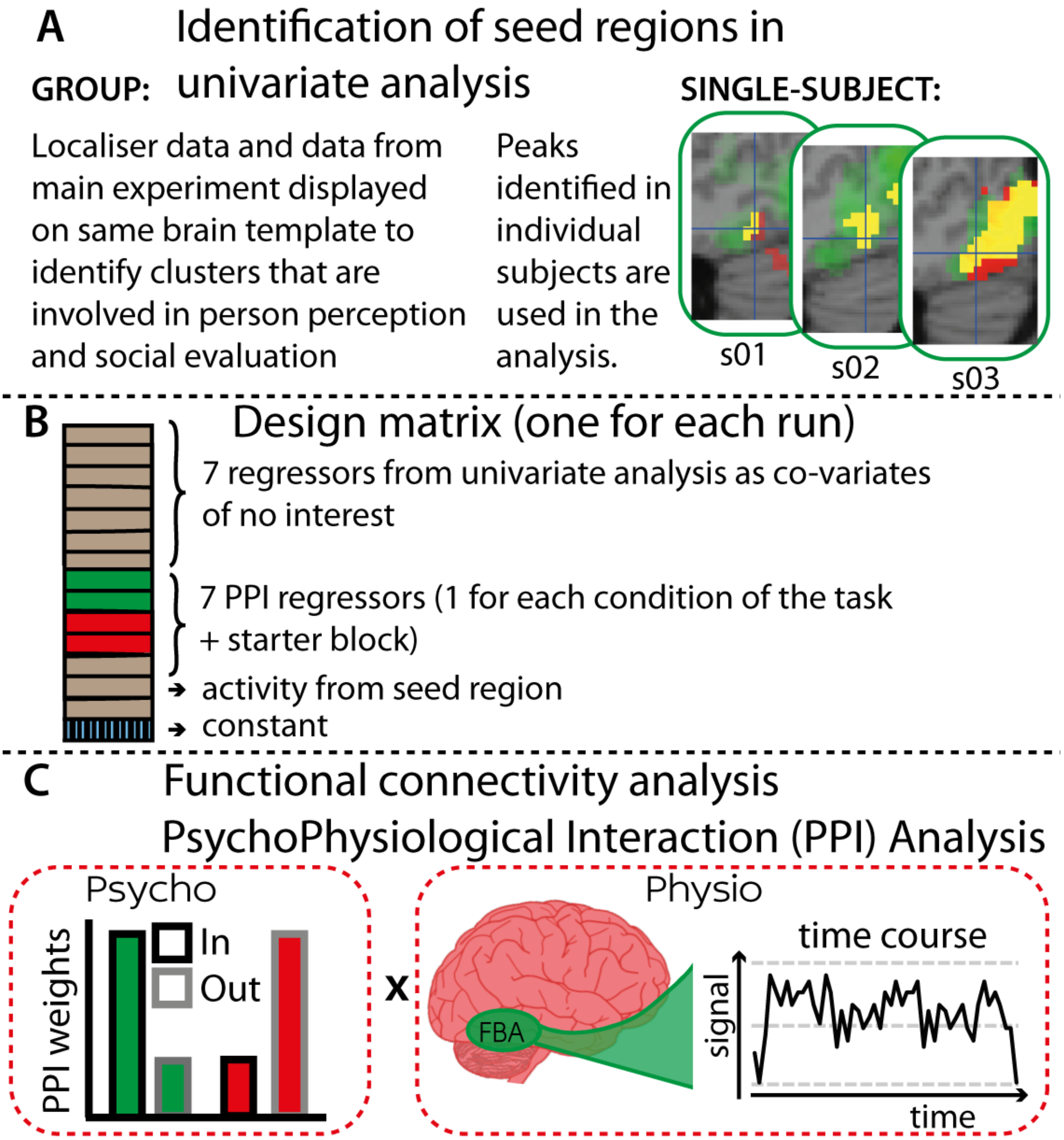

Figure 6.3. Flow chart illustrating the steps to define seed regions and run PsychoPhysiological Interactions (PPI) analyses. **A)** Identification of seed regions in the univariate analysis was done at group and single-subject level to allow for inter-individual differences in peak responses. **B)** An illustration of the design matrix (this was the same for each run), that was created for each participant. **C)** The “psychological” (task) and “physiological” (time course from seed region) inputs for the PPI analysis.

Table 6.1. Details of the body, ToM, and affective masks. Average coordinates given for each region of the body-localiser (bilateral extrastriate and fusiform body area; EBA and FBA) and ToM-localiser (bilateral temporoparietal junction (TPJ), temporal poles (TP), Precuneus, and medial Prefrontal Cortex (mPFC)). For the affective mask, coordinates of each area (amygdala, anterior and posterior insula, striatum, and five clusters within the orbitofrontal cortex (OFC)) and their source from the literature are provided.

Network	Area	L/R	Coordinate	Source
Body	EBA	Left	-51,-73,7	Functional localiser (Downing et al., 2007)
		Right	54,-70,4	
	FBA	Left	-48,-37,-23	
		Right	51,-40,-23	
ToM	TPJ	Left	-45,-64,28	Functional localiser (Dodell-Feder et al., 2011)
		Right	60,-58,25	
	TP	Left	-51,5,-32	
		Right	51,5,-32	
	mPFC		6,56,28	
	Precuneus		-9,-49,34	
Affective	Amygdala	Left	-20,-3,-20	(Ball et al., 2009)
		Right	20,-3,-20	
	Anterior insula	Left	-35,12,-4	(Kurth et al., 2010; Cerliani et al., 2012; Jakab et al., 2012; Bartra et al., 2013)
		Right	37,11,-4	
	Posterior insula	Left	-38,-9,4	
		Right	39,-6,4	
	Striatum	Left	-16,4,-4	(Tanaka et al., 2004; Seymour et al., 2007; Bartra et al., 2013)
		Right	12,6,4	
	Anterior OFC	Left	-6,40,-16	(Kahnt et al., 2012; Liu et al., 2015)
		Right	6,41,-13	
	Medial OFC	Left	-16,58,-10	
		Right	14,57,-11	
	Posterior OFC	Left	-28,39,-15	
		Right	28,41,-16	
	Intermediate OFC	Left	-42,33,-10	
		Right	43,35,-10	
	Lateral OFC	Left	-15,23,-21	
		Right	18,23,-21	

Results

Behavioural data

First, we tested if recognition performance was greater than chance for each condition. Performance was above chance (50%) for PosIn (M=55.69, CI.95 [50.55, 60.83], Cohen's d_z=0.48) and NegOut (M=55.34, CI.95 [51.23, 59.44], Cohen's d_z=0.56). However, performance was at chance for PosOut (M=49.26, CI.95 [44.08, 54.43], Cohen's d_z=0.06) and NegIn (M=48.64, CI.95 [43.98, 53.29], Cohen's d_z=0.13).

Second, we tested how performance on the recognition task varied as a function of Valence and Group using a 2x2 ANOVA. There was no main effect of either Valence (Positive or Negative; F(1,22)=0.07, p=.79, η_p^2=.003) or Group (In or Out; F(1,22)=0.002, p=.97, η_p^2<.001). There was a significant Valence*Group interaction (F(1,22)=7.71, p=.01, η_p^2 =.26), which showed better recognition of Positive compared to Negative in-group members, and vice versa for out-group members. Follow-up analyses interrogated the interaction by comparing recognition of positive and negative information for in- and out-group members separately (Figure 6.2). This revealed a difference for the in-group between positive and negative (Mean difference=7.05, CI.95 [2.22, 11.89], Cohen's d_z=0.63). There was a weaker difference for out-group (Mean difference=6.08, CI.95 [-1.27, 13.43], Cohen's d_z=0.36). Therefore, the direction of the difference was as predicted for both the in-group as well as the out-group, but the effect was stronger for the in-group than the out-group.

Neuroimaging data

Univariate analyses

Main effect: No suprathreshold clusters were revealed within either the body or ToM localiser for the main effect of Valence (Pos vs. Neg) or Group (In vs. Out).

Interaction: The Valence by Group interaction [(PosIn>PosOut) > (NegOut>NegIn)] revealed no suprathreshold clusters when masked by the body or ToM localiser. To explore this null result further, we performed a set of exploratory analyses. First, we removed the voxel extent and clusters emerged in right fusiform gyrus, which overlapped with the body-localiser (FBA), and bilateral temporal poles and left TPJ, which overlapped with the ToM-localiser (Appendix 10.A). Second, we explored the same contrast at a more liberal voxel-wise threshold of p<.05, k=10 (Appendix 10.B). At this more liberal threshold, four clusters emerged within the body-network (bilateral EBA and FBA), and five within the ToM-network (bilateral temporal poles and TPJ, and mPFC). At such a liberal threshold, we do not interpret these results as they could reflect false positives. Instead, we use these univariate analyses as a means to guide the location of seed region specification in subsequent PPI analyses. In line with Chapter 3 and 4, we will only use the clusters emerging at $p<.005$, $k=0$ as seed regions.

Psychophysiological Interaction analyses: Coordinates of overlap within individual participants were identified in right FBA (n=16), temporal poles (left: n=23; right: n=18), and left TPJ (n=19) (for more details, see Appendix 11). We hypothesized that body-selective areas, parts of an affective network and the ToM-network would interact when recalling trait information about people that fit the participant's group bias (positive in-group members and negative out-group members).

For the body-selective seed regions, we tested for connectivity within the ToM-network and affective network. Right FBA showed greater functional coupling with the ToM-network, specifically the right TPJ (Table 6.2.A; Figure 6.4.A). PPI estimates show that the functional coupling was stronger for positive compared to negative in-group members and vice versa for out-group members. In addition, right FBA was functionally coupled with parts of the affective network, including bilateral amygdala, left anterior insula, left striatum, and right OFG (Table 6.2.B; Figure 6.4.B), with the same pattern of functional coupling as described above. PPI estimates show that all clusters show the predicted pattern of response: functional coupling that was stronger for positive compared to negative in-group members and vice versa for out-group members.

For ToM seed regions, we tested for functional connectivity within the body-selective and affective networks. Left TPJ was functionally coupled with right FBA in a manner consistent with our prediction. PPI estimates revealed functional coupling that was stronger for positive compared to negative in-group members and vice versa for out-group members (Table 6.3.A; Figure 6.5.A). There was no other coupling between a ToM seed region and a body-selective region. Within the affective network, left temporal pole was functionally coupled with left anterior insula (Table 6.3.B; Figure 6.5.B). PPI estimates reveal a stronger coupling between left temporal pole and anterior insula when recalling positive in comparison to negative information about in-group members, and the opposite pattern for out-group members. Additionally, right temporal pole was functionally coupled with bilateral amygdala. In contrast to the other patterns of functional coupling, PPI estimates suggest only stronger functional coupling for negative compared to positive out-group members, but indifference in strength for in-group members.

Table 6.2. PPI results based on body-selective seed regions. Clusters revealed in the PsychoPhysiological Interaction (PPI) analysis for the Valence by Group [(PosIn>PosOut) > (NegOut > NegIn)] contrast using the body selective seed region defined by the univariate Valence by Group contrast (right FBA), **A)** masked by the ToM-localiser, and **B)** masked by the affective network.

Region	Number of voxels	Cluster P_{FWE}	Peak *T*	Montreal Neurological Institute coordinates		
				x	y	z
a) Seed region: right FBA masked by ToM-localiser						
Right TPJ	13	.74	4.23	63	-46	37
b) Seed region: right FBA masked by affective network						
Left insula	20	.65	4.17	-36	23	4
Left striatum/superior orbital gyrus	18	.68	4.08	-18	17	-14
Left hippocampus extending into amygdala	25	.57	4.07	-15	5	-26
Right middle orbital gyrus	22	.62	3.66	30	38	-14
			3.49	33	29	-17
Right amygdala	10	.81	3.16	15	11	-23
			3.06	18	2	-17

Note: Regions surviving a voxel-level threshold of p<.005 and 10 voxels are reported. Cluster-level p-values are corrected for the search volume, i.e., the mask created from the localisers. Subclusters at least 8 mm from the main peak are listed.

Table 6.3. PPI results based on theory-of-mind seed regions. Clusters revealed in the PsychoPhysiological Interaction (PPI) analysis for the Valence by Group [(PosIn>PosOut) > (NegOut > NegIn)] contrast using ToM seed regions defined by the univariate Valence by Group interaction (bilateral temporal poles (TP) and left TPJ), **A)** masked by the body-localiser, and **B)** masked by the affective network.

Region	Number of voxels	Cluster p_{FWE}	Peak *T*	Montreal Neurological Institute coordinates		
				x	y	z
a) Masked by body-localiser (EBA and FBA)						
Seed regions: bilateral TP						
No suprathreshold clusters						
Seed region: left TPJ						
Right fusiform gyrus (FBA)	70	.33	4.31	48	-43	-14
b) Masked by affective network						
Seed region: right TP						
Right amygdala	10	.77	3.92	18	5	-14
Left amygdala extending into	12	.74	3.33	-24	-4	-14
hippocampus			3.14	-15	-7	-14
Seed region: left TP						
Left insula	31	.52	3.50	-33	8	4
Seed region: left TPJ						
No suprathreshold clusters						

Note: Regions surviving a voxel-level threshold of p<.005 and 10 voxels are reported. Cluster-level p-values are corrected for the search volume, i.e., the mask created from the localisers. Subclusters at least 8 mm from the main peak are listed.

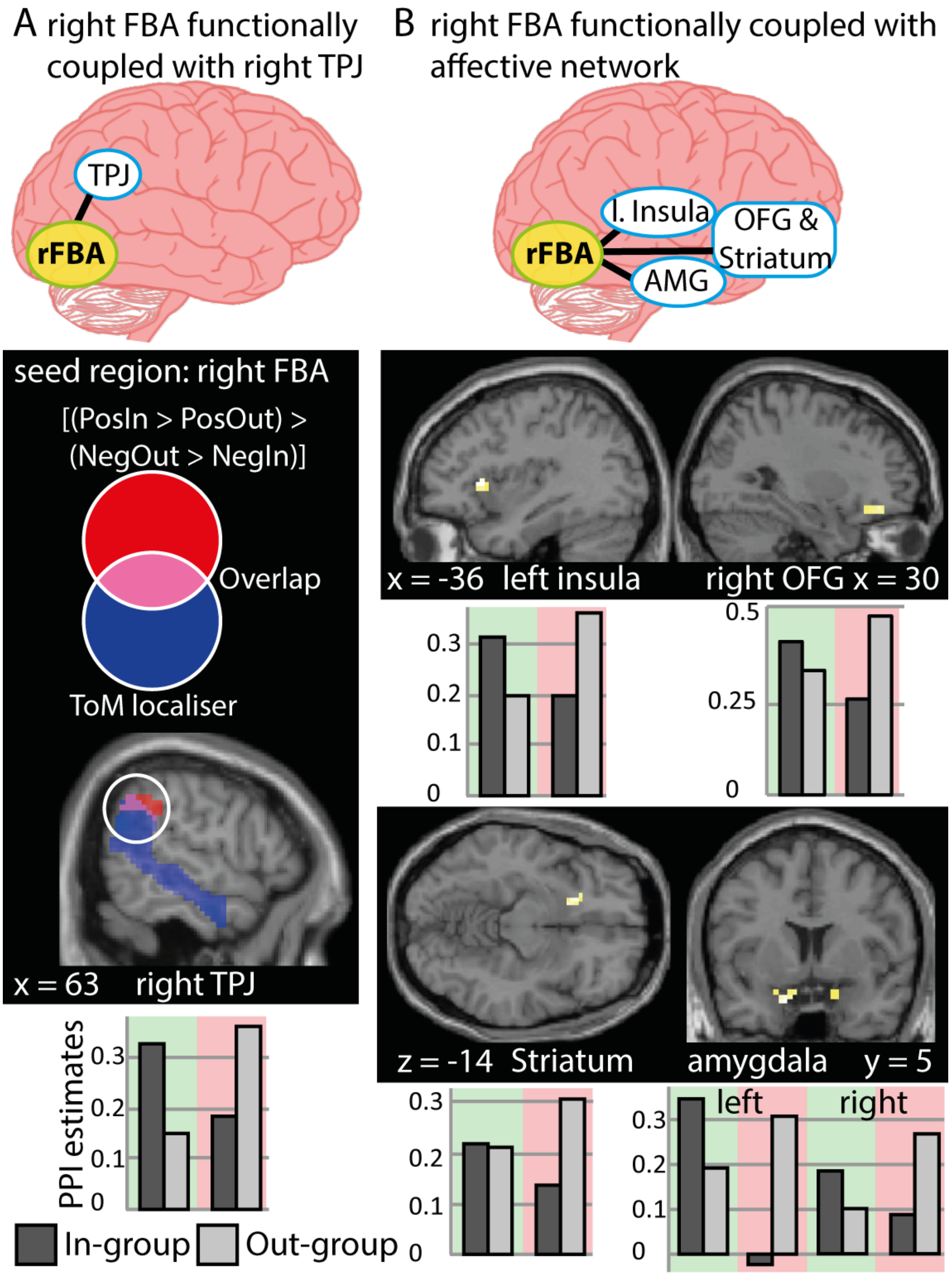

Figure 6.4. Results from the PsychoPhysiological Interaction (PPI) analysis. Seed regions were identified based on clusters emerging from the Valence by Group [(PosIn>PosOut) > (NegOut > NegIn)] contrast at the univariate level (see Appendix 10 and Appendix Figure 3). In this figure, the seed region that is part of the person perception network (right fusiform body area (FBA)) as defined by the body-localiser is presented. In this PPI analysis, right FBA was used as a seed region with the Valence by Group term as the contrast of interest. Clusters emerging from this analysis reveal the strength of correlation over time between activity in that cluster and that in the seed region as a function of the task. These PPI parameter estimates are extracted from a 4 mm sphere around the peak coordinate. **A)** The PPI analysis revealed that seed region right FBA (solid yellow circle) showed functional coupling with a node within the person knowledge network. A cluster in right temporoparietal junction showed greater functional coupling with right FBA when recalling positive and negative traits about in- and out-group members, respectively (shown in red). This area overlapped with the ToM-localiser (shown in blue; overlap is shown in pink). **B)** Seed region right FBA (solid yellow circle) showed functional coupling with several areas within the affective network; bilateral amygdala, left insula, left striatum, and right middle orbital gyrus. These areas were identified based on coordinates from the literature (see Table 6.1).

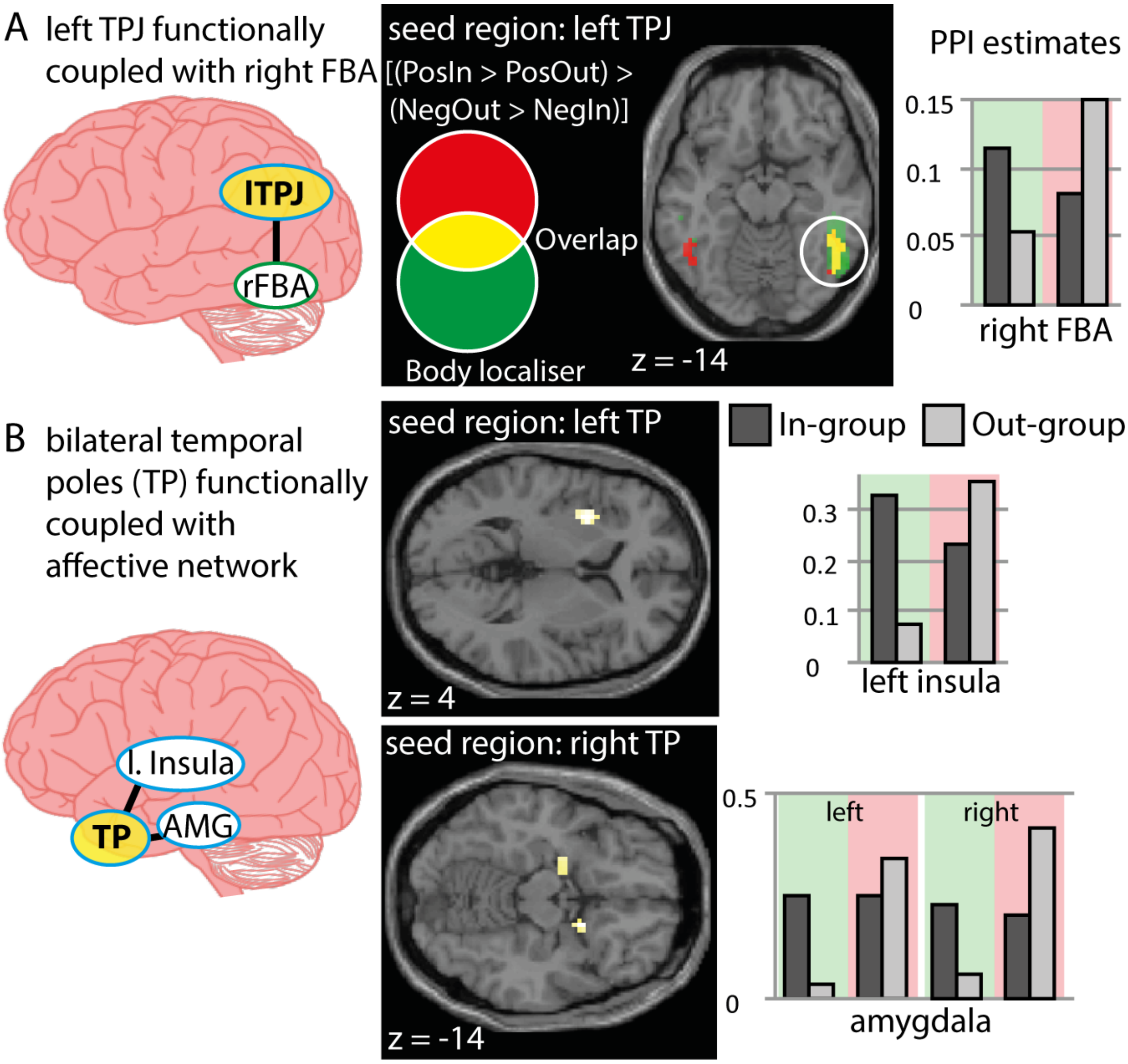

Figure 6.5. Results from the PsychoPhysiological Interaction (PPI) analysis. Seed regions were identified based on clusters emerging from the Valence by Group [(PosIn>PosOut) > (NegOut > NegIn)] contrast at the univariate level (see Appendix 10 and Appendix Figure 3). In this figure, seed regions that are part of the person knowledge network (bilateral temporal poles (TP) and left temporoparietal junction (TPJ)) as defined by the ToM-localisers are presented. In three separate PPI analyses, each identified region from the univariate analysis was used as a seed region with the Valence by Group term as the contrast of interest. Clusters emerging from these analyses reveal the strength of correlation over time between activity in that cluster and that in the seed region as a function of the task. These PPI parameter estimates are extracted from a 4 mm sphere around the peak coordinate. **A)** PPI analyses revealed that seed region left TPJ (solid yellow circle) showed functional coupling with a body-selective patch. A clusters in right FBA showed greater functional coupling with left TPJ when recalling positive and negative traits about in- and out-group members, respectively (shown in red). These areas overlapped with the body-localiser (shown in green; overlap is shown in yellow). **B)** PPI analyses revealed that both TP seed regions (solid yellow circle) showed functional coupling with areas within the affective network. Left temporal pole was coupled with left insula, while right TP showed increased functional coupling with bilateral amygdala. These areas were identified based on coordinates from the literature (see Table 6.1).

Discussion

In everyday social interactions we have only a limited amount of information to make inferences about people's traits and character. Such impoverished social knowledge typically leads to generalized judgments based on social categories, typically involving in-group favouritism and dislike of out-group members (Allport, 1954; Brewer, 1999; Stangor, 2014). Previous neuroscience research has revealed that differential engagement of perceptual, affective, and cognitive neural systems underlies such group-biases (Molenberghs, 2013; Amodio, 2014). However, the potential interaction between these widespread neural circuits as a function of group membership has received little attention. In the current study, participants observed bodies with an in-group or out-group affiliation that cued the recall of positive or negative social knowledge. We report that when body shape and posture do not differ and all bodies had previously been paired with the same type of trait-based information (positive or negative), functional coupling between perceptual, affective, and cognitive neural networks is dependent both on valence and group membership. Specifically, these three neural networks couple more when positive information is cued for in-group members and out-group members cue negative information. In sum, this study is the first demonstration of neural network integration during group bias modulation of person perception.

Neural network integration during group bias modulation of person perception

Several distinct neural circuits have been shown to contribute to detecting and managing interactions with other group members (Golby et al., 2001; Van Bavel et al., 2008; Volz et al., 2009; Contreras et al., 2012; Molenberghs et al., 2016). From these studies it is clear that a suite of functional processes and neural circuits contribute to seeing, feeling, and reasoning about others in terms of "us" and "them" (Molenberghs, 2013). Here we show that in a minimal group paradigm (Tajfel et al., 1971), three networks interact when participants form an impression of several bodies of in-group and out-group members based on what they learned about them before. The right FBA, involved in holistic body processing (Peelen and Downing, 2007; Downing and Peelen, 2011), exchanged signals with bilateral TPJ, an area associated with representing others' thoughts and traits (Saxe and Kanwisher, 2003; Mitchell, 2009; van Overwalle, 2009). Additionally, right FBA and bilateral temporal poles were connected with areas part of an affective neural network comprising the amygdala, insula, striatum, and OFC (Keysers and Gazzola, 2009; Fan et al., 2011; Bartra et al., 2013; Eres and Molenberghs, 2013). This suggests that detecting, feeling, and reasoning about in-group and out-group members involves communication between perceptual, affective, and cognitive neural network.

It has previously been revealed that core areas in the person perception network areas interact with the amygdala when processing *dynamic* features of a person, such as facial expression (Fairhall and Ishai, 2007), and with areas in the person knowledge network when associating multiple simultaneously presented features (social knowledge and bodies) online (Greven et al., 2016). The bodies in the current experiment were *static*, with a neutral posture, and the social knowledge had been associated with the bodies *prior* to scanning. Our data suggest that also when *recalling* social information cued by a body alone, "core" person perception and person knowledge areas (right FBA and right temporal pole, respectively) communicate with an extended network, and together are necessary for the (biased) evaluation of a person.

From our data, we cannot determine the functional role of the individual links revealed in this study and thereby distinguish the functional connections from each other. However, as previous work has attributed specific distinct functional roles to areas within the person perception, person knowledge, and affective networks, it is possible to speculate about the functional contribution that these separate links make to group-bias. For instance, the TPJ is consistently shown to be preferentially engaged when reasoning about another person's beliefs and mental states compared to other cognitive tasks (Carrington and Bailey, 2009; van Overwalle, 2009; Saxe, 2010; Dodell-Feder et al., 2011), and our ToM-localiser data replicates this pattern of results also. However, TPJ has also been associated with processes such as exogenous (stimulus-driven) and endogenous (influenced by motivational states) attentional guidance (Decety and Lamm, 2007; Shulman et al., 2007; Scholz et al., 2009; Frank and Sabatinelli, 2012; Donaldson et al., 2015; Krall et al., 2015). Considering the suggested stronger motivation to individuate members of the in-group compared to the out-group (Golby et al., 2001; Azevedo et al., 2013), as well as the greater sensitivity to immoral actions of out-group compared to in-group members (Molenberghs et al., 2016), the here-presented interaction between TPJ and right FBA could possibly reflect a difference in motivation to process bodies that are remembered to have characteristics consistent with the group-bias.

Both right temporal pole and right FBA interacted with bilateral amygdala, which is involved in processing the affective valence of biologically and socially relevant stimuli (Whalen, 1998; Costafreda et al., 2008; Adolphs, 2010; Morrison and Salzman, 2010; Pessoa, 2010). It is possible that in-group and out-group members who fit their social category are socially more relevant (Oakes et al., 1991; Otten and Moskowitz, 2000). The coupling between the amygdala and right temporal pole and right FBA might therefore reflect a stronger exchange of signals when processing socially relevant stimuli.

Additionally, the left temporal pole was connected with left mid to anterior insula, and right FBA with left anterior insula, an area found to be recruited in both affective and cognitive empathy (Fan et al., 2011). Because it is thought to be responsible for functional integration of different functional systems, such as emotion and memory (Kurth et al., 2010), we speculate that the left temporal pole, a core ToM node associated with recalling person knowledge (Olson et al., 2007, 2013), may communicate with the anterior insula to remember the affective value of a person based on their group membership. Lastly, right FBA was functionally coupled with left striatum and right OFC, which have commonly been associated with processing reward and subjective value (Seymour et al., 2007; Kahnt et al., 2012; Bartra et al., 2013), suggesting that participants might have assigned different weights to positive and negative trait-based information depending on group membership.

Limitations and future directions

Apart from the suggestions for functional roles given above, it may be that the stronger coupling for positive compared to negative in-group members and vice versa for out-group members reflects a difference in memory for these people. Participants had above chance-level recognition for people displaying behaviours that fit the social categorisation (positive in-group and negative out-group members), while the other were more easily forgotten (performance was at chance-level). However, such a memory bias was not observed in the pilot data, and as the retention time in the pilot experiment was shorter (~7.5 minutes) than it was in the fMRI experiment (>1 hour), it would be expected that soon after encoding, when participants were being scanned, no memory difference would be observed.

Moreover, the connectivity reported here does not survive FWE correction. As such, these results should be taken with caution. Since we considered a two-by-two factorial analysis in this study, there is less data in each regressor compared to the regressors in Chapter 5 (where Positive and Negative for Blue and Yellow combined were compared to Neutral for Blue and Yellow combined). The weaker effects in the connectivity effects could be explained by this.

Furthermore, as functional connectivity analyses are correlational, and thus bi-directional, the current study provides no direct insight into the underlying neural pathway that controls functional coupling between brain areas. Research using diffusion MRI has validated anatomical studies by imaging the white matter connectivity between several areas that are revealed in the current study (Flynn et al., 1999; Ghashghaei and Barbas, 2002; Rilling et al., 2008; Cerliani et al., 2012; Jakab et al., 2012; Le Bihan, 2012). Once we take into account the structural connections, the directional connectivity between areas within the three neural networks could be explored using event-related potentials (ERPs) from EEG. As this methodology has better temporal resolution in comparison to fMRI, directional connectivity from ERPs can investigate how perceptual nodes influence affective and cognitive nodes, as well as how they in turn alter the response in the perceptual network.

Finally, PPI does not allow for an investigation of functional connectivity between body-selective, ToM, and affective nodes that occurs during all conditions. It is possible that information about the person’s personality is shared between these nodes also when the valence does not fit with the group bias. Therefore, the results of the functional connectivity in this study reflect an exchange of information specific to bodies whose trait-characteristics fit their stereotype. However, it remains unclear what information is exchanged between these areas.

Conclusion

In sum, the valence and group dependent modulation of neural network integration during person perception found in the current experiment provides evidence that perceptual, cognitive, and affective neural networks do not work in isolation. Instead, the current study provides empirical evidence that these neuroanatomically distinct networks bias each other to give rise to a representation of another person’s identity (Haxby et al. 2000; Collins and Olson 2014; Ramsey et al. 2011; Ishai 2008; Moeller et al. 2008).

CHAPTER 7

GENERAL DISCUSSION

The studies comprising this thesis have examined the circumstances under which distributed neural networks interact with one another during the detection and recognition of others, using a neuroimaging approach with functional connectivity analyses. In all empirical chapters, I investigated how person perception and person knowledge networks interact under varying circumstances, such as when making a first impression, or when recalling that impression later on. Additionally, in Chapter 6, I investigated how both the person perception and person knowledge networks interact with an affective neural network. In the following summary section, I will highlight the main findings from each empirical chapter and briefly discuss the continuum of task-dependency on which the social judgments lie. Next, I will outline implications for research on person perception and possible mechanisms for the functional integration during social interactions. Finally, I will suggest directions for future research.

7.1. Summary of findings

In the first empirical chapter (Chapter 3) I investigated how physical features of a social agent are linked to social knowledge that could be inferred from behavioural descriptions, similarly to how we form impressions when we initially meet someone. I showed that functional connectivity between the person perception and person knowledge networks was greater when the agent was a body (rather than a name) paired with trait-based (rather than neutral) information. These data suggest that person perception and person knowledge networks are not completely encapsulated and resistant to influence from other brain systems.

In order to investigate how social signals are extracted from the visual image of the body alone, in Chapter 4 the body shapes differed across conditions. Body-type conditions were created based on an item-analysis of two separate pilot experiments to invoke distinct judgments (i.e., muscular and obese bodies were rated differently to neutral bodies on perceptions of personality and health). However, a ‘social evaluation’ vs. ‘neutral’ comparison in the neuroimaging analyses (both univariate and functional connectivity) did not reveal a difference in the neural networks that support person perception when performing a purely perceptual task. It may be that the links between person perception and person knowledge networks are subtle and our study was not sensitive enough to detect them.

In Chapter 5, I investigated neural network integration when social knowledge is recalled based on physical features of the body. While in Chapter 3 impressions were formed online, in this chapter participants relied on the impression they had previously formed of each person during a prior task outside the scanner. Our data revealed stronger neural network integration when recalling trait-based rather than neutral information. This extends previous work demonstrating the involvement of, but not interaction between, both perceptual and inferential neural networks when encoding and recalling social information about a person (Mitchell et al., 2004; Todorov et al., 2007; Vrtička et al., 2009; Cloutier et al., 2011; Gilron and Gutchess, 2012).

Unlike the previous chapters, where evaluative judgments were compared to neutral information, the analyses presented in Chapter 6 differentiated between affective valences of trait-based judgments. While Todorov et al. (2007) demonstrated the involvement of an area within the ToM-network when spontaneously recalling negative compared to positive social knowledge, this study sought to investigate the influence of both valence and group membership on the interaction between perceptual, inferential, and affective neural networks. Behavioural research has shown that we better remember behavioural descriptions that fit with a person’s stereotypical social category (Oakes et al., 1991; Otten and Wentura, 2001). Furthermore, neuroimaging research has demonstrated that we are more sensitive to positive and negative behaviour displayed by the in-group and out-group, respectively (Molenberghs et al., 2016). The data in Chapter 6 provide insight into the complex nature of neural network integration when recalling trait-based information that was cued by bodies who were either in-group or out-group members. Specifically, person perception, person knowledge, and affective neural networks show a stronger functional coupling when positive information is cued for in-group members and out-group members cue negative information.

Taken together, the chapters in this thesis provide empirical evidence supporting the view that a “who” system for social cognition spans perceptual and inferential mechanisms and that these mechanisms communicate to each other when forming a representation of another’s identity (Haxby et al. 2000; Collins and Olson 2014; Ramsey et al. 2011; Ishai 2008; Moeller et al. 2008). It adds to a growing body of research demonstrating that complex social interactions rely on equally complex interactions between neuroanatomically distinct circuits, and that the integration depends on the type of task participants have been given.

7.2. Task-dependency of social inferences

In everyday life, the intentionality of the inferences we make varies. When on a first date, you will do your best to see what your prospective partner is like, while also figuring out what they might think of you. In other circumstances, for instance when walking down the street, you might be thinking about what you will have for lunch, and you pay little attention to the people around you. Suddenly, you notice a person with broad shoulders and tremendously muscular arms, and you might think about how they must be vain, but still very disciplined. Likewise, the inferences made in psychological experiments vary in intentionality, or task-dependency. As I will outline below, the chapters in this thesis show that functional integration between neuroanatomically distinct networks varies with the degree of task-dependency, from no functional integration (when social inferences were entirely task-independent) to functional integration between different nodes within perceptual, inferential, and affective networks (during task-dependent social inferences).

The study presented in Chapter 4 lies on one end of a continuum of task-dependency. Participants were not informed of the different body-types they would observe in the scanner. Moreover, they were not instructed to form impressions or make social judgments, but instead to press a button whenever they saw the exact same body twice in a row. Therefore, any functional integration between person perception and person knowledge networks when observing the bodies that give rise to a more salient social inference would reflect spontaneous or task-independent social judgments. Although the study yielded no significant interactions, we will not interpret these null results as evidence that participants did not socially evaluate these bodies, for two reasons. First, classical null-hypothesis statistical testing procedures do not allow us to quantify the degree of evidence in favour of the null-hypothesis (e.g., Schervish, 1996). Second, our pilot studies for Chapter 4 as well as a plethora of behavioural and neuroscientific research show that the observer's social inferences and empathetic responses differ depending on people's body-type (Puhl and Heuer, 2009; Sell et al., 2009; Azevedo et al., 2014; Stulp et al., 2015).

In a previous experiment employing a perceptual 1-back task, Todorov et al. (2007) demonstrated the spontaneous involvement of the person perception and person knowledge networks when observing faces that had previously been associated with social knowledge versus novel faces. This task resembles the one employed in Chapter 4, and can be placed close to it on the task-dependency continuum: while the impressions formed during the 1-back task were spontaneous, participants had actively associated social information prior to entering the scanner. In Chapter 5, I aimed to extend Todorov et al.'s findings by examining the functional integration of person perception and person knowledge networks during recall of social information cued by physical features. Participants were explicitly asked to recall what they had previously learned about that person and to base their impressions on that. Results revealed stronger neural network integration during recall of trait-based rather than neutral information, suggesting that social information stored in memory is sufficient to prompt the interaction between person perception and person knowledge nodes. Additionally, EBA and FBA are functionally connected under the same circumstances. The interaction between EBA and FBA – with FBA holding a holistic representation of bodies – could reveal a reciprocal exchange of visual information that contributes to determining a person's identity (Taylor et al., 2007; Ewbank et al., 2011; Brandman and Yovel, 2016).

With the completely task-independent Chapter 4 on one end of the continuum, Chapter 3 can be placed at the other end. Here, participants were asked to form an impression of the people they saw based on the concurrently presented behavioural descriptions. Consistent with Chapter 5, functional connectivity between person perception and person knowledge circuits was strongest for impressions made when bodies were paired with trait-based information. Unlike Chapter 5, the results did not reveal functional connectivity within the person perception network. As participants in this study saw each body for the first time and only once, it is possible that the interaction between EBA and FBA is not only dependent on the task, but also on whether the representation of a person's identity has already been stored.

These tasks all relied on the assumption that participants made individuated social judgments. In Chapter 6, participants were still asked to make individualised judgments, but the analyses allowed for an examination of judgments that relied on social categorisations. Previous work has demonstrated stronger functional coupling between the person perception network and dorsolateral prefrontal cortex (DLPFC) when participants categorised, based on gender, people who wore outfits that defied gender norms (Quadflieg et al., 2011). The authors concluded that this domain-general area was likely to be involved in limiting stereotypical thinking by influencing person perception areas to stay focused on the task (Mansouri et al., 2009). In Chapter 6, participants were not instructed to limit their stereotypical thinking, nor were they explicitly instructed to make different judgments based on group membership. Therefore, the valence-dependent group bias modulation of functional connectivity between person perception, person knowledge, and affective neural networks might have given rise to biased judgments that are task-independent.

The chapters in this thesis thus lend empirical support to the view that, in order to accomplish cognitively elaborate functions, functionally segregated patches of cortex should flexibly interact with each other in a way that is context- or task-dependent (Mesulam, 1990; Friston and Price, 2001).

7.3. Implications for person perception

7.3.1. Degrees of modularity in the person perception network

In the general introduction I described the distinct patches of cortex along the ventral visual stream that respond selectively to bodies: EBA is involved in featural processing of whole bodies and body parts (Downing et al., 2001; Pourtois et al., 2007; Urgesi et al., 2007), whereas FBA is involved in a more holistic processing of the body (Peelen and Downing, 2005; Taylor et al., 2007; Brandman and Yovel, 2016). The localiser used throughout this thesis confirmed that these two areas respond stronger to bodies in comparison to cars.

However, this level of specificity is still contested (Kanwisher and Dilks, 2013). While many researchers agree that the high-order perception of bodies is regionally specific to EBA and FBA, they broaden the scope of what these areas can accomplish. Whereas Mesulam (1990) noted that complex cognitive problems cannot be solved by one region alone, several researchers have expanded the functional specificity of EBA and FBA to include the selective coding for bodily actions, embodiment, aesthetic perception, and mental imagery (Astafiev et al., 2004; Arzy et al., 2006; Kable and Chatterjee, 2006; Blanke et al., 2010; Calvo-Merino et al., 2010; Marsh et al., 2010; Limanowski et al., 2014).

The debate on whether or not the functional specificity of these regions is limited to the visual analysis of bodies risks to be fruitless (Colombo, 2013). Instead, it should be acknowledged that brain regions can be both category-specific and, at the same time, be part of complex neural networks where individual regions interact with each other to accomplish cognitively elaborate tasks (Mesulam, 1990; Fuster, 1997; Sporns et al., 2005; Downing and Peelen, 2011; Colombo, 2013; Sporns, 2014). Functional segregation might even be the result of functional coupling among distributed regions. It has been demonstrated that organisation of category-selectivity in the occipitotemporal cortex may have emerged because of the connectivity constraints imposed by a widely distributed network (Mahon and Caramazza, 2011; Hutchison et al., 2014; He et al., 2015). Functional segregation and functional integration are therefore not mutually exclusive.

In an attempt to explain some of the claims described above, inspiration could be drawn from the extensive literature on face perception, which has highlighted the exchange of signals between core and extended networks (e.g., Mechelli et al., 2004; Zhen et al., 2013; He et al., 2015; Hermann et al., 2015). For instance, Mechelli et al. (2004) demonstrated that category-specific patterns of activation observed during visual perception and imagery are mediated by bottom-up and top-down mechanisms, respectively. Specifically, when observing faces and objects, category-specific patterns of activation are mediated by increased bottom-up connectivity from early visual cortex (inferior occipital cortex). On the other hand, category-specific activation as a result of imagining faces or objects was associated with increased top-down connectivity from prefrontal cortex. Likewise, the greater activation in EBA seen when mentally imagining oneself in a certain position (Arzy et al., 2006; Blanke et al., 2010) may instead be the result of top-down influence from anterior brain regions.

7.3.2. Implications for a middle ground view

The results presented in this thesis add to a middle ground view stating that patches of cortex in the person perception network, although selectively responding to bodies, are not completely impermeable to influences from other brain regions. Chapters 3, 5, and 6 demonstrate that, in different situations, different parts of the core person perception network interact with extended networks that are tasked with reasoning about and empathising with the observed person.

The work in my thesis is not the first to propose this view (Haxby et al., 2000; Gobbini and Haxby, 2007; Minnebusch and Daum, 2009; Kanwisher, 2010; Amoruso et al., 2011). Kanwisher (2010) noted that “most questions about biological systems are matters of degree, and so too is the question of functional specialisation in the cortex”. She added that the response in functionally specialised regions can be strongly modulated, for instance, by visual attention (Wojciulik et al., 1998; Seidl et al., 2012). One possible example of attentional modulation in the current thesis is the functional coupling of FBA with TPJ found in Chapter 6. Although part of the ToM-network, TPJ has also been associated with exogenous (stimulus-driven) and endogenous (influenced by motivational states) attentional guidance (Decety and Lamm, 2007; Shulman et al., 2007; Scholz et al., 2009; Frank and Sabatinelli, 2012; Donaldson et al., 2015; Krall et al., 2015). Functional coupling was found under circumstances that could reflect a difference in motivation to individuate members of the group who displayed behaviours stereotypically consistent with their group membership (Oakes et al., 1991; Golby et al., 2001; Otten and Wentura, 2001; Azevedo et al., 2013;

Molenberghs et al., 2016). Under these circumstances, the responses in FBA are still domain-specific but are modulated by a difference in motivation to reason about people.

Neuronal activity in perceptual regions is also strongly modulated by the emotional content of stimuli, and the amygdala plays a key role in this process through reciprocal connections with perceptual regions (Phelps, 2004; Adolphs, 2010). Additionally, the amygdala is involved in processing socially relevant stimuli (Whalen, 1998; Costafreda et al., 2008; Adolphs, 2010; Morrison and Salzman, 2010; Pessoa, 2010). In the task employed in Chapters 5 and 6, a participant might instantly recognise the person they see because they associated that person with social information that strongly mattered to them (e.g., “His hamster died because he forgot to feed it”). Prior research suggests that positive information was more important for in-group members while, for out-group members, negative information was more relevant (Oakes et al., 1991; Otten and Wentura, 2001). When observing bodies that cued recall of bias relevant information (positive for in-group and negative for out-group members), FBA was functionally coupled with bilateral amygdala. This is in line with the results from Schiller et al. (2009), who showed that the amygdala was active when encoding social information that was relevant for the subsequent evaluation of a person compared to when social information was irrelevant. It may thus be that the amygdala interacted with FBA to enhance perception and potentially prioritise the encoding of emotional events (Phelps, 2004; Phelps and LeDoux, 2005).

Thus, I am not debating the domain-specificity of responses in EBA and FBA. The thorough investigation of domain-specificity has provided strong evidence that there are cortical regions responsible for the privileged and accurate detection of another person in complex natural scenes (Downing et al., 2004; Peelen and Downing, 2007; Bindemann et al., 2010; Stein et al., 2012; van Koningsbruggen et al., 2013; Downing and Peelen, 2015). However, the rapidly acquired visual analysis of a person needs to be shared with other brain regions to influence behaviour. Imagine it is late at night and you are at the train station. You see a tall figure, his broad shoulders hunched and his huge arms folded, standing on the platform where you need to be. Had you not known him, you would have kept your distance to avoid potential harm, as his posture seems intimidating. However, possibly through the influence of the temporal poles, you recognise him and recall what you know about him (it’s your colleague, Harm, who is good-natured and likes to play the piano). So, instead of avoiding him, you decide to approach him. While the perceptual input is the same, the behavioural outcomes differ. In the latter situation, it is probable that person perception nodes are more active compared to when you observe someone with a less intimidating body shape whom you do not know. Instead of expanding the functional role of the person perception network to include social evaluation, it is important to examine the brain areas with which this network interacts during person perception. Indeed my thesis has shown that, in order for social interactions in a complex environment to run smoothly, it is necessary for functionally segregated patches to pass signals back and forth to other brain areas.

7.4. Future research

Although the studies in my thesis demonstrate that domain-specific areas interact with neural networks involved in affective and cognitive processes, the correlational functional connectivity analyses provide no direct insight into either the direction of the interactions or the underlying neural pathways. Furthermore, PPI does not allow for an investigation of functional connectivity that is present during all conditions. In Chapter 4, where participants performed a perceptual task with silhouettes of bodies that differed categorically in shape, the apparent lack of functional interplay between person perception and person knowledge could be the result of a functional connectivity that is always present. Additionally, as PPI cannot detect learning, it is possible that there was functional interplay during the first run, but disappeared as participants learned what stimuli would be presented, causing them to lose sensitivity. I will suggest several methodological approaches that can help advance our knowledge of the neural pathways that underlie functional relationships between person perception and person knowledge systems.

7.4.1. Structural connectivity

Functional connectivity between body-selective nodes and bilateral temporal poles was found in both Chapters 3 and 5. Neuroanatomical studies as well as studies using diffusion MRI (Le Bihan, 2012) have provided evidence that the occipital and anterior temporal regions are connected via a white matter associative tract, the inferior longitudinal fasciculus (Catani et al., 2003; Saygin et al., 2012; Gomez et al., 2015; Hodgetts et al., 2015). While it is possible for the functional connectivity between these areas to reflect a direct connection, it is not possible to infer what is exactly accomplished through this interaction.

It has been suggested that the temporal poles may bind together complex information from different modalities together (e.g., physical features and trait-based information; Olson et al., 2007, 2013). The functional interaction with FBA revealed in Chapter 3 could thus reflect the stream of information about the physical features to the temporal poles, where it is stored for later use. Indeed, when recalling trait-based information that was cued by a person's physical features, as was done in Chapter 5, the temporal poles functionally interacted with body-selective nodes. Although much research supports the view that the temporal poles are involved in retrieving social knowledge specifically (Simmons and Martin, 2009; Simmons et al., 2010; Drane et al., 2013), it has also been argued that it serves a more general function related to conceptual knowledge (Rogers et al., 2004, 2006; Patterson et al., 2007). Future research will need to distinguish the particular circumstances that modulate the direct interaction between these areas.

Another area within the person knowledge network that has been proposed to both encode person specific information and accurately retrieve social knowledge from semantic memory is mPFC (Mitchell et al., 2004; Gilron and Gutchess, 2012; Satpute et al., 2013; Welborn and Lieberman, 2014). The results in Chapter 5 reveal stronger functional coupling between mPFC and body-selective areas, which is unlikely to be the result of a direct anatomical connection. The reason is that the human brain has greater local interconnectivity with a short mean distance between connected brain regions (small-world brain network; Bassett and Bullmore 2006; Gong et al. 2009; Vaessen et al. 2010). The functional coupling with mPFC could instead reflect an indirect pathway via other areas within the ToM-network, such as the temporal poles. While individual areas within the person knowledge network likely interact with each other, this was outside the scope of my thesis, which investigated the functional integration of neuroanatomically distinct networks.

Chapter 6 revealed complex interactions between regions within the affective network (amygdala and left anterior insula) and right FBA as well as bilateral temporal poles. It is known that the amygdala receives and sends projections to a variety of regions in the brain, among which the occipital and insular cortices and temporal poles (Aggleton et al., 1980; Amaral and Price, 1984; Iwai and Yukie, 1987; Catani et al., 2003; LeDoux, 2007). It is thus possible that FBA and the temporal poles exchange signals with the amygdala directly, which in turn exchanges signals with the insula. Alternatively, FBA and the temporal poles could interact directly with both the amygdala and insula. The analyses employed in the current thesis cannot distinguish between these options, but structural connectivity approaches might help.

7.4.2. Effective connectivity

Investigating the effective connectivity between brain areas that are anatomically connected can further inform us on the direction of such interactions under varying circumstances and in different contexts (Friston et al., 2003; Stephan and Friston, 2010). These connectivity methods (e.g., dynamic causal modelling [DCM]) rely on Bayesian statistics, where the evidence for different models is estimated. These models need to be carefully motivated, since they should accurately explain the data while still having minimal complexity (Stephan et al., 2010). The brain regions used in this method (nodes) and the input from one node to the other is pre-specified. These nodes can be chosen based on anatomical connections (e.g., the inferior longitudinal fasciculus connecting the temporal poles and occipitotemporal cortex; Catani et al., 2003) and/or prior research that has demonstrated a robust and replicable involvement of a circuit during a specific function (e.g., activation of the ventral premotor cortex and inferior frontal gyrus during the observation and execution of actions; Kilner et al., 2007a; Kilner and Lemon, 2013). The way in which these nodes potentially influence each other (through top-down or bottom-up effects) can then be modelled by specifying how deterministic inputs (e.g., images of bodies) and internal states (e.g., attention) exert changes on connectivity. Even with the minimal amount of nodes, this can result in a large number of models that need to be tested (e.g., 59 models for 2 nodes: Ewbank et al., 2011). The method in the current thesis used a whole-brain approach, and could identify and has indeed identified which nodes within the person perception and person knowledge networks functionally interact. Future research could use these nodes to test the effective connectivity between them, not only under varying circumstances, but also whether this connectivity occurs for each condition.

During first impressions, the person perception network will respond to the physical features of an individual, while inferring character traits from their behaviour will engage the person knowledge network. When no prior knowledge is present, information about these physical features will be associated to knowledge of their traits, a process thought to be subserved by the temporal poles (Olson et al., 2007, 2013). The functional coupling found in Chapter 3 could therefore reflect a feed-forward connection from FBA to the temporal poles. The temporal poles will hold a personal memory for the multiple features that together represent a person’s identity, and can in turn influence the person perception network when this individual will be encountered again in the future. In Chapter 5, participants were told they would see the exact same pictures of bodies again. In the scanner, the bodies were grouped together according to the type of information they were associated with (positive, negative, neutral). After the first two bodies cued the recall of positive social knowledge, the participant might start expecting to see a person that had been associated with positive knowledge. Thus, these results could reflect a connection from the temporal poles to EBA and FBA to predict what the visual input will be.

The functional interactions found in Chapter 6 are more complicated, as both perceptual and mentalizing nodes coupled with several regions within the affective network. Given the poor temporal resolution of fMRI, it is impossible to determine whether these functional interactions represent parallel as opposed to sequential processes, where information about the body's identity is sent to the amygdala, which in turn exchanges information with the temporal poles about the behaviours associated with that particular body. Effective connectivity analyses could be conducted on electroencephalography (EEG) data, which has better temporal resolution in comparison to fMRI. Together, these analyses can better investigate how perceptual, cognitive, and affective nodes influence each other.

7.4.3. What causes the integration to happen?

Many different proposals have been put forward to explain how signals are exchanged between functionally segregated patches of cortex: Mesulam (1990) proposed simultaneous interactions, while others proposed a hierarchical organisation (Fuster, 1997). I want to consider how functions associated with person perception can be understood within a predictive coding framework, where perceptual information is processed in a hierarchical manner in order to minimise the prediction error through recurrent or reciprocal interactions (Kilner et al., 2007b; Friston and Kiebel, 2009; Friston, 2010). Information extracted from a person's physical features is passed on by forward connections (feedforward model) to regions that hold a personal memory for this person along with all the associated social knowledge (e.g., temporal poles, Olson et al., 2007, 2013). Implicit in the hierarchical predictive coding framework is that in addition to the feedforward model, anterior regions can form a prediction of what the visual input is going to be at the lower processing level.

With increasing experience (e.g., seeing a person from different viewpoints or in various types of clothing that influence how much of the body shape is occluded), the predictions for the possible perceptual input will become more and more accurate. Not only prior experience with a person's physical features, but also the context and environment in which you see them, influences person identification. When I am in Bangor, I will easily and quickly recognise my colleague. Even under conditions where visual input is impoverished (it rains a lot here), her thin frame, long brown hair, and gait will quickly inform me on her identity. In this case, the temporal poles would generate a prediction of what the person looks like, which is then compared to the actual visual input in EBA and FBA. However, when I am in my hometown in the Netherlands, I do not expect to see her. In this different setting, I could see her and initially think she is someone else who happens to have similar physical features. The prediction generated by temporal poles would, in this case, be false. As perceptual evidence accumulates in the body patches, the recognition of my colleague may depend on a feedforward model where EBA and FBA provide information to anterior brain regions (Ploran et al., 2007, 2011).

Apart from increased experience with a person's physical features, you also gain more experience with their trait characteristics. If you get to know someone as conscientious, responsible, and empathetic, you will not expect people to refer to him when they say that his hamster died because he forgot to feed it. In this example, the valence of the traits changed but not the intensity. It could also be that you've learned about someone as an even-tempered person, who is generally nice but not in an exceptional way. Your prior experience in this example will not lead to expect behaviours, positive or negative, such as donated a large sum of money to charity, becoming a foster parent, or driving off after causing an accident. Future research could investigate whether more extreme traits lead to increased functional or effective connectivity between body-selective, ToM, and affective nodes, and whether (violations of) expectations on the extremity can change the direction of influence between these nodes.

The predictive coding framework offers explanations of a potential mechanism for how familiarity and different contexts influence recognition. While this is definitely not the only framework that can explain functional integration, predictive coding has shown much promise (e.g., Rao and Ballard, 1999; Rauss et al., 2011; Apps and Tsakiris, 2013).

7.5. Conclusions

The results of the work described in this thesis provide novel insights into the circumstances under which neuroanatomically distinct networks communicate during social interactions. Both when forming a first impression and when recalling this impression at a later time point, body-selective nodes are functionally coupled with areas associated with person knowledge processes. The visual analysis of bodies that are often socially stereotyped and stigmatized did not show statistically significant neural network integration compared to neutral bodies. Conversely, when forming an impression was explicitly requested and social evaluation on group membership was task-independent, person perception and person knowledge circuits reliably communicated with regions involved in affective processing.

These findings highlight the importance of an integrative perspective when investigating the role of functionally segregated brain regions in a larger interconnected network. Such a multifaceted approach will better inform us on the role that purely perceptual areas play in cognitively elaborate functions, ultimately elucidating how neural network integration is flexibly modified by perceptual, cognitive, and social contexts.

7. GENERAL DISCUSSION

REFERENCES

Adolphs R (1999) Social cognition and the human brain. Trends in Cognitive Sciences 3:469–479.

Adolphs R (2009) The social brain: neural basis of social knowledge. Annual Review of Psychology 60:693–716.

Adolphs R (2010) What does the amygdala contribute to social cognition? Annals of the New York Academy of Sciences 1191:42–61.

Adolphs R, Tranel D, Damasio AR (2003) Dissociable neural systems for recognizing emotions. Brain and Cognition 52:61–69.

Aggleton JP, Burton MJ, Passingham RE (1980) Cortical and subcortical afferents to the amygdala of the rhesus monkey (Macaca mulatta). Brain Research 190:347–368.

Aguirre GK (2007) Continuous carry-over designs for fMRI. NeuroImage 35:1480–1494.

Allport GW (1954) The Nature of Prejudice. Cambridge, Massachusets: Addison-Wesley Publication company.

Amaral DG, Price JL (1984) Amygdalo-cortical projections in the monkey (Macaca fascicularis). Journal of Comparative Neurology 230:465–496.

Amodio DM (2014) The neuroscience of prejudice and stereotyping. Nature Reviews Neuroscience 15:670–682.

Amoruso L, Couto B, Ibáñez A (2011) Beyond extrastriate body area (EBA) and fusiform body area (FBA): context integration in the meaning of actions. Frontiers in Human Neuroscience 5:1–3.

Apperly IA (2013) Can theory of mind grow up? Mindreading in adults, and its implications for the development and neuroscience of mindreading. In: Understanding other Minds, 3rd ed. (Baron-Cohen S, Tager-Flusberg HB, Lombardo M, eds). Oxford University Pres.

Apps MAJ, Tsakiris M (2013) Predictive codes of familiarity and context during the perceptual learning of facial identities. Nature communications 4:1–10.

Arzy S, Thut G, Mohr C, Michel CM, Blanke O (2006) Neural basis of embodiment: distinct contributions of temporoparietal junction and extrastriate body area. Journal of Neuroscience 26:8074–8081.

Astafiev S V, Stanley CM, Shulman GL, Corbetta M (2004) Extrastriate body area in human occipital cortex responds to the performance of motor actions. Nature Neuroscience 7:542–548.

Atkinson AP, Dittrich WH, Gemmell AJ, Young AW (2004) Emotion perception from dynamic and static body expressions in point-light and full-light displays. Perception 33:717–746.

Aviezer H, Trope Y, Todorov A (2012) Body cues, not facial expressions, discriminate between intense positive and negative emotions. Science 338:1225–1229.

Azevedo RT, Macaluso E, Avenanti A, Santangelo V, Cazzato V, Aglioti SM (2013) Their pain is not our pain: Brain and autonomic correlates of empathic resonance with the pain of same and different race individuals. Human Brain Mapping 34:3168–3181.

Azevedo RT, Macaluso E, Viola V, Sani G, Aglioti SM (2014) Weighing the stigma of weight: An fMRI study of neural reactivity to the pain of obese individuals. NeuroImage 91:109–119.

Baldauf D, Desimone R (2014) Neural Mechanisms of Object-Based Attention. Science 344:424–427.

Ball T, Derix J, Wentlandt J, Wieckhorst B, Speck O, Schulze-Bonhage A, Mutschler I (2009) Anatomical specificity of functional amygdala imaging of responses to stimuli with positive and negative emotional valence. Journal of Neuroscience Methods 180:57–70.

Bar M (2004) Visual objects in context. Nature Reviews Neuroscience 5:617–629.

Barker AT, Jalinous R, Freeston IL (1985) Non-invasive magnetic stimulation of human motor cortex. The Lancet 325:1106–1107.

Bartra O, McGuire JT, Kable JW (2013) The valuation system: A coordinate-based meta-analysis of BOLD fMRI experiments examining neural correlates of subjective value. NeuroImage 76:412–427.

Bassett DS, Bullmore E (2006) Small-World Brain Networks. The Neuroscientist 12:512–523.

Bastiaansen JACJ, Thioux M, Keysers C (2009) Evidence for mirror systems in emotions. Philosophical transactions of the Royal Society of London Series B, Biological sciences 364:2391–2404.

Batson CD (2009) These Things Called Empathy: Eight Related but Distinct Phenomena. In: The Social Neuroscience of Empathy (Decety J, Ickes W, eds), pp 3–16. MIT Press.

Bayliss AP, Naughtin CK, Lipp O V, Kritikos A, Dux PE (2012) Make a lasting impression: The neural consequences of re-encountering people who emote inappropriately. Psychophysiology 49:1571–1578.

Berker EA, Berker AH, Smith A (1986) Translation of Broca’s 1865 report. Localization of speech in the third left frontal convolution. Archives of Neurology 43:1065–1072.

Bernstein MJ, Young SG, Hugenberg K (2007) The Cross-Category Effect: Mere Social Categorization Is Sufficient to Elicit an Own-Group Bias in Face Recognition. Psychological Science 18:706–712.

Bindemann M, Scheepers C, Ferguson HJ, Burton AM (2010) Face, body, and center of gravity mediate person detection in natural scenes. Journal of Experimental Psychology: Human Perception and Performance 36:1477–1485.

Blank H, Kiebel SJ, von Kriegstein K (2015) How the human brain exchanges information across sensory modalities to recognize other people. Human Brain Mapping 36:324–339.

Blanke O, Ionta S, Fornari E, Mohr C, Maeder P (2010) Mental imagery for full and upper human bodies: common right hemisphere activations and distinct extrastriate activations. Brain Topography 23:321–332.

Borhani K, Làdavas E, Maier ME, Avenanti A, Bertini C (2015) Emotional and movement-related body postures modulate visual processing. Social Cognitive and Affective Neuroscience 10:1092–1101.

Borkenau P, Liebler A (1992) Trait Inferences: Sources of Validity at Zero Acquaintance. Journal of Personality and Social Psychology 62:645–657.

Brandman T, Yovel G (2016) Bodies are Represented as Wholes Rather Than Their Sum of Parts in the Occipital-Temporal Cortex. Cerebral Cortex 26:530–543.

Brewer MB (1999) The psychology of prejudice: Ingroup love our outgroup hate? Journal of Social Issues 55:429–444.

Brothers L (1990) The social brain: a project for integrating primate behavior and neurophysiology in a new domain. Concepts in Neuroscience 1:27–51.

Bruce V, Young A (1986) Understanding face recognition. British Journal of Psychology 77:305–327.

Brüne M, Brüne-Cohrs U (2006) Theory of mind-evolution, ontogeny, brain mechanisms and psychopathology. Neuroscience and Biobehavioral Reviews 30:437–455.

Cacioppo JT, Berntson GG (1992) Social psychological contributions to the decade of the brain. Doctrine of multilevel analysis. American Psychologist 47:1019–1028.

Calvo-Merino B, Urgesi C, Orgs G, Aglioti SM, Haggard P (2010) Extrastriate body area underlies aesthetic evaluation of body stimuli. Experimental Brain Research 204:447–456.

Caramazza A, Anzellotti S, Strnad L, Lingnau A (2014) Embodied Cognition and Mirror Neurons: A Critical Assessment. Annual Review of Neuroscience 37:1–15.

Carels RA, Musher-Eizenman DR (2010) Individual differences and weight bias: Do people with an anti-fat bias have a pro-thin bias? Body Image 7:143–148.

Carrington SJ, Bailey AJ (2009) Are there theory of mind regions in the brain? A review of the neuroimaging literature. Human Brain Mapping 30:2313–2335.

Catani M, Jones DK, Donato R, Ffytche DH (2003) Occipito-temporal connections in the human brain. Brain 126:2093–2107.

Cauda F, D'Agata F, Sacco K, Duca S, Geminiani G, Vercelli A (2011) Functional connectivity of the insula in the resting brain. NeuroImage 55:8–23.

Cauda F, Vercelli A (2013) How many clusters in the insular cortex? Cerebral Cortex 23:2779–2780.

Cavanna AE, Trimble MR (2006) The precuneus: A review of its functional anatomy and behavioural correlates. Brain 129:564–583.

Cerliani L, Thomas RM, Jbabdi S, Siero JCW, Nanetti L, Crippa A, Gazzola V, D'Arceuil H, Keysers C (2012) Probabilistic tractography recovers a rostrocaudal trajectory of connectivity variability in the human insular cortex. Human Brain Mapping 33:2005–2034.

Chan AW-Y, Peelen MV, Downing PE (2004) The effect of viewpoint on body representation in the extrastriate body area. Neuroreport 15:2407–2410.

Chao I (2008) Read my mind. Nature Milestones Spin 462:1.

Chiavarino C, Apperly IA, Humphreys GW (2012) Understanding Intentions: Distinct Processes for Mirroring, Representing, and Conceptualizing. Current Directions in Psychological Science 21:284–289.

Cloutier J, Gyurovski I (2014) Ventral medial prefrontal cortex and person evaluation: Forming impressions of others varying in financial and moral status. NeuroImage 100:535–543.

Cloutier J, Kelley WM, Heatherton TF (2011) The influence of perceptual and knowledge-based familiarity on the neural substrates of face perception. Social Neuroscience 6:63–75.

Cohen J (1988) Statistical Power Analysis for the Behavioral Sciences (Associates LE, ed).

Cohen J (1992) A power primer. Psychological Bulletin 112:155–159.

Collins JA, Olson IR (2014) Knowledge is power: how conceptual knowledge transforms visual cognition. Psychonomic Bulletin and Review 21:843–860.

Colombo M (2013) Moving Foward (and Beyond) the Modularity Debate: A Network Perspective. Philosophy of Science 80:356–377.

Contreras JM, Banaji MR, Mitchell JP (2012) Dissociable neural correlates of stereotypes and other forms of semantic knowledge. Social Cognitive and Affective Neuroscience 7:764–770.

Cosmides L, Tooby J (1994) Origins of domain specificity: The evolution of functional organization. In: Mapping the Mind: Domain Specificity in Cognition and Culture (Hirschfeld L, Gelman S, eds), pp 84–116. New York: Cambridge University Press.

Costafreda SG, Brammer MJ, David AS, Fu CHY (2008) Predictors of amygdala activation during the processing of emotional stimuli: A meta-analysis of 385 PET and fMRI studies. Brain Research Reviews 58:57–70.

Coulson M (2004) Attributing emotion to static body postures: Recognition accuracy, confusions, and viewpoint dependence. Journal of Nonverbal Behavior 28:117–139.

Cumming G (2014) The New Statistics: Why and How. Psychological Science 25:7–29.

Damasio H, Grabowski T, Frank R, Galaburda AM, Damasio AR (1994) The return of Phineas Gage: Clues about the brain from the skull of a famous patient. Science 264:1102–1105.

de Gelder B (2006) Towards the neurobiology of emotional body language. Nature Reviews Neuroscience 7:242–249.

de Gelder B, Snyder J, Greve D, Gerard G, Hadjikhani N (2004) Fear fosters flight: a mechanism for fear contagion when perceiving emotion expressed by a whole body. Proceedings of the National Academy of Sciences of the United States of America 101:16701–16706.

de Gelder B, van den Stock J, Meeren HKM, Sinke CBA, Kret ME, Tamietto M (2010) Standing up for the body. Recent progress in uncovering the networks involved in the perception of bodies and bodily expressions. Neuroscience and Biobehavioral Reviews 34:513–527.

De Silva PR, Bianchi-Berthouze N (2004) Modeling human affective postures: An information theoretic characterization of posture features. Computer Animation and Virtual Worlds 15:269–276.

Decety J, Lamm C (2007) The Role of the Right Temporoparietal Junction in Social Interaction: How Low-Level Computational Processes Contribute to Meta-Cognition. The Neuroscientist 13:580–593.

Deen B, Pitskel NB, Pelphrey KA (2011) Three systems of insular functional connectivity identified with cluster analysis. Cerebral Cortex 21:1498–1506.

Desimone R, Albright TD, Gross CG, Bruce C (1984) Stimulus-selective neurons in the macaque. Journal of Neuroscience 4:2051–2062.

Devue C, Collette F, Balteau E, Degueldre C, Luxen A, Maquet P, Brédart S (2007) Here I am: The cortical correlates of visual self-recognition. Brain Research 1143:169–182.

Dodell-Feder D, Koster-Hale J, Bedny M, Saxe RR (2011) fMRI item analysis in a theory of mind task. NeuroImage 55:705–712.

Donaldson P, Rinehart NJ, Enticott PG (2015) Noninvasive stimulation of the temporoparietal junction: A systematic review. Neuroscience and Biobehavioral Reviews 55:547–572.

Donnellan MB, Oswald FL, Baird BM, Lucas RE (2006) The mini-IPIP scales: tiny-yet-effective measures of the Big Five factors of personality. Psychological Assessment 18:192–203.

Downing PE, Bray D, Rogers J, Childs C (2004) Bodies capture attention when nothing is expected. Cognition 93:27–38.

Downing PE, Jiang Y, Shuman M, Kanwisher N (2001) A cortical area selective for visual processing of the human body. Science 293:2470–2473.

Downing PE, Peelen MV (2011) The role of occipitotemporal body-selective regions in person perception. Cognitive Neuroscience 2:186–226.

Downing PE, Peelen MV (2015) Body selectivity in occipitotemporal cortex: Causal evidence. Neuropsychologia in press:1–11.

Downing PE, Wiggett AJ, Peelen MV (2007) Functional magnetic resonance imaging investigation of overlapping lateral occipitotemporal activations using multi-voxel pattern analysis. Journal of Neuroscience 27:226–233.

Drane DL, Ojemann JG, Phatak V, Loring DW, Gross RE, Hebb AO, Silbergeld DL, Miller JW, Voets NL, Saindane AM, Barsalou L, Meador KJ, Ojemann GA, Tranel D (2013) Famous face identification in temporal lobe epilepsy: Support for a multimodal integration model of semantic memory. Cortex 49:1648–1667.

Eickhoff SB, Stephan KE, Mohlberg H, Grefkes C, Fink GR, Amunts K, Zilles K (2005) A new SPM toolbox for combining probabilistic cytoarchitectonic maps and functional imaging data. NeuroImage 25:1325–1335.

Eliot SA ed. (1911) John M. Harlow. In: Biographical History of Massachusetts: Biographies and Autobiographies of the Leading Men in the State, 1st ed. Massachusetts Biographical Society.

Eres R, Molenberghs P (2013) The influence of group membership on the neural correlates involved in empathy. Frontiers in Human Neuroscience 7:1–6.

Ewbank MP, Lawson RP, Henson RN, Rowe JB, Passamonti L, Calder AJ (2011) Changes in “top-down” connectivity underlie repetition suppression in the ventral visual pathway. Journal of Neuroscience 31:5635–5642.

Fairhall SL, Ishai A (2007) Effective connectivity within the distributed cortical network for face perception. Cerebral Cortex 17:2400–2406.

Fan Y, Duncan NW, de Greck M, Northoff G (2011) Is there a core neural network in empathy? An fMRI based quantitative meta-analysis. Neuroscience and Biobehavioral Reviews 35:903–911.

Fitzgerald PB, Fountain S, Daskalakis ZJ (2006) A comprehensive review of the effects of rTMS on motor cortical excitability and inhibition. Clinical Neurophysiology 117:2584–2596.

Flynn FG, Benson DF, Ardila A (1999) Anatomy of the insula functional and clinical correlates. Aphasiology 13:55–78.

Frank DW, Sabatinelli D (2012) Stimulus-driven reorienting in the ventral frontoparietal attention network: the role of emotional content. Frontiers in Human Neuroscience 6:1–5.

Friston K (2010) The free-energy principle: a unified brain theory? Nature Reviews Neuroscience 11:127–138.

Friston KJ (1994) Functional and Effective Connectivity in Neuroimaging: A Synthesis. Human Brain Mapping 2:56–78.

Friston KJ, Buechel C, Fink GR, Morris J, Rolls E, Dolan RJ (1997) Psychophysiological and modulatory interactions in neuroimaging. NeuroImage 6:218–229.

Friston KJ, Harrison L, Penny WD (2003) Dynamic causal modelling. NeuroImage 19:1273–1302.

Friston KJ, Kiebel S (2009) Predictive coding under the free-energy principle. Philosophical transactions of the Royal Society of London Series B, Biological sciences 364:1211–1221.

Friston KJ, Price CJ (2001) Generative models, brain function and neuroimaging. Scandinavian Journal of Psychology 42:167–177.

Frith CD (2007) The social brain? Philosophical transactions of the Royal Society of London Series B, Biological sciences 362:671–678.

Frith CD, Frith U (1999) Interacting Minds--A Biological Basis. Science 286:1692–1695.

Frith U, Frith C (2010) The social brain: allowing humans to boldly go where no other species has been. Philosophical transactions of the Royal Society of London Series B, Biological sciences 365:165–176.

Fuster JM (1997) Network memory. Trends in Neurosciences 20:451–459.

Fyock J, Stangor C (1994) The role of memory biases in stereotype maintenance. British Journal of Social Psychology 33:331–343.

Gallese V, Keysers C, Rizzolatti G (2004) A unifying view of the basis of social cognition. Trends in Cognitive Sciences 8:396–403.

Gauthier I, Tarr MJ, Moylan J, Skudlarski P, Gore JC, Anderson AW (2000) The Fusiform "Face Area" is part of a network that processes faces at the individual level. Journal of Cognitive Neuroscience 12:495–504.

Georgieff N, Jeannerod M (1998) Beyond consciousness of external reality: a "who" system for consciousness of action and self-consciousness. Consciousness and Cognition 7:465–477.

Gershberg FB, Shimamura AP (1994) Serial Position Effects in Implicit and Explicit Tests of Memory. Journal of Experimental Psychology: Learning, Memory, and Cognition 20:1370–1378.

Ghashghaei HT, Barbas H (2002) Pathways for emotion: Interactions of prefrontal and anterior temporal pathways in the amygdala of the rhesus monkey. Neuroscience 115:1261–1279.

Gilron R, Gutchess AH (2012) Remembering first impressions: Effects of intentionality and diagnosticity on subsequent memory. Cognitive Affective and Behavioral Neuroscience 12:85–98.

Gitelman DR, Penny WD, Ashburner J, Friston KJ (2003) Modeling regional and psychophysiologic interactions in fMRI: the importance of hemodynamic deconvolution. NeuroImage 19:200–207.

Glezer LS, Riesenhuber M (2013) Individual Variability in Location Impacts Orthographic Selectivity in the "Visual Word Form Area." Journal of Neuroscience 33:11221–11226.

Gobbini MI, Haxby JV (2007) Neural systems for recognition of familiar faces. Neuropsychologia 45:32–41.

Golby AJ, Gabrieli JDE, Chiao JY, Eberhardt JL (2001) Differential responses in the fusiform region to same-race and other-race faces. Nature Neuroscience 4:845–850.

Gomez J, Pestilli F, Witthoft N, Golarai G, Liberman A, Poltoratski S, Yoon J, Grill-Spector K (2015) Functionally Defined White Matter Reveals Segregated Pathways in Human Ventral Temporal Cortex Associated with Category-Specific Processing. Neuron 85:216–228.

Gong G, He Y, Concha L, Lebel C, Gross DW, Evans AC, Beaulieu C (2009) Mapping anatomical connectivity patterns of human cerebral cortex using in vivo diffusion tensor imaging tractography. Cerebral Cortex 19:524–536.

Gopnik A, Astington JW (1988) Children's understanding of representational change and its relation to the understanding of false belief and the appearance-reality distinction. Child Development 59:26–37.

Greven IM, Downing PE, Ramsey R (2016) Linking person perception to person knowledge in the human brain. Social Cognitive and Affective Neuroscience.

Grèzes J, Adenis MS, Pouga L, Armony JL (2013) Self-relevance modulates brain responses to angry body expressions. Cortex 49:2210–2220.

Grèzes J, Pichon S, de Gelder B (2007) Perceiving fear in dynamic body expressions. NeuroImage 35:959–967.

Gross CG (2008) Single neuron studies of inferior temporal cortex. Neuropsychologia 46:841–852.

Gross CG, Bender DB, Rocha-Miranda CE (1969) Visual receptive fields of neurons in inferotemporal cortex of the monkey. Science 166:1303–1306.

Gross CG, Rocha-Miranda CE, Bender DB (1972) Visual properties of neurons in inferotemporal cortex of the Macaque. Journal of Neurophysiology 35:96–111.

Hadjikhani N, de Gelder B (2003) Seeing Fearful Body Expressions Activates the Fusiform Cortex and Amygdala. Current Biology 13:2201–2205.

Harlow JM (1993) Recovery from the passage of an iron bar through the head. History of Psychiatry 4:274–281.

Harris LT, Fiske ST (2007) Social groups that elicit disgust are differentially processed in mPFC. Social Cognitive and Affective Neuroscience 2:45–51.

Hassabis D, Spreng RN, Rusu AA, Robbins CA, Mar RA, Schacter DL (2014) Imagine all the people: How the brain creates and uses personality models to predict behavior. Cerebral Cortex 24:1979–1987.

Haxby JV, Hoffman EA, Gobbini MI (2000) The distributed human neural system for face perception. Trends in Cognitive Sciences 4:223–233.

He W, Garrido MI, Sowman PF, Brock J, Johnson BW (2015) Development of effective connectivity in the core network for face perception. Human Brain Mapping 36:2161–2173.

Hecaen H, Angelergues R (1962) Agnosia for faces (prosopagnosia). Archives of Neurology 7:92–100.

Heider JD, Scherer CR, Skowronski JJ, Wood SE, Edlund JE, Hartnett JL (2007) Trait expectancies and stereotype expectancies have the same effect on person memory. Journal of Experimental Social Psychology 43:265–272.

Hermann P, Bankó ÉM, Gál V, Vidnyánszky Z (2015) Neural Basis of Identity Information Extraction from Noisy Face Images. Journal of Neuroscience 35:7165–7173.

Herrington JD, Taylor JM, Grupe DW, Curby KM, Schultz RT (2011) Bidirectional communication between amygdala and fusiform gyrus during facial recognition. NeuroImage 56:2348–2355.

Hertel G, Kerr NL (2001) Priming In-Group Favoritism: The Impact of Normative Scripts in the Minimal Group Paradigm. Journal of Experimental Social Psychology 37:316–324.

Heyes C (2014) False belief in infancy: a fresh look. Developmental Science 17:647–659.

Hirst W, Echterhoff G (2012) Remembering in Conversations: The Social Sharing and Reshaping of Memories. Annual Review of Psychology 63:55–79.

Hodgetts CJ, Postans M, Shine JP, Jones DK, Lawrence AD, Graham KS (2015) Dissociable roles of the inferior longitudinal fasciculus and fornix in face and place perception. eLife 4:1–25.

Hodzic A, Kaas A, Muckli L, Stirn A, Singer W (2009a) Distinct cortical networks for the detection and identification of human body. NeuroImage 45:1264–1271.

Hodzic A, Muckli L, Singer W, Stirn A (2009b) Cortical responses to self and others. Human Brain Mapping 30:951–962.

Hutchison RM, Culham JC, Everling S, Flanagan JR, Gallivan JP (2014) Distinct and distributed functional connectivity patterns across cortex reflect the domain-specific constraints of object, face, scene, body, and tool category-selective modules in the ventral visual pathway. NeuroImage 96:216–236.

Ishai A (2008) Let’s face it: It's a cortical network. NeuroImage 40:415–419.

Ito TA, Bartholow BD (2009) The Neural Correlates of Race. Trends in Cognitive Sciences 13:524–531.

Iwai E, Yukie M (1987) Amygdalofugal and amygdalopetal connections with modality-specific visual cortical areas in macaques (Macaca fuscata, M. mulatta, and M. fascicularis). Journal of Comparative Neurology 261:362–387.

Izuma K, Saito DN, Sadato N (2008) Processing of Social and Monetary Rewards in the Human Striatum. Neuron 58:284–294.

Jabbi M, Swart M, Keysers C (2007) Empathy for positive and negative emotions in the gustatory cortex. NeuroImage 34:1744–1753.

Jakab A, Molnár PP, Bogner P, Béres M, Berényi EL (2012) Connectivity-based parcellation reveals interhemispheric differences in the insula. Brain Topography 25:264–271.

Josephs O, Henson RNA (1999) Event-related functional magnetic resonance imaging: modelling, inference and optimization. Philosophical transactions of the Royal Society of London Series B, Biological sciences 354:1215–1228.

Kable JW, Chatterjee A (2006) Specificity of action representations in the lateral occipitotemporal cortex. Journal of Cognitive Neuroscience 18:1498–1517.

Kahnt T, Chang LJ, Park SQ, Heinzle J, Haynes J-D (2012) Connectivity-Based Parcellation of the Human Orbitofrontal Cortex. Journal of Neuroscience 32:6240–6250.

Kanwisher N (2010) Functional specificity in the human brain: a window into the functional architecture of the mind. Proceedings of the National Academy of Sciences of the United States of America 107:11163–11170.

Kanwisher N, Dilks DD (2013) The Functional Organization of the Ventral Visual Pathway in Humans. In: The New Visual Neurosciences (Chalupa L, Werner J, eds).

Kanwisher N, McDermott J, Chun MM (1997) The fusiform face area: a module in human extrastriate cortex specialized for face perception. Journal of Neuroscience 17:4302–4311.

Keysers C, Gazzola V (2009) Expanding the mirror: vicarious activity for actions, emotions, and sensations. Current Opinion in Neurobiology 19:666–671.

Kilner JM, Friston KJ, Frith CD (2007a) The mirror-neuron system: a Bayesian perspective. NeuroReport 18:619–623.

Kilner JM, Friston KJ, Frith CD (2007b) Predictive coding: an account of the mirror neuron system. Cognitive Processing 8:159–166.

Kilner JM, Lemon RN (2013) What we know currently about mirror neurons. Current Biology 23:R1057–R1062.

Klapper A, Ramsey R, Wigboldus DHJ, Cross ES (2014) The Control of Automatic Imitation Based on Bottom-Up and Top-Down Cues to Animacy: Insights from Brain and Behavior. Journal of Cognitive Neuroscience 26:2503–2513.

Krall SC, Rottschy C, Oberwelland E, Bzdok D, Fox PT, Eickhoff SB, Fink GR, Konrad K (2015) The role of the right temporoparietal junction in attention and social interaction as revealed by ALE meta-analysis. Brain Structure and Function 220:587–604.

Kramer RSS, Ward R (2010) Internal facial features are signals of personality and health. Quarterly Journal of Experimental Psychology 63:2273–2287.

Kriegeskorte N, Simmons WK, Bellgowan PSF, Baker CI (2009) Circular analysis in systems neuroscience: the dangers of double dipping. Nature Neuroscience 12:535–540.

Kubota JT, Banaji MR, Phelps EA (2012) The neuroscience of race. Nature Neuroscience 15:940–948.

Kurth F, Zilles K, Fox PT, Laird AR, Eickhoff SB (2010) A link between the systems: functional differentiation and integration within the human insula revealed by meta-analysis. Brain Structure and Function 214:519–534.

Kuzmanovic B, Bente G, von Cramon DY, Schilbach L, Tittgemeyer M, Vogeley K (2012) Imaging first impressions: Distinct neural processing of verbal and nonverbal social information. NeuroImage 60:179–188.

Lakens D (2013) Calculating and reporting effect sizes to facilitate cumulative science: a practical primer for t-tests and ANOVAs. Frontiers in Psychology 4:1–12.

Lamm C, Singer T (2010) The role of anterior insular cortex in social emotions. Brain Structure and Function 214:579–591.

Le Bihan D (2012) Diffusion, confusion and functional MRI. NeuroImage 62:1131–1136.

LeDoux J (2007) The amygdala. Current Biology 17:868–874.

Leichtman MD, Ceci SJ (1995) The effects of stereotypes and suggestions on preschoolers' reports. Developmental Psychology 31:568–578.

Levy DJ, Glimcher PW (2012) The root of all value: A neural common currency for choice. Current Opinion in Neurobiology 22:1027–1038.

Liang X, Zebrowitz LA, Aharon I (2009) Effective connectivity between amygdala and orbitofrontal cortex differentiates the perception of facial expressions. Social Neuroscience 4:185–196.

Lieberman MD, Cunningham WA (2009) Type I and Type II error concerns in fMRI research: re-balancing the scale. Social Cognitive and Affective Neuroscience 4:423–428.

Limanowski J, Lutti A, Blankenburg F (2014) The extrastriate body area is involved in illusory limb ownership. NeuroImage 86:514–524.

Lin A, Adolphs R, Rangel A (2012) Social and monetary reward learning engage overlapping neural substrates. Social Cognitive and Affective Neuroscience 7:274–281.

Liu H, Qin W, Qi H, Jiang T, Yu C (2015) Parcellation of the human orbitofrontal cortex based on gray matter volume covariance. Human Brain Mapping 36:538–548.

Ma N, Vandekerckhove M, van Hoeck N, van Overwalle F (2012) Distinct recruitment of temporo-parietal junction and medial prefrontal cortex in behavior understanding and trait identification. Social Neuroscience 7:37–41.

Ma N, Vandekerckhove M, van Overwalle F, Seurinck R, Fias W (2011) Spontaneous and intentional trait inferences recruit a common mentalizing network to a different degree: spontaneous inferences activate only its core areas. Social Neuroscience 6:123–138.

Macrae CN, Quadflieg S (2010) Perceiving People. In: Handbook of Social Psychology, pp 2:11:12. John Wiley & Sons, Inc.

Mahon BZ, Caramazza A (2011) What drives the organization of object knowledge in the brain? Trends in Cognitive Sciences 15:97–103.

Malach R, Reppas JB, Benson RR, Kwong KK, Jiang H, Kennedy WA, Ledden PJ, Brady TJ, Rosen BR, Tootell RBH (1995) Object-related activity revealed by functional magnetic resonance imaging in human occipital cortex. Proceedings of the National Academy of Sciences of the United States of America 92:8135–8139.

Malpass RS, Kravitz J (1969) Recognition for faces of own and other race. Journal of Personality and Social Psychology 13:330–334.

Mansfield P (1977) Multi-planar image formation using NMR spin echoes. Journal of Physics C: Solid State Physics 10:55–58.

Marsh AA, Kozak MN, Wegner DM, Reid ME, Yu HH, Blair RJR (2010) The neural substrates of action identification. Social Cognitive and Affective Neuroscience 5:392–403.

Martin-Malivel J, Okada K (2007) Human and chimpanzee face recognition in chimpanzees (Pan troglodytes): role of exposure and impact on categorical perception. Behavioral Neuroscience 121:1145–1155.

McKone E, Kanwisher N, Duchaine BC (2007) Can generic expertise explain special processing for faces? Trends in Cognitive Sciences 11:8–15.

McLaren DG, Ries ML, Xu G, Johnson SC (2012) A generalized form of context-dependent psychophysiological interactions (gPPI): a comparison to standard approaches. NeuroImage 61:1277–1286.

Mechelli A, Price CJ, Friston KJ, Ishai A (2004) Where Bottom-up Meets Top-down: Neuronal Interactions during Perception and Imagery. Cerebral Cortex 14:1256–1265.

Mende-Siedlecki P, Cai Y, Todorov A (2013) The neural dynamics of updating person impressions. Social Cognitive and Affective Neuroscience 8:623–631.

Mesulam M (1990) Large-Scale Neurocognitive Networks and Distributed Processing for Attention, Language, and Memory. Annals of Neurology 28:597–613.

Minnebusch DA, Daum I (2009) Neuropsychological mechanisms of visual face and body perception. Neuroscience and Biobehavioral Reviews 33:1133–1144.

Mitchell JP (2009) Inferences about mental states. Philosophical transactions of the Royal Society of London Series B, Biological sciences 364:1309–1316.

Mitchell JP, Cloutier J, Banaji MR, Macrae CN (2006) Medial prefrontal dissociations during processing of trait diagnostic and nondiagnostic person information. Social Cognitive and Affective Neuroscience 1:49–55.

Mitchell JP, Heatherton TF, Macrae CN (2002) Distinct neural systems subserve person and object knowledge. Proceedings of the National Academy of Sciences of the United States of America 99:15238–15243.

Mitchell JP, Macrae CN, Banaji MR (2004) Encoding-specific effects of social cognition on the neural correlates of subsequent memory. Journal of Neuroscience 24:4912–4917.

Mitchell JP, Macrae CN, Banaji MR (2005) Forming impressions of people versus inanimate objects: social-cognitive processing in the medial prefrontal cortex. NeuroImage 26:251–257.

Moeller S, Freiwald WA, Tsao DY (2008) Patches with Links: A Unified System for Processing Faces in the Macaque Temporal Lobe. Science 320:1355–1359.

Molenberghs P (2013) The neuroscience of in-group bias. Neuroscience and Biobehavioral Reviews 37:1530–1536.

Molenberghs P, Gapp J, Wang B, Louis WR, Decety J (2016) Increased Moral Sensitivity for Outgroup Perpetrators Harming Ingroup Members. Cerebral Cortex 26:225–233.

Molenberghs P, Morrison S (2014) The role of the medial prefrontal cortex in social categorization. Social Cognitive and Affective Neuroscience 9:292–296.

Moro V, Pernigo S, Avesani R, Bulgarelli C, Urgesi C, Candidi M, Aglioti SM (2012) Visual body recognition in a prosopagnosic patient. Neuropsychologia 50:104–117.

Moro V, Urgesi C, Pernigo S, Lanteri P, Pazzaglia M, Aglioti SM (2008) The Neural Basis of Body Form and Body Action Agnosia. Neuron 60:235–246.

Morrison SE, Salzman CD (2010) Re-valuing the amygdala. Current Opinion in Neurobiology 20:221–230.

Narasimhan PT, Jacobs RE (1996) Neuroanatomical Mircromagnetic Resonance Imaging. In: Brain Mapping: The Methods, 2nd ed. (Toga AW, Mazziotta JC, eds), pp 399–421. Elsevier Science.

Naumann LP, Vazire S, Rentfrow PJ, Gosling SD (2009) Personality judgments based on physical appearance. Personality and Social Psychology Bulletin 35:1661–1671.

O'Reilly JX, Woolrich MW, Behrens TEJ, Smith SM, Johansen-Berg H (2012) Tools of the trade: Psychophysiological interactions and functional connectivity. Social Cognitive and Affective Neuroscience 7:604–609.

O'Toole AJ, Phillips PJ, Weimer S, Roark DA, Ayyad J, Barwick R, Dunlop J (2011) Recognizing people from dynamic and static faces and bodies: dissecting identity with a fusion approach. Vision Research 51:74–83.

Oakes PJ, Turner JC, Haslam SA (1991) Perceiving people as group members: The role of fit in the salience of social categorizations. British Journal of Social Psychology 30:125–144.

Ochsner KN, Lieberman MD (2001) The emergence of social cognitive neuroscience. American Psychologist 56:717–734.

Ogawa S, Lee TM, Kay AR, Tank DW (1990) Brain magnetic resonance imaging with contrast dependent on blood oxygenation. Proceedings of the National Academy of Sciences of the United States of America 87:9868–9872.

Ogawa S, Tank DW, Menon R, Ellermann JM, Kim SG, Merkle H, Ugurbil K (1992) Intrinsic signal changes accompanying sensory stimulation: functional brain mapping with magnetic resonance imaging. Proceedings of the National Academy of Sciences of the United States of America 89:5951–5955.

Olson IR, McCoy D, Klobusicky E, Ross LA (2013) Social cognition and the anterior temporal lobes: a review and theoretical framework. Social Cognitive and Affective Neuroscience 8:123–133.

Olson IR, Plotzker A, Ezzyat Y (2007) The Enigmatic temporal pole: a review of findings on social and emotional processing. Brain 130:1718–1731.

Otten S, Moskowitz GB (2000) Evidence for Implicit Evaluative In-Group Bias: Affect-Biased Spontaneous Trait Inference in a Minimal Group Paradigm. Journal of Experimental Social Psychology 36:77–89.

Otten S, Wentura D (2001) Self-Anchoring and In-Group Favoritism: An Individual Profiles Analysis. Journal of Experimental Social Psychology 37:525–532.

Parr LA, De Waal FBM (1999) Visual kin recognition in chimpanzees. Nature 399:647.

Pascalis O, Bachevalier J (1998) Face recognition in primates: a cross-species study. Behavioural Processes 43:87–96.

Patterson K, Nestor PJ, Rogers TT (2007) Where do you know what you know? The representation of semantic knowledge in the human brain. Nature Reviews Neuroscience 8:976–987.

Paulus FM, Müller-Pinzler L, Jansen A, Gazzola V, Krach S (2015) Mentalizing and the Role of the Posterior Superior Temporal Sulcus in Sharing Others' Embarrassment. Cerebral Cortex 25:2065–2075.

Peelen MV, Downing PE (2005) Selectivity for the human body in the fusiform gyrus. Journal of Neurophysiology 93:603–608.

Peelen MV, Downing PE (2007) The neural basis of visual body perception. Nature Reviews Neuroscience 8:636–648.

Perrett DI, Hietanen JK, Oram MW, Benson PJ (1992) Organization and function of cells responsive to faces in the temporal cortex. Philosophical transactions of the Royal Society of London 335:23–30.

Perrett DI, Smith PAJ, Potter DD, Mistlin AJ, Head AS, Milner AD, Jeeves MA (1985) Visual cells in the temporal cortex sensitive to face view and gaze direction. Proceedings Royal Society of London B 223:293–317.

Pessoa L (2010) Emotion and cognition and the amygdala: From "what is it?" to "what's to be done?" Neuropsychologia 48:3416–3429.

Phelps EA (2004) Human emotion and memory: Interactions of the amygdala and hippocampal complex. Current Opinion in Neurobiology 14:198–202.

Phelps EA, LeDoux JE (2005) Contributions of the amygdala to emotion processing: From animal models to human behavior. Neuron 48:175–187.

Philips Medical Systems . (1984) Basic Principles of MR Imaging.

Pinsk MA, Arcaro M, Weiner KS, Kalkus JF, Inati SJ, Gross CG, Kastner S (2009) Neural representations of faces and body parts in macaque and human cortex: a comparative FMRI study. Journal of Neurophysiology 101:2581–2600.

Pinsk MA, DeSimone K, Moore T, Gross CG, Kastner S (2005) Representations of faces and body parts in macaque temporal cortex: a functional MRI study. Proceedings of the National Academy of Sciences of the United States of America 102:6996–7001.

Pitcher D, Charles L, Devlin JT, Walsh V, Duchaine B (2009) Triple dissociation of faces, bodies, and objects in extrastriate cortex. Current Biology 19:319–324.

Ploran EJ, Nelson SM, Velanova K, Donaldson DI, Petersen SE, Wheeler ME (2007) Evidence accumulation and the moment of recognition: dissociating perceptual recognition processes using fMRI. Journal of Neuroscience 27:11912–11924.

Ploran EJ, Tremel JJ, Nelson SM, Wheeler ME (2011) High quality but limited quantity perceptual evidence produces neural accumulation in frontal and parietal cortex. Cerebral Cortex 21:2650–2662.

Pourtois G, Peelen MV, Spinelli L, Seeck M, Vuilleumier P (2007) Direct intracranial recording of body-selective responses in human extrastriate visual cortex. Neuropsychologia 45:2621–2625.

Pourtois G, Schettino A, Vuilleumier P (2013) Brain mechanisms for emotional influences on perception and attention: What is magic and what is not. Biological Psychology 92:492–512.

Premack D, Woodruff G (1978) Does the chimpanzee have a theory of mind? Behavioral and Brain Sciences 4:515–526.

Puhl RM, Heuer CA (2009) The stigma of obesity: a review and update. Obesity 17:941–964.

Quadflieg S, Flannigan N, Waiter GD, Rossion B, Wig GS, Turk DJ, Macrae CN (2011) Stereotype-based modulation of person perception. NeuroImage 57:549–557.

Quadflieg S, Rossion B (2011) When perception and attention collide: Neural processing in EBA and FBA. Cognitive Neuroscience 2:209–210.

Ramsey R, van Schie HT, Cross ES (2011) No two are the same: Body shape is part of identifying others. Cognitive Neuroscience 2:207–208.

Rao RPN, Ballard DH (1999) Predictive coding in the visual cortex: a functional interpretation of some extra-classical receptive-field effects. Nature Neuroscience 2:79–87.

Rauss K, Schwartz S, Pourtois G (2011) Top-down effects on early visual processing in humans: A predictive coding framework. Neuroscience and Biobehavioral Reviews 35:1237–1253.

Repacholi BM, Gopnik A (1997) Early reasoning about desires: evidence from 14- and 18-month-olds. Developmental Psychology 33:12–21.

Rhodes G, Jeffery L, Boeing A, Calder AJ (2013) Visual coding of human bodies: perceptual aftereffects reveal norm-based, opponent coding of body identity. Journal of Experimental Psychology: Human Perception and Performance 39:313–317.

Rice A, Phillips PJ, Natu V, An X, O'Toole AJ (2013) Unaware person recognition from the body when face identification fails. Psychological Science 24:2235–2243.

Rilling JK, Glasser MF, Preuss TM, Ma X, Zhao T, Hu X, Behrens TEJ (2008) The evolution of the arcuate fasciculus revealed with comparative DTI. Nature Neuroscience 11:426–428.

Rogers TT, Hocking J, Noppeney U, Mechelli A, Gorno-Tempini ML, Patterson K, Price CJ (2006) Anterior temporal cortex and semantic memory: reconciling findings from neuropsychology and functional imaging. Cognitive Affective and Behavioral Neuroscience 6:201–213.

Rogers TT, Lambon Ralph MA, Garrard P, Bozeat S, McClelland JL, Hodges JR, Patterson K (2004) Structure and Deterioration of Semantic Memory: A Neuropsychological and Computational Investigation. Psychological Review 111:205–235.

Rojas MM, Masip D, Todorov A, Vitria J (2011) Automatic prediction of facial trait judgments: Appearance vs. structural models. PloS one 6:1–12.

Rorden C, Karnath H-O (2004) Using human brain lesions to infer function: a relic from a past era in the fMRI age? Nature Reviews Neuroscience 5:813–819.

Rule NO, Ambady N (2008) The Face of Success. Psychological Science 19:109–111.

Samson D, Apperly IA (2010) There is more to mind reading than having theory of mind concepts: New directions in theory of mind research. Infant and Child Development 19:443–454.

Saper CB, Iversen S, Frackowiak R (2000) Integration of Sensory and Motor Function: The Association Areas of the Cerebral Cortex of the Brain. In: Principles of Neural Science, 4th ed. (Kandel ER, Schwartz JH, Jessell TM, eds), pp 349–380. McGraw-Hill.

Satpute AB, Badre D, Ochsner KN (2013) Distinct Regions of Prefrontal Cortex Are Associated with the Controlled Retrieval and Selection of Social Information. Cerebral Cortex 24:1269–1277.

Saxe R (2010) The right temporo-parietal junction: a specific brain region for thinking about thoughts. In: Handbook of Theory of Mind (Leslie AM, German TC, eds).

Saxe RR (2006a) Why and how to study Theory of Mind with fMRI. Brain Research 1079:57–65.

Saxe RR (2006b) Uniquely human social cognition. Current Opinion in Neurobiology 16:235–239.

Saxe RR, Jamal N, Powell L (2006) My Body or Yours? The Effect of Visual Perspective on Cortical Body Representations. Cerebral Cortex 16:178–182.

Saxe RR, Kanwisher N (2003) People thinking about thinking peopleThe role of the temporo-parietal junction in "theory of mind." NeuroImage 19:1835–1842.

Saygin ZM, Osher DE, Koldewyn K, Reynolds G, Gabrieli JDE, Saxe RR (2012) Anatomical connectivity patterns predict face selectivity in the fusiform gyrus. Nature Neuroscience 15:321–327.

Schiller D, Freeman JB, Mitchell JP, Uleman JS, Phelps EA (2009) A neural mechanism of first impressions. Nature Neuroscience 12:508–514.

Scholz J, Triantafyllou C, Whitfield-Gabrieli S, Brown EN, Saxe R (2009) Distinct regions of right temporo-parietal junction are selective for theory of mind and exogenous attention. PloS one 4:1–7.

Schurz M, Radua J, Aichhorn M, Richlan F, Perner J (2014) Fractionating theory of mind: A meta-analysis of functional brain imaging studies. Neuroscience and Biobehavioral Reviews 42:9–34.

Seidl KN, Peelen MV, Kastner S (2012) Neural evidence for distracter suppression during visual search in real-world scenes. Journal of Neuroscience 32:11812–11819.

Sell A, Cosmides L, Tooby J, Sznycer D, von Rueden C, Gurven M (2009) Human adaptations for the visual assessment of strength and fighting ability from the body and face. Proceedings Royal Society of London B 276:575–584.

Seymour B, Daw N, Dayan P, Singer T, Dolan RJ (2007) Differential Encoding of Losses and Gains in the Human Striatum. Journal of Neuroscience 27:4826–4831.

Shulman GL, Astafiev S V, McAvoy MP, D'Avossa G, Corbetta M (2007) Right TPJ deactivation during visual search: Functional significance and support for a filter hypothesis. Cerebral Cortex 17:2625–2633.

Simmons WK, Martin A (2009) The anterior temporal lobes and the functional architecture of semantic memory. Journal of the International Neuropsychology Society 15:645–649.

Simmons WK, Reddish M, Bellgowan PSF, Martin A (2010) The selectivity and functional connectivity of the anterior temporal lobes. Cereb Cortex 20:813–825.

Singer T, Dolan RJ, Frith CD (2004) Empathy for Pain Involves the Affective but not Sensory Components of Pain. Science 303:1157–1162.

Sinke CBA, Kret ME, de Gelder B (2012) Body Language: Embodied Perception of Emotion. In: Measurements with persons: theory, methods and implementation areas (Berglund B, Rossi GB, Townsend JT, Pendrill LR, eds). Psychology Press / Taylor & Francis.

Slaughter V, Stone VE, Reed C (2004) Perception of Faces and Bodies: Similar or Different? Current Directions in Psychological Science 13:219–223.

Snyder M, Swann WBJ (1978) Behavioral confirmation in social interaction: From social perception to social reality. Journal of Experimental Social Psychology 162:148–162.

Spiridon M, Fischl B, Kanwisher N (2006) Location and spatial profile of category-specific regions in human extrastriate cortex. Human Brain Mapping 27:77–89.

Sporns O (2014) Contributions and challenges for network models in cognitive neuroscience. Nature Neuroscience 17:652–660.

Sporns O, Tononi G, Kötter R (2005) The human connectome: A structural description of the human brain. PLoS Computational Biology 1:0245–0251.

Spunt RP, Lieberman MD (2012) Dissociating Modality-Specific and Supramodal Neural Systems for Action Understanding. Journal of Neuroscience 32:3575–3583.

Stangor C (2014) Principles of Social Psychology – 1st International Edition (Jhangiani R, Tarry H, eds).

Stanislaw H, Todorov N (1999) Calculation of signal detection theory measures. Behavior Research Methods, Instruments, and Computers 31:137–149.

Stein T, Sterzer P, Peelen MV (2012) Privileged detection of conspecifics: Evidence from inversion effects during continuous flash suppression. Cognition 125:64–79.

Stephan KE, Friston KJ (2010) Analyzing effective connectivity with fMRI. Wiley Interdisciplinary Review of Cognitive Science 1:446–459.

Stephan KE, Penny WD, Moran RJ, den Ouden HEM, Daunizeau J, Friston KJ (2010) Ten simple rules for dynamic causal modeling. NeuroImage 49:3099–3109.

Stevens JR, Cushman FA, Hauser MD (2005) Evolving the Psychological Mechanisms for Cooperation. Annual Review of Ecology, Evolution, and Systematics 36:499–518.

Stoddart A (2008) From spectrum to snapshot. Nature Milestones Spin 462:1.

Stulp G, Buunk AP, Verhulst S, Pollet T V (2015) Human Height Is Positively Related to Interpersonal Dominance in Dyadic Interactions. PloS one 10:1–18.

Sugiura M (2014) Neuroimaging studies on recognition of personally familiar people. Frontiers in Bioscience 19:672–686.

Sugiura M, Sassa Y, Watanabe J, Akitsuki Y, Maeda Y, Matsue Y, Fukuda H, Kawashima R (2006) Cortical mechanisms of person representation: Recognition of famous and personally familiar names. NeuroImage 31:853–860.

Szwed M, Dehaene S, Kleinschmidt A, Eger E, Valabrègue R, Amadon A, Cohen L (2011) Specialization for written words over objects in the visual cortex. NeuroImage 56:330–344.

Tajfel H, Billig MG, Bundy RP, Flament C (1971) Social Categorization and Intergroup Behaviour. European Journal of Social Psychology 1:149–177.

Tanaka SC, Doya K, Okada G, Ueda K, Okamoto Y, Yamawaki S (2004) Prediction of immediate and future rewards differentially recruits cortico-basal ganglia loops. Nature Neuroscience 7:887–893.

Taylor JC, Wiggett AJ, Downing PE (2007) Functional MRI analysis of body and body part representations in the extrastriate and fusiform body areas. Journal of Neurophysiology 98:1626–1633.

Thoresen JC, Vuong QC, Atkinson AP (2012) First impressions: gait cues drive reliable trait judgements. Cognition 124:261–271.

Todorov A, Gobbini MI, Evans KK, Haxby JV (2007) Spontaneous retrieval of affective person knowledge in face perception. Neuropsychologia 45:163–173.

Tomasello M, Call J, Hare B (1998) Five primate species follow the visual gaze of conspecifics. Animal Behaviour 55:1063–1069.

Tsao DY, Freiwald WA, Knutsen TA, Mandeville JB, Tootell RBH (2003) Faces and objects in macaque cerebral cortex. Nature Neuroscience 6:989–995.

Tsukiura T, Mochizuki-Kawai H, Fujii T (2006) Dissociable roles of the bilateral anterior temporal lobe in face-name associations: an event-related fMRI study. NeuroImage 30:617–626.

Uleman JS, Adil Saribay S, Gonzalez CM (2008) Spontaneous inferences, implicit impressions, and implicit theories. Annual Review of Psychology 59:329–360.

Urgesi C, Berlucchi G, Aglioti SM (2004) Magnetic Stimulation of Extrastriate Body Area Impairs Visual Processing of Nonfacial Body Parts. Current Biology 14:2130–2134.

Urgesi C, Candidi M, Ionta S, Aglioti SM (2007) Representation of body identity and body actions in extrastriate body area and ventral premotor cortex. Nature Neuroscience 10:30–31.

Vaessen MJ, Hofman PAM, Tijssen HN, Aldenkamp AP, Jansen JFA, Backes WH (2010) The effect and reproducibility of different clinical DTI gradient sets on small world brain connectivity measures. NeuroImage 51:1106–1116.

Van Bavel JJ, Packer DJ, Cunningham WA (2008) The Neural Substrates of In-Group Bias: A functional magnetic resonance imaging investigation. Psychological Science 19:1131–1139.

Van Bavel JJ, Packer DJ, Cunningham WA (2011) Modulation of the Fusiform Face Area following Minimal Exposure to Motivationally Relevant Faces: Evidence of In-group Enhancement (Not Out-group Disregard). Journal of Cognitive Neuroscience 23:3343–3354.

van Koningsbruggen MG, Peelen MV, Downing PE (2013) A causal role for the extrastriate body area in detecting people in real-world scenes. Journal of Neuroscience 33:7003–7010.

van Overwalle F (2009) Social cognition and the brain: a meta-analysis. Human Brain Mapping 30:829–858.

van Overwalle F, van den Eede S, Baetens K, Vandekerckhove M (2009) Trait inferences in goal-directed behavior: ERP timing and localization under spontaneous and intentional processing. Social Cognitive and Affective Neuroscience 4:177–190.

Vocks S, Busch M, Grönemeyer D, Schulte D, Herpertz S, Suchan B (2010) Differential neuronal responses to the self and others in the extrastriate body area and the fusiform body area. Cognitive Affective and Behavioral Neuroscience 10:422–429.

Vokey JR, Rendall D, Tangen JM, Parr LA, de Waal FBM (2004) Visual kin recognition and family resemblance in chimpanzees (Pan troglodytes). Journal of Comparative Psychology 118:194–199.

Volz KG, Kessler T, von Cramon DY (2009) In-group as part of the self: In-group favoritism is mediated by medial prefrontal cortex activation. Social Neuroscience 4:244–260.

Vrtička P, Andersson F, Sander D, Vuilleumier P (2009) Memory for friends or foes: The social context of past encounters with faces modulates their subsequent neural traces in the brain. Social Neuroscience 4:384–401.

Wager TD, Nichols TE (2003) Optimization of experimental design in fMRI: a general framework using a genetic algorithm. NeuroImage 18:293–309.

Walker MB, Trimboli A (1989) Communicating affect: the role of verbal and nonverbal content. Journal of Language and Social Psychology 8:229–248.

Walsh V, Cowey A (2000) Transcranial magnetic stimulation and cognitive neuroscience. Nature Reviews Neuroscience 1:73–79.

Ware JEJR, Kosinski M, Keller SD (1996) A 12-Item Short-Form Health Survey: Construction of Scales and Preliminary Tests of Reliability and Validity. Medical Care 34:220–233.

Webb R (2008) New resonance. Nature Milestones Spin 462:1.

Welborn BL, Lieberman MD (2014) Person-specific Theory of Mind in Medial pFC. Journal of Cognitive Neuroscience 27:1–12.

Whalen PJ (1998) Fear, vigilance, and ambiguity: initial neuroimaging studies of the human amygdala. Current Directions in Psychological Science 7:177–188.

Wheeler ME, Fiske ST (2005) Controlling Racial Prejudice. Social-Cognitive Goals Affect Amygdala and Stereotype Activation. Psychological Science 16:56–63.

Wimmer H, Perner J (1983) Beliefs about beliefs: Representation and constraircing function of wrong bekfs in young children’s understanding of deception. Cognition 13:103–128.

Wojciulik E, Kanwisher N, Driver J (1998) Covert visual attention modulates face-specific activity in the human fusiform gyrus: fMRI study. Journal of Neurophysiology 79:1574–1578.

Xiu D, Geiger MJ, Klaver P (2015) Emotional face expression modulates occipital-frontal effective connectivity during memory formation in a bottom-up fashion. Frontiers in Behavioral Neuroscience 9:1–11.

Young L, Dodell-Feder D, Saxe RR (2010) What gets the attention of the temporo-parietal junction? An fMRI investigation of attention and theory of mind. Neuropsychologia 48:2658–2664.

Zaki J, Ochsner KN, Hanelin J, Wager TD, Mackey SC (2007) Different circuits for different pain: patterns of functional connectivity reveal distinct networks for processing pain in self and others. Social Neuroscience 2:276–291.

Zhen Z, Fang H, Liu J (2013) The Hierarchical Brain Network for Face Recognition. PLoS one 8:1–9.

Zimmermann M, Toni I, de Lange FP (2013) Body posture modulates action perception. Journal of Neuroscience 33:5930–5938.

APPENDICES

APPENDIX 1

Additional univariate results (Chapter 3)

Appendix 1. Results from the univariate analysis: a) the main effect of social agent (Names > Bodies), b) the main effect of social knowledge (Neutral > Traits), and c) the social agent by social knowledge interaction [(NamesTraits > NamesNeutral) > (BodiesTraits > BodiesNeutral)].

Region	Number of voxels	*T*	Montreal Neurological Institute coordinates		
			x	y	z
a) Main effect Social Agent: Names > Bodies					
Left thalamus extending into hippocampus	**325**	**6.42**	**-9**	**-34**	**13**
		5.41	**39**	**-43**	**1**
		5.13	**-18**	**-43**	**7**
Right angular gyrus extending into right inferior parietal lobule	**189**	**6.26**	**60**	**-55**	**37**
		5.79	**57**	**-49**	**49**
		4.80	**54**	**-58**	**46**
Left supramarginal gyrus	**508**	**6.18**	**-45**	**-43**	**37**
		4.89	**-36**	**-55**	**46**
		4.72	**-30**	**-61**	**40**
Right middle temporal gyrus	130	5.79	63	-19	-14
		3.68	60	-4	-11
Left insula	**461**	**5.36**	**-45**	**11**	**1**
		4.89	**-51**	**5**	**10**
		4.60	**-42**	**5**	**19**
Right insula	35	5.13	39	17	4
Left middle orbital gyrus	**208**	**4.76**	**-33**	**47**	**4**
		4.14	**-30**	**53**	**13**
Left middle frontal gyrus	28	4.67	-21	32	37
Left supplementary motor area	123	4.60	-12	-1	67
		4.30	-3	5	55
Left precentral gyrus	58	4.60	-30	-10	52
Right middle frontal gyrus	48	4.39	33	38	25
		4.19	30	56	4
		3.77	33	50	19

Right caudate	16	4.28	21	20	7
Left middle temporal gyrus	33	4.13	-66	-31	-2
Right cerebellum	17	4.07	27	-79	-50
		3.64	36	-76	-50
Caudate	54	3.90	3	5	16
		3.59	-6	-1	22
Left middle frontal gyrus	17	3.21	-42	29	31
		3.15	-36	26	25
b) Main effect Social Knowledge: Neutral > Traits					
Left middle occipital gyrus	52	5.91	-36	-85	31
Left calcarine gyrus	171	5.61	-15	-64	22
Left fusiform gyrus	169	5.60	-33	-37	-20
Right calcarine gyrus	**375**	**5.27**	**12**	**-61**	**19**
		4.50	**-9**	**-70**	**49**
		3.87	**9**	**-73**	**43**
Left middle frontal gyrus	64	4.53	-21	17	49
Left inferior frontal gyrus (pars triangularis)	120	4.48	-36	32	16
		4.37	-27	35	-17
Right middle frontal gyrus	**369**	**4.36**	**33**	**32**	**34**
		4.19	**30**	**35**	**43**
		4.14	**42**	**44**	**16**
Right middle cingulate cortex	116	4.26	3	-28	40
		3.53	-6	-28	34
Left orbitofrontal cortex	15	3.85	-27	59	-8
Right anterior cingulate cortex	10	3.83	15	23	16
Right medial frontal gyrus	38	3.77	9	35	31
		3.16	15	35	19
Left insula	35	3.57	-39	-10	-11
Left intraparietal sulcus	16	3.45	-57	-43	49
Right hippocampus	12	3.27	24	-37	-8
		2.88	33	-37	-17
Right postcentral gyrus	19	3.17	63	-40	43
Left postcentral gyrus	12	3.12	-60	-31	34

c) Interaction: Social agent * knowledge [(NamesTraits > NamesNeutral) > (BodiesTraits > BodiesNeutral)]

Left superior temporal gyrus	56	4.65	-42	-16	4
		3.24	-51	-13	-5
Right caudate	12	4.47	24	5	25
Left postcentral gyrus	111	4.44	-63	-25	22
		3.83	-48	-28	13
		3.68	-45	-25	34
Right cuneus	154	4.15	12	-73	43
		4.08	15	-70	31
		3.85	12	-76	25
Right superior parietal lobule	48	4.06	15	-31	43
Left middle occipital gyrus	25	4.02	-24	-100	-8
Right inferior parietal lobule	40	3.85	60	-37	34
Right inferior parietal lobule	75	3.82	39	-31	40
		3.27	42	-46	43
		2.90	33	-46	40
Left cerebellum	16	3.53	-27	-37	-41
		3.11	-33	-40	-47
Right middle frontal gyrus	10	3.19	42	56	13

Note: Regions surviving a voxel-level threshold of p<.005 and 10 voxels are reported. Areas in bold survive FWE cluster correction for multiple comparisons. Subclusters at least 8 mm from the main peak are listed.

APPENDICES

APPENDIX 2

Additional univariate results at reduced threshold to help identify seed regions (Chapter 3)

Appendix 2. Exploratory analysis of the univariate interaction analysis in body-selective regions. The social agent by social knowledge interaction [(BodiesTraits > BodiesNeutral) > (NamesTraits > NamesNeutral)] is masked by the body-localiser.

Region	Number of voxels	*T*	Montreal Neurological Institute coordinates		
			x	y	z
Interaction: Social agent * knowledge					
Right fusiform gyrus	44	2.94	45	-46	-11
		2.84	48	-43	-8
		2.28	48	-43	1
Left middle temporal gyrus	12	2.60	-45	-64	19

Note: Regions surviving a voxel-level threshold of p<.05 and 10 voxels are reported. Subclusters at least 8 mm from the main peak are listed. These results are exclusively masked by the NamesNeutral > NamesTraits contrast to make sure that any interaction result does not include (Neutral > Traits) when paired with names.

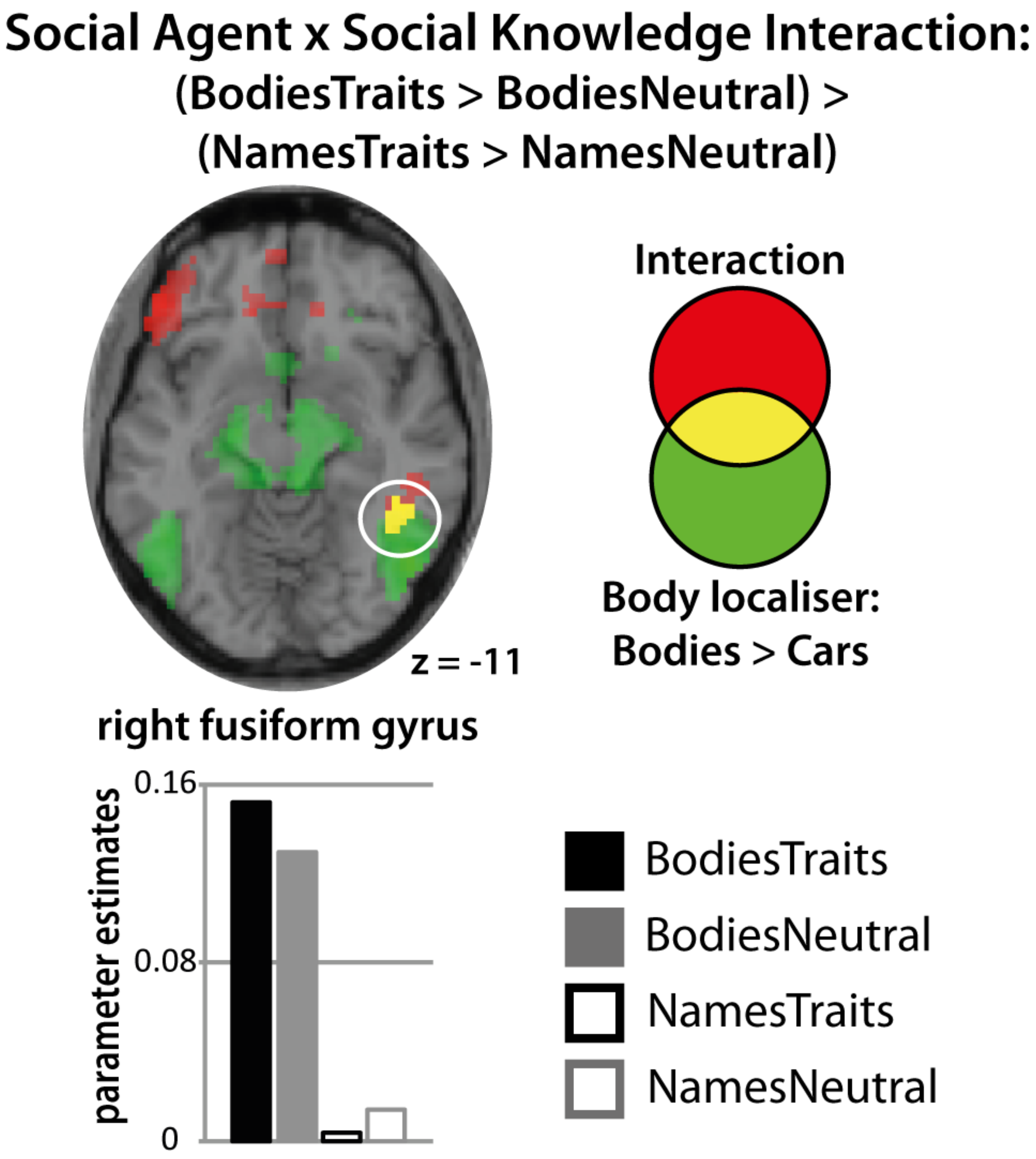

Appendix Figure 1. Results from the univariate analysis at a reduced threshold (p<.05, k=10). The Social Agent by Social Knowledge interaction ([BodiesTraits > BodiesNames] > [NamesTraits > NamesNeutral]) revealed a clusters right fusiform gyrus, which overlapped with the body-localiser (overlap is shown in yellow). These parameter estimates are extracted from a 4 mm sphere around the peak coordinate within the body-localiser.

APPENDIX 3

Details for PPI analyses (Chapter 3)

Appendix 3. Details of individual subjects' overlap between social agent and social knowledge interaction and the ToM (for seed regions left temporoparietal junction, medial prefrontal cortex, and left temporal pole) and body (for right fusiform gyrus) localisers. The details in this table are not intended to be interpreted on their own.

Seed-region	*Interaction threshold at which overlap was found in individual subjects*								
	p<.001	p<.005	p<.01	p<.05	p<.1	p<.2	p<.3	p<.4	p<.5
Left temporoparietal junction (n=17)	1	1	2	10	-	1	-	2	-
Medial prefrontal cortex (n=17)	1	1	-	15	-	-	-	-	-
Left temporal pole (n=15)	-	2	4	8	-	-	1	-	-
Right fusiform gyrus (n=19)	-	7	-	2	2	3	5	-	-

APPENDICES

APPENDIX 4

Additional information about the methods in pilot experiment 1 and 2 (Chapter 4)

Selection and validation of stimuli: To select and validate stimuli, we ran two behavioural pilot experiments requiring participants to make socially-relevant judgments about silhouettes either presented under unlimited viewing conditions (Pilot 1) or presented briefly (Pilot 2). The participants in pilot experiments did not complete the fMRI study. First we made series of body images that represented three different body shapes: muscular, obese, and slim. These categories were chosen so that we could compare the perception of bodies where a social evaluation is more extreme (muscular and obese) to a body where social evaluations are relatively neutral (slim). Because the focus of our research question was on body shape and posture only, we used body silhouettes with heads removed. Bodies were selected to have a posture that was as neutral as possible (no crossed arms or slouching postures). Images were gathered from various websites, converted into silhouettes, and cropped using GIMP 2.8 (www.gimp.org). To validate that our stimuli were indeed socially evaluated differently, in two separate experiments we asked participants to rate bodies. Stimuli were presented using an iMac computer and Matlab software using Psychtoolbox 3.

In both pilot studies, all bodies were presented upright as well as inverted. Inverted bodies were included to address an additional question (not reported here). All analyses reported here are based on upright bodies. In pilot Experiment 1, 14 participants evaluated 85 upright bodies by rating them on how well the statement matched the image of a body (with 1 being ‘completely disagree’ and 9 being ‘completely agree’). Like prior work on the evaluation of faces (e.g., Kramer and Ward 2010), statements were taken from Big-5 personality measures (Extraversion, Conscientiousness, Agreeableness; Donnellan et al. 2006), as well as physical health (Ware et al., 1996). For instance, to assess physical health, participants rated how well each body matched the statement “Accomplishes less due to health problems”. Participants completed one of two versions of the task. Both versions were identical with the exception of the content of the questions that were asked. In each version, two questions (one positive and one negative) were asked for each of the four measures, resulting in 8 questions. Each question was asked for each body. Ratings for each condition were compared using a repeated-measures Analysis of Variance, and subsequently in two planned comparisons (slim vs. muscular and slim vs. obese).

In pilot Experiment 2 (n=23), we wanted to find out whether these silhouettes gave rise to a social inference during a brief presentation, which would be more akin to conditions during the fMRI experiment. To do so, each body was presented for 330 ms, after which it was backward masked for 300 ms. The question then remained on screen until a response was made. Participants were asked to assess how confident they were about the answer they gave. Participants completed one of two versions of the task. These were identical, with the exception of how the bodies were paired with the questions. In each version, two questions (one positive and one negative) were asked for each of the four measures, resulting in 8 questions. Each of the bodies was rated on all measures.

APPENDIX 5

Additional univariate results at reduced threshold to help identify seed regions (Chapter 4)

Appendix 5. Univariate results masked by the body-localiser (p<.005, k=10) at a) p-uncorrected<.005, k=0, and b) at p-uncorr<.05, k=10.

Region	Number of voxels	Cluster *P FWE*	*T*	Montreal Neurological Institute coordinates		
				x	y	z
a) Social Evaluation > Neutral masked by body-localiser at p<.005, k=0						
Left inferior occipital gyrus (EBA)	1	.72	3.12	-48	-82	-5
b) Social Evaluation > Neutral masked by body-localiser at p<.05, k=10						
Left inferior occipital gyrus (EBA)	61	.96	2.98	-48	-82	-5
			2.60	-48	-73	-8
			2.58	-45	-67	-5
Left fusiform gyrus (FBA)	58	.96	2.69	-42	-55	-11
			2.65	-45	-49	-11
			2.55	-45	-43	-14
			2.39	-42	-43	-26
			2.36	-48	-46	-23

Note: Cluster-level p-values are corrected for the search volume, i.e., the mask created from the localisers. Subclusters at least 8 mm from the main peak are listed.

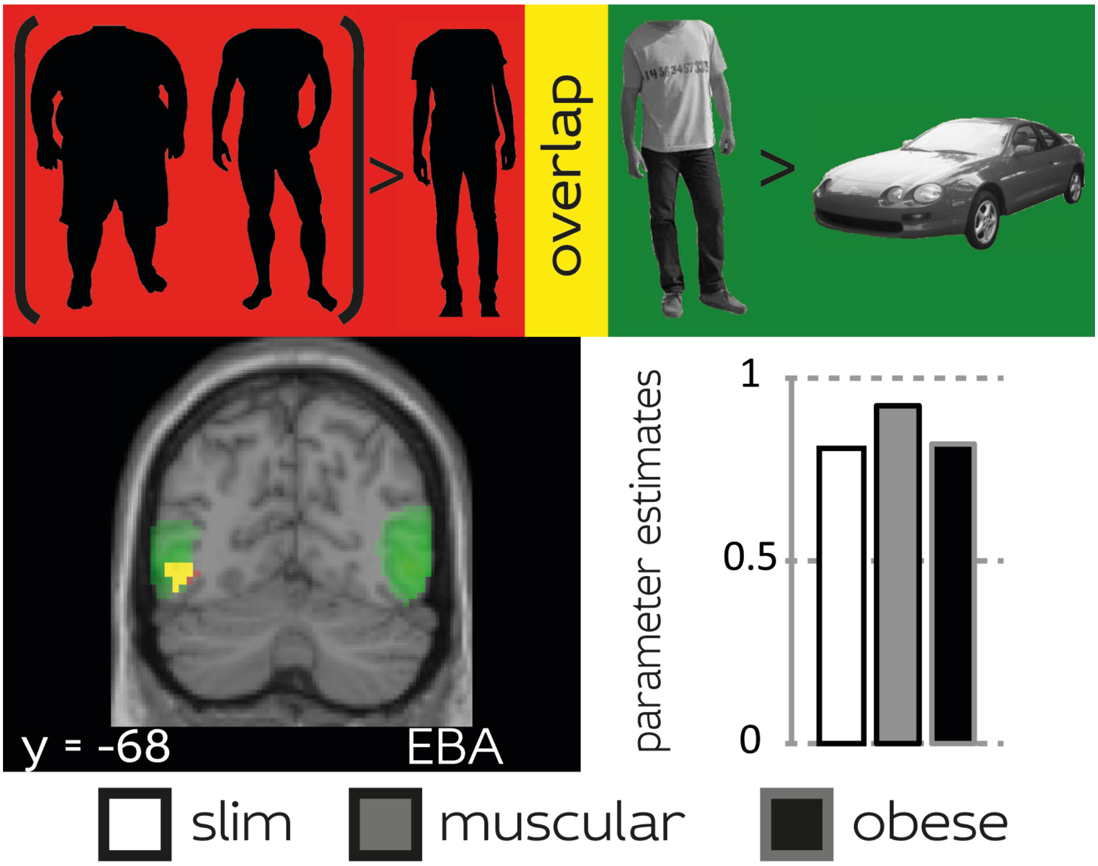

Appendix Figure 2. Results from the univariate analysis at a reduced threshold (p<.05, k=10). The Social Evaluation > Neutral contrast revealed a clusters left occipital and fusiform gyrus, which overlapped with the body-localiser (overlap is shown in yellow). These parameter estimates are extracted from a 4 mm sphere around the peak coordinate within the body localiser.

APPENDIX 6

Details for PPI analysis (Chapter 4)

Appendix 6. Details of individual subjects' overlap between Social Evaluation > Neutral contrast and the body-localiser.

Seed-region	*Main task threshold at which overlap was found in individual subjects*								
	p<.001	p<.005	p<.01	p<.05	p<.1	p<.2	p<.3	p<.4	p<.5
Left EBA (n=24)	3	1	-	1	6	2	6	4	1

APPENDICES

APPENDIX 7

Details for PPI analyses with seed regions taken from the body- and Theory-of-Mind (ToM) localisers (Chapter 4)

		Body-localiser		ToM-localiser			
		EBA	FBA	TPJ	TP	Precuneus	mPFC
Number of subjects (total 26)	Left	26	16	25	25	23	26
	Right	26	23	24	26		
Mean coordinate	Left	-51,-79,1	-48,-43,-23	-54,-58,16	-51,5,-35	0,-64,28	-15,47,34
	Right	51,-76,-5	48,-40,-23	54,-67,22	57,2,-32		
SD coordinate	X	L=3.70; R=4.13	L=4.17; R=4.01	L=6.56; R=6.53	L=5.63; R=4.20	7.38	9.31
	Y	L=6.29; R=4.49	L=9.67; R=9.12	L=6.42; R=6.50	L=5.98; R=7.43	6.22	6.84
	Z	L=5.80; R=4.24	L=5.70; R=5.70	L=5.58; R=6.06	L=8.32; R=6.09	7.98	15.32

Appendix 7. Details of amount of subjects showing results within each region of the body-localiser (bilateral extrastriate and fusiform body area; EBA and FBA) and ToM-localiser (bilateral temporoparietal junction (TPJ), temporal poles (TP), Precuneus, and medial Prefrontal Cortex (mPFC)). Further details are provided on the mean coordinate, and the standard deviation from the mean coordinate for x, y, and z separately.

APPENDICES

APPENDIX 8

Exploratory analyses regarding neural sensitivity to the Muscular > Slim and Obese > Slim contrast (Chapter 4)

Appendix 8. Results from the **A)** Univariate and **B)** PPI analyses for the Muscular > Slim (1) and Obese > Slim (2) contrasts are presented **a)** masked by the body-localiser (focussing on EBA and FBA), and **b)** masked by the ToM-localiser. The seed region (left EBA) is defined by the univariate contrast (Social Evaluation > Neutral).

Region	Number of voxels	Cluster P_{FWE}	Peak T	Montreal Neurological Institute coordinates		
				x	y	z
A) Univariate results:						
1) Muscular > Slim						
1.a) Masked by body localiser (EBA and FBA)						
Left inferior occipital gyrus (EBA)	18	.40	5.32	-48	-82	-5
Left fusiform gyrus (FBA)	39	.23	3.91	-45	-40	-14
			3.39	-42	-52	-14
			3.04	-48	-46	-23
Right inferior occipital gyrus (EBA)	11	.49	3.43	45	-79	-5
1.b) Masked by ToM-localiser						
No suprathreshold clusters						
2) Obese > Slim						
No suprathreshold clusters masked by either localiser						
B) PPI results, seed region defined by univariate analysis (left EBA):						
1) Muscular > Slim						
No suprathreshold clusters masked by either localiser						
2) Obese > Slim						
No suprathreshold clusters masked by either localiser						

Note: Regions surviving a voxel-level threshold of $p<.005$ and 10 voxels are reported. Cluster-level p-values are corrected for the search volume, i.e., the mask created from the localisers. Subclusters at least 8 mm from the main peak are listed.

APPENDICES

APPENDIX 9

Details for PPI analyses with seed regions taken from the body- and Theory-of-Mind (ToM) localisers (Chapter 5)

Appendix 9. Details of amount of subjects showing results within each region of the body-localiser (bilateral extrastriate and fusiform body area; EBA and FBA) and ToM-localiser (bilateral temporoparietal junction (TPJ), temporal poles (TP), Precuneus, and medial Prefrontal Cortex (mPFC)). Further details are provided on the mean coordinate, and the standard deviation from the mean coordinate for x, y, and z separately.

		Body-localiser		ToM-localiser			
		EBA	FBA	TPJ	TP	Precuneus	mPFC
Number of subjects (total 24)	Left	24	13	22	22	22	22
	Right	24	19	23	22		
Mean coordinate	Left	-51,-73,7	-48,-37,-23	-45,-64,28	-51,5,-32	-9,-49,34	6,56,28
	Right	54,-70,4	51,-40,-23	60,-58,25	51,5,-32		
SD coordinate	X	L=4.72; R=4.18	L=7.57; R=5.60	L=7.03; R=5.50	L=6.12; R=4.41	7.21	7.46
	Y	L=5.08; R=4.71	L=7.08; R=8.09	L=5.60; R=5.96	L=6.06; R=5.46	6.39	6.34
	Z	L=5.66; R=7.34	L=10.63; R=6.02	L=7.07; R=7.51	L=6.80; R=7.03	6.46	16.28

APPENDICES

APPENDIX 10

Additional univariate results at reduced threshold to help identify seed regions (Chapter 6)

Appendix 10. Univariate results of the BiasConsistent [(PosIn>PosOut) > (NegOut > NegIn)] contrast masked by A) the body-localiser at 1) p<.005, k=0, and 2) p<.05, k=10, and B) by the ToM-localiser at 1) p<.005, k=0, and 2) p<.05, k=10.

Region	Number of voxels	Cluster P_{FWE}	Peak T	Montreal Neurological Institute coordinates		
				x	y	z
A) Masked by body-localiser (EBA and FBA)						
1) Thresholded at p<.005, k=0						
Right fusiform gyrus	5	.97	3.19	45	-37	-14
2) Thresholded at p<.05, k=10						
Right fusiform gyrus (FBA)	102	1	3.76	42	-19	-23
			3.19	45	-37	-14
Left middle temporal gyrus (EBA)	46	1	2.75	-57	-52	-5
			2.61	-66	-49	1
			2.38	-60	-55	16
			2.19	-63	-55	10
Left middle occipital gyrus (EBA)	22	1	2.72	-39	-79	4
Right middle temporal gyrus extending into inferior occipital gyrus (EBA)	22	1	2.4	51	-76	13
			2.25	48	-79	19
			2.14	54	-73	16
			1.82	48	-82	4
Right inferior temporal gyrus (FBA)	19	1	2.4	42	-55	-5
B) Masked by ToM-localiser						
1) Thresholded at p<.005, k=0						
Left temporal pole	7	.83	3.69	-42	8	-41
Left temporal pole	2	.91	3.42	-42	23	-20
Right temporal pole	2	.91	3.42	30	17	-29
Left temporal pole	3	.90	2.90	-30	14	-29
Right temporal pole	5	.86	2.99	36	14	-38
Left middle temporal gyrus	1	.93	2.97	-63	-55	16
Right temporal pole	2	.91	2.90	39	17	-23

2) Thresholded at p<.05, k=10						
Left temporal pole	70	.99	3.69	-42	8	-41
			3.13	-30	14	-29
			2.48	-51	8	-29
			2.31	-39	17	-32
Left temporal pole	12	1	3.42	-42	23	-20
Right temporal pole	80	.99	3.42	30	17	-29
			2.99	36	14	-38
			2.90	39	17	-23
			2.79	42	5	-50
			2.08	51	14	-32
Left middle temporal gyrus	50	.99	2.97	-63	-55	16
			1.87	-63	-46	31
Right supramarginal gyrus	24	1	2.53	57	-40	31
			1.96	63	-46	37
Left superior medial gyrus	10	1	2.45	-6	62	22

Note: Cluster-level p-values are corrected for the search volume, i.e., the mask created from the localisers. Subclusters at least 8 mm from the main peak are listed.

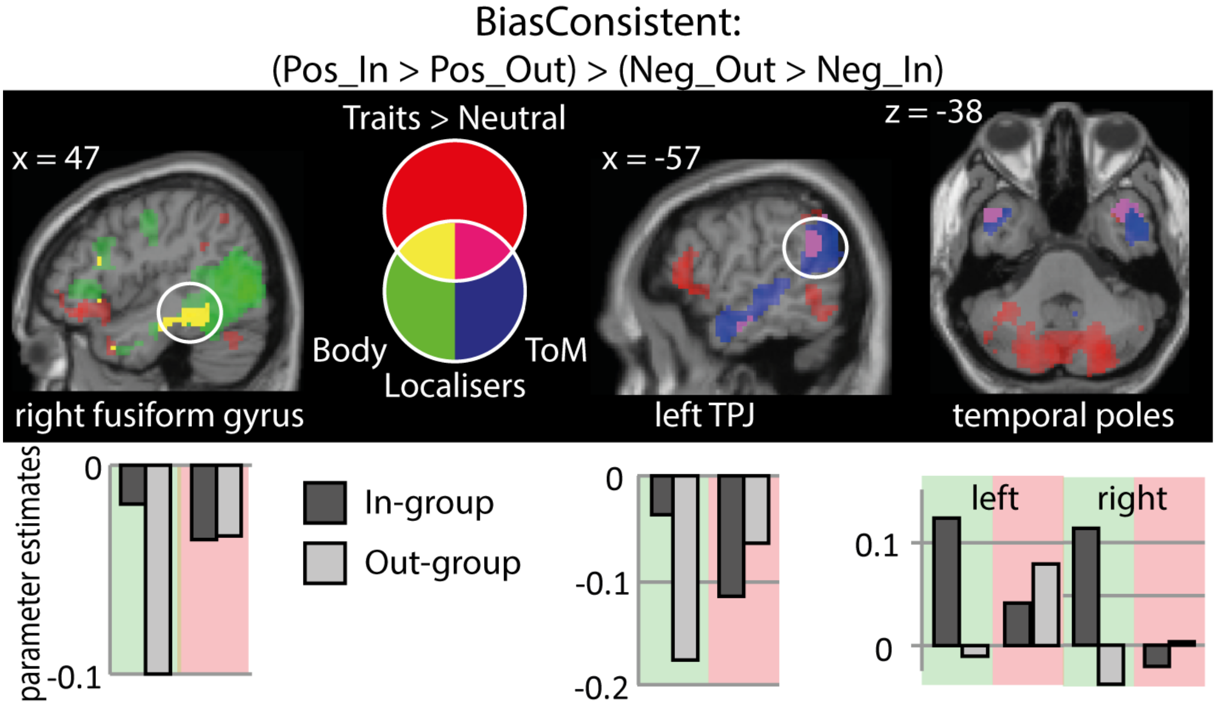

Appendix Figure 3. Results from the univariate analysis at a reduced threshold (p<.05, k=10). The Valence by Group or BiasConsistent [(PosIn>PosOut) > (NegOut > NegIn)] contrast revealed clusters (shown in red) in right fusiform gyrus, which overlapped with the body-localiser (localiser in green, overlap is shown in yellow), bilateral temporal poles, and left TPJ, which overlapped with the ToM-localiser (localiser in blue, overlap is shown in pink). These parameter estimates are extracted from a 4 mm sphere around the peak coordinate.

APPENDICES

APPENDIX 11

Details for PPI analysis (Chapter 6)

Appendix 11. Details of individual subjects' overlap between social BiasConsistent [(PosIn>PosOut) > (NegOut > NegIn)] contrast and the body and ToM localisers.

Seed-region	*Main task threshold at which overlap was found in individual subjects*								
	p<.001	p<.005	p<.01	p<.05	p<.1	p<.2	p<.3	p<.4	p<.5
Right FBA (n=16)	1	2	-	2	3	4	3	1	-
Left TPJ (n=19)	2	3	2	2	2	4	2	1	1
Left TP (n=23)	-	-	-	5	6	5	5	1	1
Right TP (n=18)	-	1	-	4	5	4	3	1	-

Ceterum censeo Carthaginem delendam esse

- Cato Maior